UNIVERSITÀ
DEGLI STUDI
DI PADOVA

University of Padua

Department of Cardiac, Thoracic and Vascular Sciences

PhD PROGRAMME IN MEDICAL, CLINICAL AND EXPERIMENTAL SCIENCES

CURRICULUM: CARDIOVASCULAR SCIENCES

29th SERIES

STERILISATION METHODS FOR DECELLULARISED SCAFFOLDS

This research was supported by the People Programme (Marie Curie Actions) of the European Union's Seventh Framework Programme FP7/2007-2013/ under REA grant agreement n° 317512.

Coordinator: Prof. Gaetano Thiene

Supervisor: Prof. Gino Gerosa

Co-Supervisor: Dr. Paola Aguiari

PhD Student: Cátia Fidalgo

STERILISATION METHODS FOR DECELLULARISED SCAFFOLDS

By

Cátia Fidalgo, Eng.

Submitted in Accordance with the Requirements for the Degree of

Doctor of Philosophy

UNIVERSITÀ DEGLI STUDI DI PADOVA

University of Padua

Marie Skłodowska-Curie Initial Training Network

"Tissue Engineering Solutions for Cardiovascular Surgery"

November 2016

“Deus quer,

O Homem sonha,

A Obra nasce”

Fernando Pessoa

“God wills,

Man dreams,

The work is born”

ABSTRACT

The lack of adequate sterilisation procedures represents one of the main hindrance for clinical adoption of cardiovascular substitutes composed of xenogeneic decellularised material. Effective methods are required to be tailored and optimized for the utilization on tissues derived from animal sources and should not impair the functional properties of the original scaffolds. The purpose of this study is to establish two protocols for sterilisation of pericardial decellularised scaffolds: Sterilisation Protocol 1, based on antibiotic/antimycotic (AA) + peracetic acid (PAA) treatments; and Sterilisation Protocol 2, based on γ-irradiation.

Assessment of the sterility effectiveness of the proposed methods required the design of a novel proper rigorous protocol. The sterilisation assessment methodology consists in the verification of sterility and subsequent quantification/qualification of the bioburden. A preliminary controlled contamination (CC) with $Gram^+$ and $Gram^-$ bacteria was performed on all scaffolds to assess the effectiveness of the developed sterilisation protocols. Sterility test was performed according to the European Pharmacopoeia guidelines by inoculation of a small amount of sample or its rinsing solution in bacteria media. Turbid medium is indicative of contaminated samples while clear medium indicates that the sample is sterile. Identification of contaminants was assessed by MALDI-TOF (Matrix-Assisted Laser Desorption/Ionization Time-of-Flight) mass spectrometry, while microorganism quantification was performed by Most Probable Number (MPN) method. This method was applied to evaluate both sterilisation methods in study, however it can also be tailored to other sterilisation methodologies or scaffolds.

The scaffold subjected to sterilisation are pericardia form porcine and bovine origin, decellularised according to an established protocol called TRICOL. The Sterilisation Protocol 1 consists in the incubation of tissues with a cocktail of AA comprising vancomycin, gentamicin, cefoxitin and amphotericin B during 24 h at 37 °C followed by treatment with PAA at 0.05% and 0.1% (v/v) for 3h at 27 °C. The second protocol developed (Sterilisation Protocol 2) consists in the application of five dosages of γ-irradiation: 1.5, 5, 10, 15 and 25 kGy.

Sterility assessment was carried out through the sterilisation assessment protocol developed. The effects of the sterilisation on the pericardial scaffolds were evaluated by histology, biochemical and biomechanical tests, scanning electron microscopy (SEM) analysis and cell seeding experiments with human bone marrow mesenchymal stem cells (hBM-MSC) for evaluation of cytotoxicity and cell proliferation.

The outcomes of the Sterilisation Protocol 1 showed that AA+PAA treatment provides sterile tissues in both concentrations tested. Histological, biomechanical and biochemical evaluation demonstrated that AA+PAA at both concentrations does not lead to substantial modifications of the decellularised pericardial scaffolds in terms of collagen fibres architecture, ECM protein content and appearance. However, the higher concentration of PAA has been shown to induce damages on porcine pericardial scaffolds ECM, as collagen network fragmentation. In addition, biomechanical evaluation demonstrates the preservation of mechanical properties of bovine scaffolds, whereas for porcine differences were observed after PAA treatments. Cell seeding experiments disclosed the non-cytotoxic effect of treatments in both pericardial scaffolds, as a sustained cell proliferation was observed in all tissues during time. Furthermore, histological assessment of cell seeded sterilised scaffolds showed the presence of a uniform monolayer of cells on scaffold surface after 14 days.

The Sterilisation Protocol 2, based on γ-irradiation treatment, was proven effective in the complete elimination of all the contaminants from both porcine and bovine pericardial scaffolds, even in the lower dosage applied. In addition, the biological indicator for this treatment (spore form of *Bacilus Pumilus*), employed to simulate the worst-case scenario, was removed after all the dosages employed in the test. Furthermore, after histological, biochemical and SEM analyses a general well preserved ECM was observed.

In summary, in this PhD project a sterilisation assessment protocol has been designed. This protocol has been designed for the verification of the effectiveness of two different sterilisation methods for decellularised animal biomaterials. In addition, the two sterilisation protocols (Sterilisation Protocol 1, comprising AA + 0.05% PAA and Sterilisation Protocol 2, dosage 1.5kGy) were both adequate in the effective sterilisation

of pericardial decellularised tissues without affecting ECM structure and functionality. In addition, the sterilisation methodologies developed were optimised for the tissues in study but can be putatively applied on any decellularised animal scaffold. Furthermore, they can be easily exploited in research laboratories and in tissue banks, since they do not require expensive and complex equipment to be implemented.

TABLE OF CONTENTS

CHAPTER I

INTRODUCTION

1.1 Heart

The heart has been correctly assumed since ancient Chinese, Egyptian, Greek and Roman scholars as a pump for filling the vessels with blood. Leonardo da Vinci (1452-1519) contributes with his drawings and notes to the understanding of several systems of the human body (Figure 1.1). His drawings and notes of the heart anatomy and function are one of the first references to the complexity of this organ (Leonardo, Keele et al. 1983).

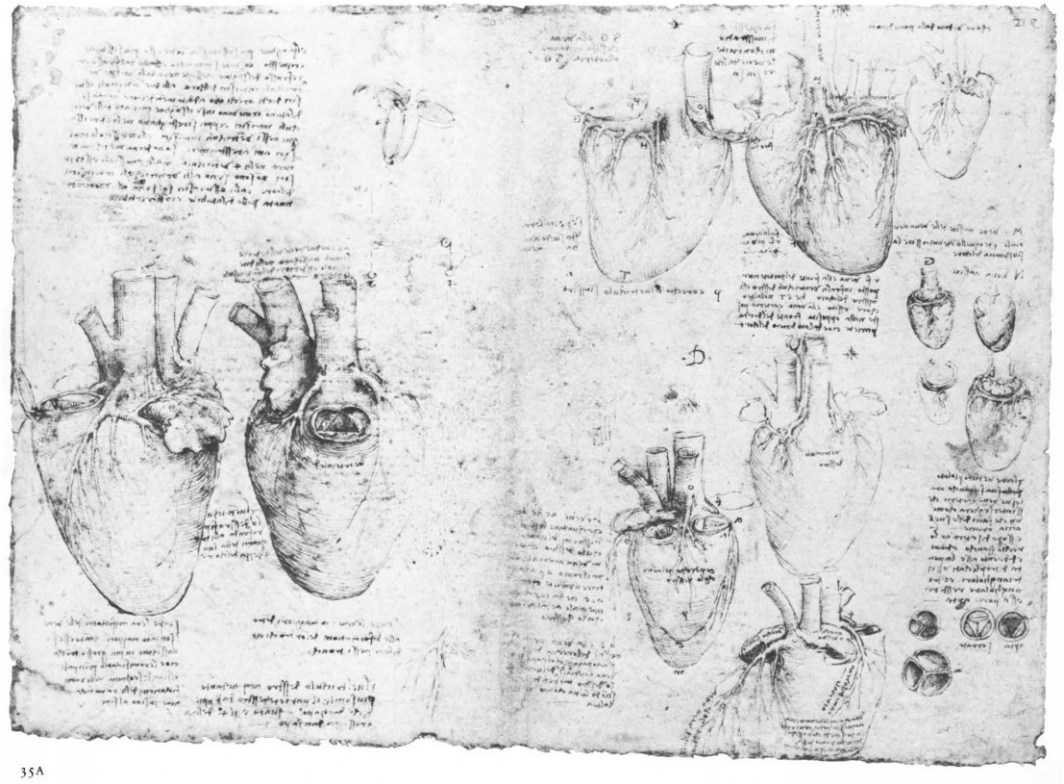

Figure 1.1 Heart drawings and notes by Leonardo da Vinci. Adapted from (Leonardo, Keele et al. 1983).

1.1.1 Anatomy

The heart is a four-chambered muscular pump, located in the thoracic cavity in the mediastinum behind the sternum and between the lungs (Figure 1.2). It is enclosed and protected by pericardium. Pericardial fluid is present between pericardium and heart in the pericardial cavity and the major function is to lubricate the membranes to reduce the friction during heart contraction.

The inferior portion of the heart is called apex, while the superior portion is known as base. The apex has a conical shape and is located immediately above the diaphragm. The base is the point of attachment of great vessels that transport the blood to and from the heart. In an anterior observation, the heart is inclined to the left, about 2/3 located in the left median plane. An adult heart is about 9 cm wide at the base, 13 cm from the base to the apex and 6 cm from anterior to posterior (approximately the size of a closed fist), weighting about 300 g (Saladin 2010).

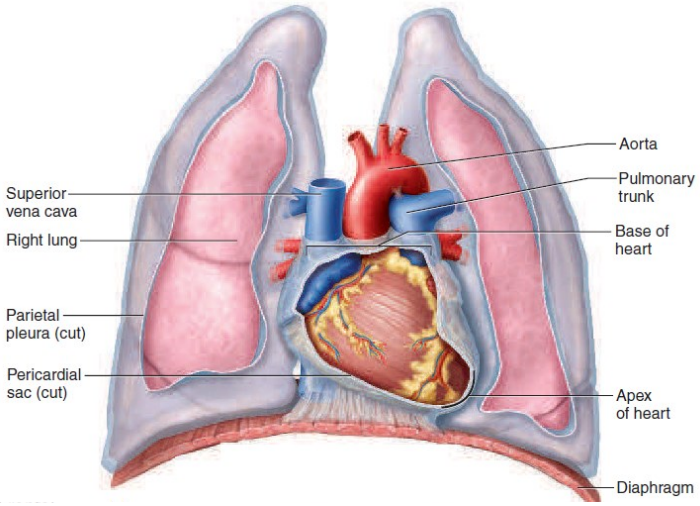

Figure 1.2 Anatomic location of the human heart. Adapted from (Saladin 2010).

Heart's four chambers can be divided in: two atria, which receive blood from veins and two ventricles that push blood towards organs through the arteries. The atria are located in the base of the heart, while the ventricles are located at the apex. From an anterior vision, between each atrium and ventricle, the extension of the atria named auricles can be observed (Figure 1.3). The sulcus around the heart defines the boundaries of the four chambers, constituted by adipose tissue and coronary blood

vessels. The coronary blood vessels have the important function of ensure blood circulation through the myocardium. In order to maintain the unidirectional flow of the blood, the heart is provided with valves between the atria/ventricle and ventricle to pulmonary and aortic arteries.

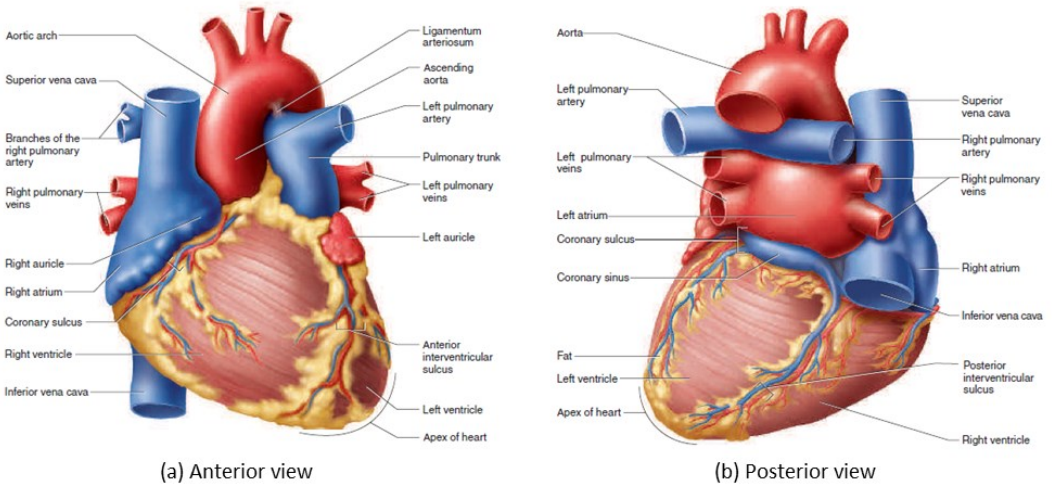

Figure 1.3 External anatomy of heart: (a) anterior view; (b) posterior view. Adapted from (Saladin 2010).

Since the heart is a muscle that supports strong effort during a lifetime - at rest, a healthy adult heart pumps approximately 5 L/min that can increase to 20 L/min during vigorous exercise – it is required to have a resilient structure. The heart wall is structured in three different layers of tissue: epicardium, myocardium and endocardium (Figure 1.4). The epicardium is a serous membrane in the outer layer of the heart. It consists of a thin layer of aerolar tissue (loose connective tissue with small spaces for interstitial fluid) enclosed with a simple squamous endothelium layer. It encloses also the coronary blood vessels around the heart. Endocardium is the inner layer that is in direct contact with blood. It consists on connective tissue covered by a simple squamous epithelium, similar to epicardium but without adipose tissue. The endocardium permit the smooth flow of the blood on its surface, covering also the valve surfaces and continuous with the endothelium of blood vessels. Myocardium is the ticker middle layer of the heart, responsible for the contraction of the heart chambers. It is composed of cardiac muscle cells. The thickness of the myocardium is proportional on the workload of cardiac chambers, thus having high variability on the different chambers (Saladin 2010, Tate 2012).

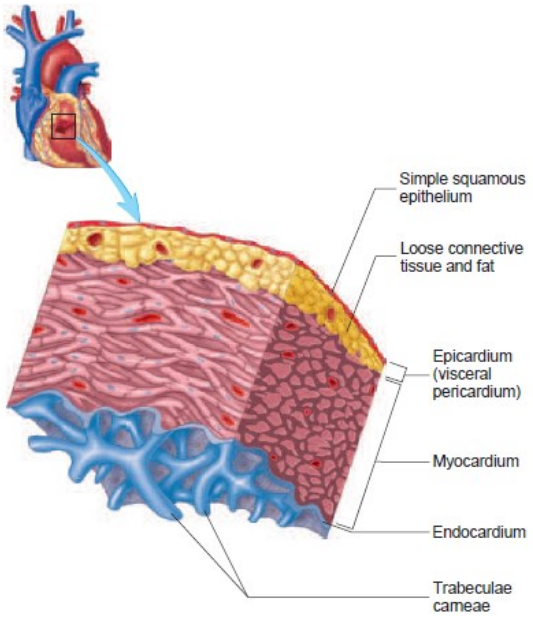

Figure 1.4 Structure of heart wall. Adapted from (Tate 2012).

Cardiac muscle cells, also referred as cardiomyocytes, are branching cells with centrally located nuclei typically with 50 to 100 µm long and 10 to 20 µm wide (Figure 1.5). Cardiomyocytes contain myosin and actin filaments organized to form the contractile unites called sarcomeres. These structures are responsible for muscle contraction and their organization resulted in the striated appearance, more evident in the skeletal muscle. In cardiomyocytes, the plasma membrane (called sarcolemma) forms deep invaginations called transverse tubules (T tubules), which run transversely through the muscle fibre and associate with the sarcoplasmic reticulum. Through T tubules electrical impulses are transmitted from the sarcoplasm to the fibre's interior. The T tubules in cardiomyocytes are larger than the ones present in the skeletal muscle. To activate muscle contraction during excitation of the cell, T tubules stimulate release of calcium ions from the sarcoplasmic reticulum. Calcium released from the sarcoplasmic reticulum is required for fibres contraction as it triggers the sliding of myosin filaments on actin ones, causing the shortening of the sarcomere length. Supplement of calcium in cardiomyocytes is supplied from the extracellular fluid. Mitochondria present in cardiomyocytes produces energy in form of adenosine triphosphate (ATP) by aerobic respiration, necessary to cardiac muscle contraction. They are present in higher number in comparison with skeletal muscle cells. Since cardiomyocytes have limited ability for

ATP production through anaerobic glycolysis, constant supply of oxygen and nutrients from blood is essential for their correct function. Intercalated disks are tick connections that bond cardiomyocytes laterally and end-to-end. These disks increase cell contact due to some characteristics that are not present in the skeletal muscle as interdigitating folds, mechanical junctions and electrical junctions. The gap junctions allow the passage of action potentials from one cell to the other through electrical synapses and thus cells contract as a single unit. This functional characteristic is essential for the highly coordinated contractions of the heart (Saladin 2010, Tate 2012).

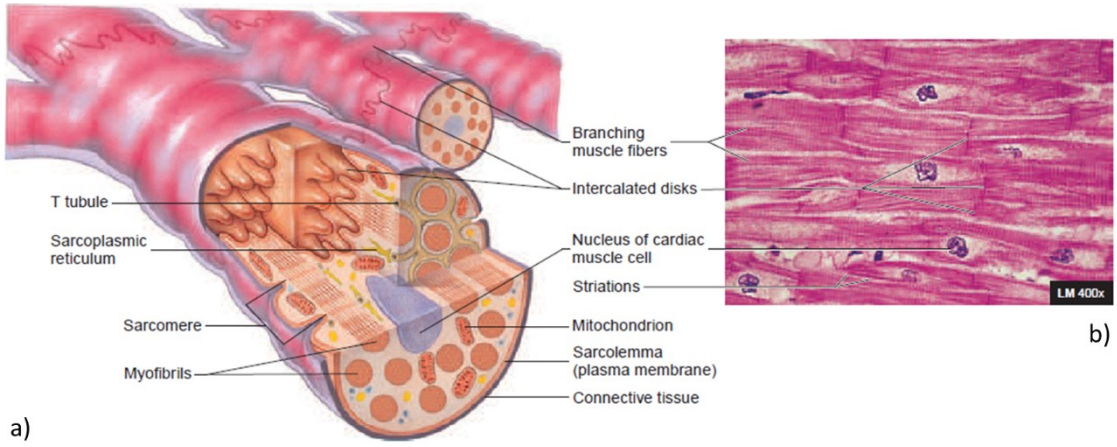

Figure 1.5 (a) Detailed structure of cardiac muscle cell and (b) light micrograph of cardiac muscle tissue. Adapted from (Tate 2012).

1.1.2 Function

The heart operates as a pump that permit the blood flow through the body. It displays three major functions: 1) the contraction of the heart generates blood pressure required for the blood flow; 2) the changes in contraction rate and force regulate the blood supply to the organism according to the metabolic requirements and 3) the double pump function of the heart provides supply of blood to both pulmonary and systemic circulation. To accomplish these functions, a complex system of blood vessels to reach all parts of the organism is present.

The heart and blood vessels (arteries, veins and capillaries) form the cardiovascular system, which ensures the circulating blood is able to transport oxygen and nutrients to tissues and cells and collect their waste products to be eliminated. This system consists

in two separate circuits: pulmonary and systemic. Pulmonary circuit carries the blood from and to the lungs for gas exchange (O_2 and CO_2), while systemic circuit supplies blood to all organs and tissues of the body. The right side of the heart is responsible to provide blood to the pulmonary circuit – lungs receive the venous blood (not oxygenated) from pulmonary artery and return oxygenated blood (named arterial blood) to the heart through pulmonary vein. The left side of the heart is responsible for the systemic circuit – arterial blood is distributed through aorta to organs and tissues, returning to the heart through inferior and superior vena cava (Figure 1.6) (Saladin 2010, Tate 2012).

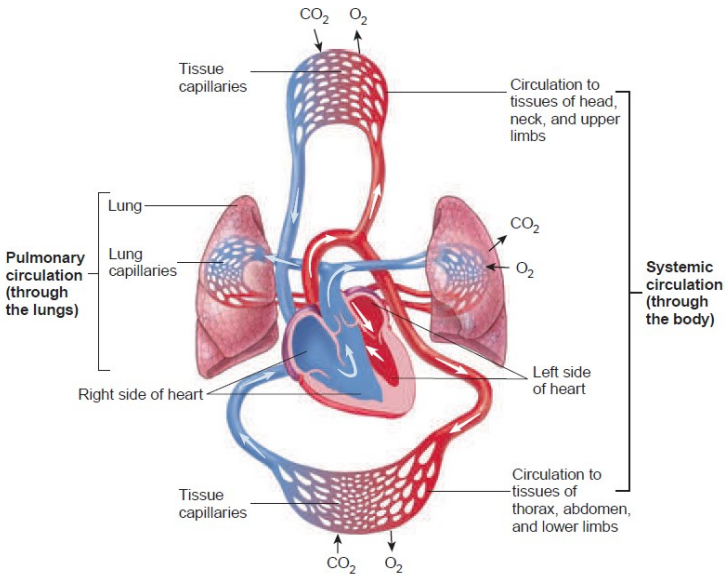

Figure 1.6 Human cardiovascular system. Adapted from (Tate 2012).

1.1.3 Conduction System and Cardiac Cycle

The cardiac conduction system comprises the coordinated contraction of the atria and ventricles by an internal pacemaker that transmits action potential through the myocardium (Figure 1.7). The sinoatrial (SA) node (pacemaker) is located in the right atrium near vena cava. Action potentials originated from SA node are spread in both right and left atria, causing their contraction. These signals reach the atrioventricular (ATV) node in the lower portion of the right atrium. ATV node give rise to the ATV bundle or bundle of His. This bundle reach the interventricular septum by a small opening in the fibrous skeleton that electrically separates action potentials from the atria and the

ventricles, to allow their separate contraction. The ATV bundle divides into the left and right bundle branches descending through the interventricular septum till the apex of the heart. There, they subdivide in smaller bundles named Purkinje fibres that distribute the action potentials to cardiomyocytes of the ventricular walls (Saladin 2010, Tate 2012).

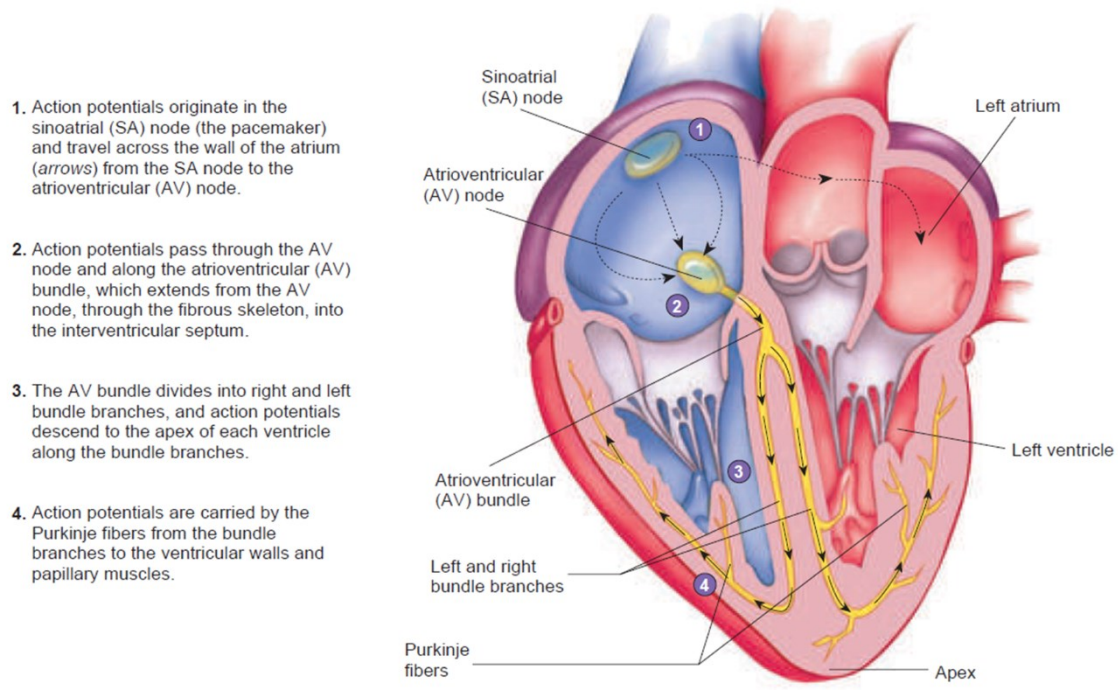

Figure 1.7 Conduction system of the heart. Adapted from (Tate 2012).

The cardiac cycle refers to the repetitive pressure changes caused by systole and diastole of the four heart chambers: right and left atria and ventricle (Figure 1.8). A complete cycle has a total duration of 0.8 second in a resting person. Systole refers to the contraction while diastole refers to expansion of atria or ventricle. In ventricular diastole, the ventricles are expanded and pressure is lower than the one in the atria, causing the opening of the ATV valves and blood flow to the ventricles. As the ventricle pressure rises, the atrial pressure drop and atrial systole finish to fill the ventricle. While the atria repolarize, relax and remain in diastole, the ventricles begin to contract. The pressure in the ventricles rises and close the ATV valve, while the semilunar (SL) valves are still closed. Ventricles continue to contract and when ventricular pressure exceed arterial pressure, SL valves open and blood flows to pulmonary trunk and aorta.

Ventricles then start to relax and ventricular pressures decrease below the ones in pulmonary trunk and aorta. SL valves close due to the flow back of the blood toward the ventricle. Through ventricular systole and beginning of diastole, the atria relax and start to fill with blood from the veins. Atrial pressure increases and the cycle starts again (Saladin 2010, Tate 2012).

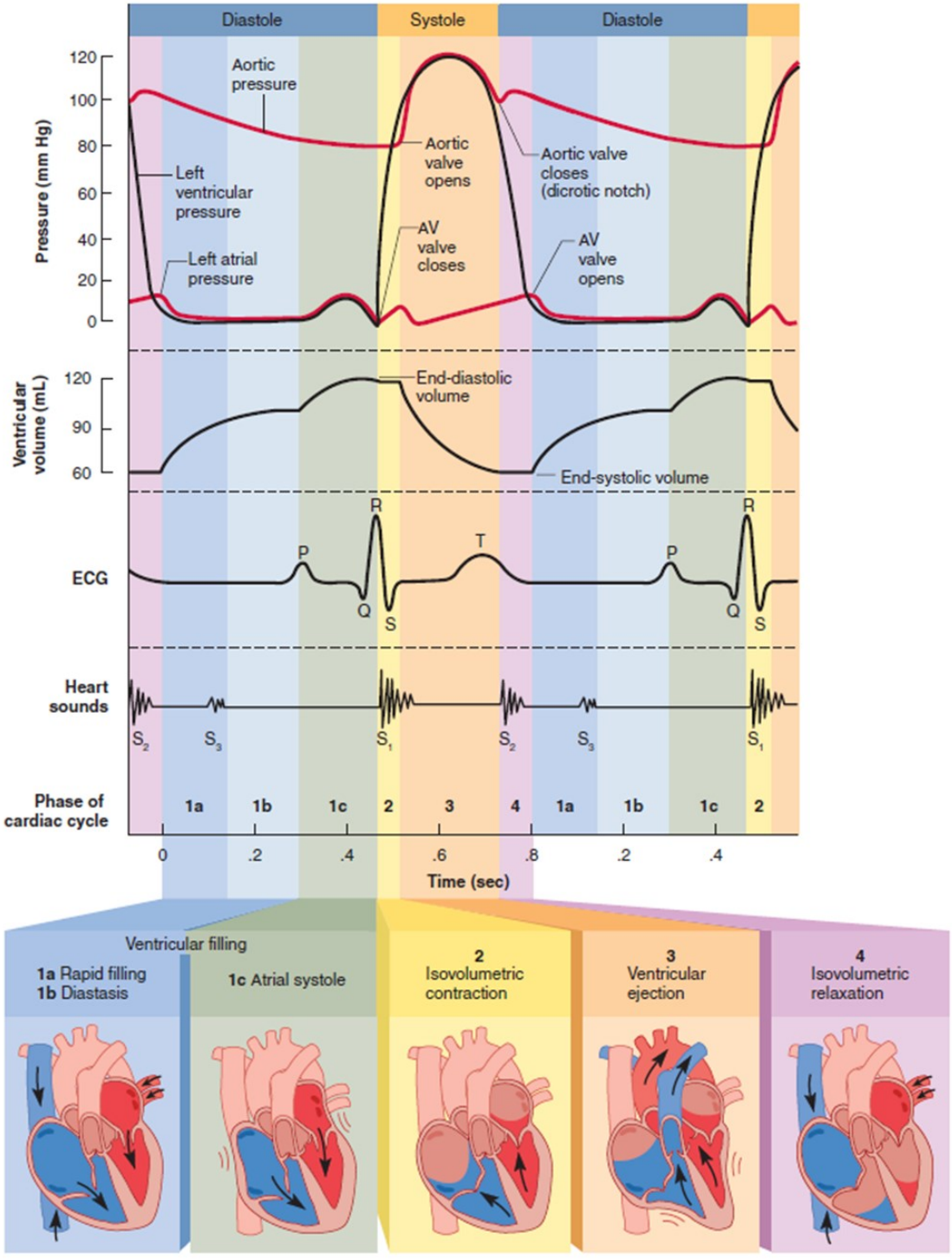

Figure 1.8 Events of the cardiac cycle. Adapted from (Saladin 2010).

1.2 Pericardium

Pericardium is a double layer sac that involves the heart. It consists in two layers: fibrous pericardium and serous pericardium (Figure 1.9). Fibrous pericardium is the outer layer, composed of fibrous connective tissue. Serous pericardium is constituted of parietal pericardium lining the fibrous pericardium and the visceral pericardium that covers the heart surface. Pericardial cavity is located between parietal and visceral pericardia and is filled with pericardial fluid produced by serous pericardium. The pericardial fluid reduces the friction caused by the contraction of the heart (Saladin 2010, Tate 2012).

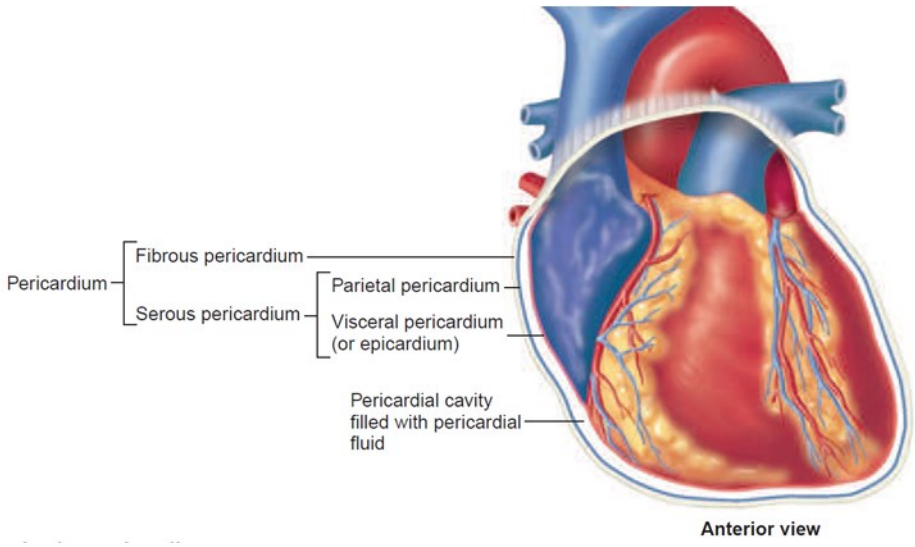

Figure 1.9 Components of the pericardium. Adapted from (Tate 2012).

The serosa layer of the pericardium is composed of a surface layer of mesothelial cells and narrow submesothelial space, while the fibrosa contains connective tissue with compact collagen bundles, small vessels and elastic fibres. In general, pericardium is a soft tissue rich in collagen (mostly collagen type I), glycoproteins, glycosaminoglycans (GAGs) and its constitutive cells (Figure 1.10 (a) and (d)). Under polarized light can also be observed the layers and the wavy appearance of the collagen fibres (Figure 1.10 (b)). The mechanical features of the pericardium are related with the distribution and orientation of the collagen fibres as well as interaction between them and other components of the pericardium as proteoglycans (Figure 1.10 (c)) (Ishihara, Ferrans et al. 1980) (Rémi, Khelil et al. 2011).

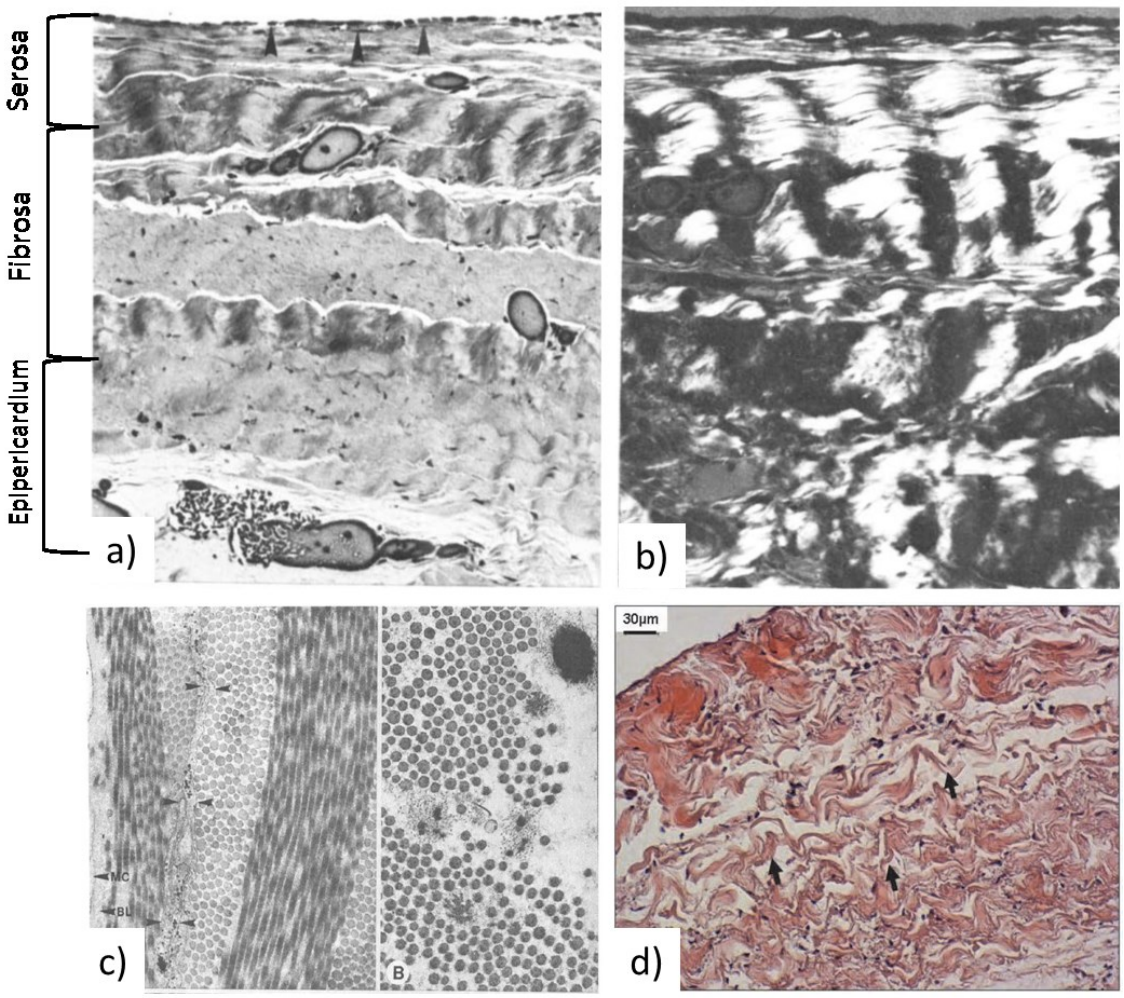

Figure 1.10 (a) Structure of human pericardium: serosa, fibrosa and epipericardium; (b) pericardium under polarized light; (c) transmission electron micrograph of pericardium with several collagen fibres oriented; (Adapted from (Ishihara, Ferrans et al. 1980)) (d) Haematoxylin-eosin staining of ovine pericardium. Adapted from (Rémi, Khelil et al. 2011).

Since the fibres of soft biological tissues have preferred directions and orientation, the mechanical behaviour of these tissues is anisotropic. Soft tissues can be deformed when compared with hard tissues and their tensile strength depends on the strain rate. The viscoelastic behaviour of the soft tissues is related with their tissue matrix composition and the shear interaction of collagen fibres with the proteoglycans. During a mechanical tensile test, three phases can be observed for soft tissues as pericardium (Figure 1.11). In a first phase, it starts the fibre recruitment while fibres are with different degrees of orientation. In the second phase, fibres start to gradually elongate and bear the load while lining in the direction of the load. In the third phase, the fibres become straight and elongated. They align in the direction of the load applied (Holzapfel 2000).

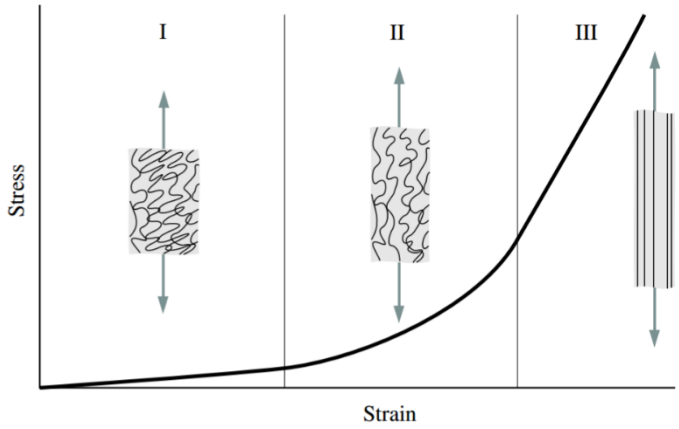

Figure 1.11 Schematic diagram of a typical stress-strain curve for soft tissues with the associated collagen fibre morphology. Adapted from (Holzapfel 2000).

1.3 Heart Valves

Heart valves play a major role in preventing the blood from flowing in the reverse direction. As for the heart anatomy and function, Leonardo da Vinci studied and made one of the first references to the general anatomy and function of the heart valves (Figure 1.12).

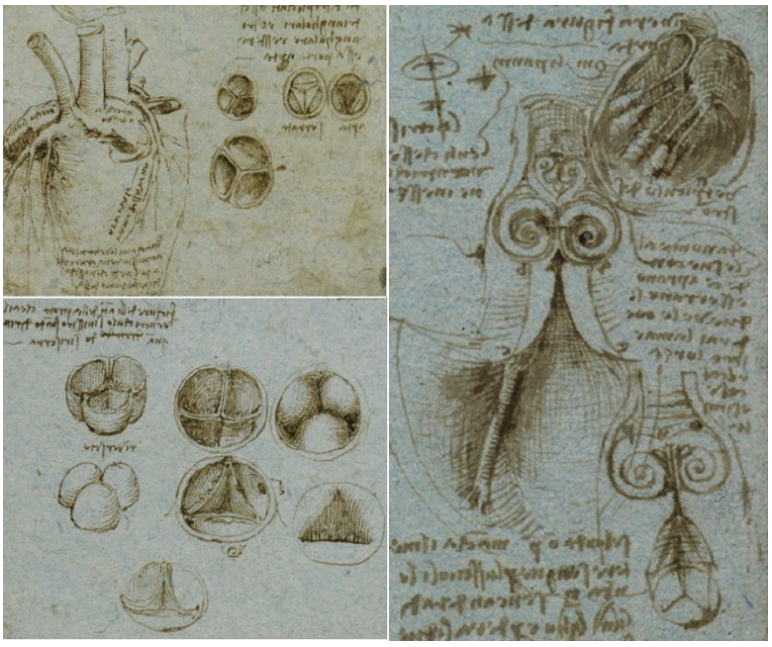

Figure 1.12 Heart valve drawings by Leonardo da Vinci. Adapted from (C. Wells 2013).

The heart presents four valves: ATV valves between the atria and ventricles and SL valves between the ventricles and pulmonary and aortic arteries. The main function of the heart valves is to ensure that the blood is effectively pumped in a one-way flow – from the atria to ventricles to the great arteries (Figure 1.13). They open and close once per second counting ≈ 40 million times in a year and more than 3 billion times over an average lifetime (Schoen 2012). Another important feature of the heart valves is that the open and closure is due to differences in pressure – they remain closed until the pressure behind is high enough to cause the blood to flow forward (Waite and Fine 2007).

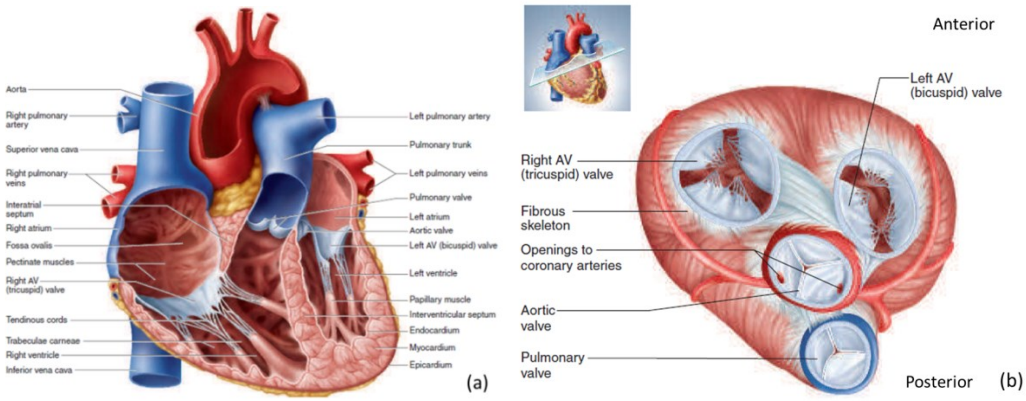

Figure 1.13 (a) Internal anatomy of the heart in a frontal plane section from an anterior view; (b) Superior view for the ATV and SL valves. Adapted from (Saladin 2010).

1.3.1 Atrioventricular Valves

The ATV valves regulate the flow from the atria into the ventricles, preventing blood flowing back into the atria. The right ATV valve is called tricuspid valve and presents three leaflets. This valve controls the blood flow from the right atria to right ventricle. The left ATV valve is called bicuspid or mitral, due to the similarity to a headdress of a church bishop, present only two leaflets. This is the only heart valve with two leaflets, controlling the blood flow from the left atria to left ventricle. Both ATV valves are connected to papillary muscles in each ventricle by thin, string-like and strong connective tissue strings called chordae tendineae. These chordae tendineae prevent the ATV valves by flipping into the atria due to the contraction of papillary muscles during the ventricle contraction (Figure 1.13) (Saladin 2010, Tate 2012).

Another component of the ATV valves is the valve annulus formed in the base of the leaflets. It consists of dense collagenous tissue surrounded by muscle that forms an elliptical ring on the base of both valves. Due to high pressures in the mitral valve, the circumference of the annulus is variable. Normal values for the mitral annulus are from 3-3.5 cm during ventricular diastole, when the blood is flowing through the mitral valve. During ventricular systole, the mitral valve closes due to the blood pressure and the circumference of the annulus is reduced (Waite and Fine 2007).

1.3.2 Semilunar Valves

The SL valves control the blood flow during the ventricle contraction/relaxation into the great arteries. The pulmonary valve (PV) is located on the pulmonary trunk and aortic valve (AV) is situated on aorta, controlling the blood flow from the right and left ventricle, respectively (Figure 1.13). Each SL valve is constituted by three leaflets, similar to shirt pockets when closed.

On the contrary of ATV valves, SL valves do not present tendinous cords connecting the leaflets to the muscular tissue. The SL valves are opening and closing due to differences of blood pressure caused by contraction and relaxation of the ventricles. The AV opens when the left ventricle is contracting, causing an increase of blood pressure on the ventricle that push the leaflets against aorta wall. When the ventricle starts to relax, the blood tends to flow back to the ventricle but instead enters in the pockets of the AV. At this point, the three leaflets of AV meet in the midline of the aorta, preventing the flow back of blood to the left ventricle. On the right part of the heart, PV is working in a similar way (Saladin 2010, Tate 2012).

SL valves leaflets are embedded within connective tissue, attached to a fibrous ring in the ventricular septum. They consist on three layers: fibrosa, ventricularis and spongiosa (Figure 1.14). Fibrosa is referred as the fibrous layer adjacent to aorta, while the ventricularis is the layer adjacent to the ventricle. The ventricularis is thinner and very smooth comparing to fibrosa. Since it is smoother, ventricularis allow the easy blood flow through the valve. Spongiosa is located at the central part of the leaflet and usually not present vascularization (Waite and Fine 2007).

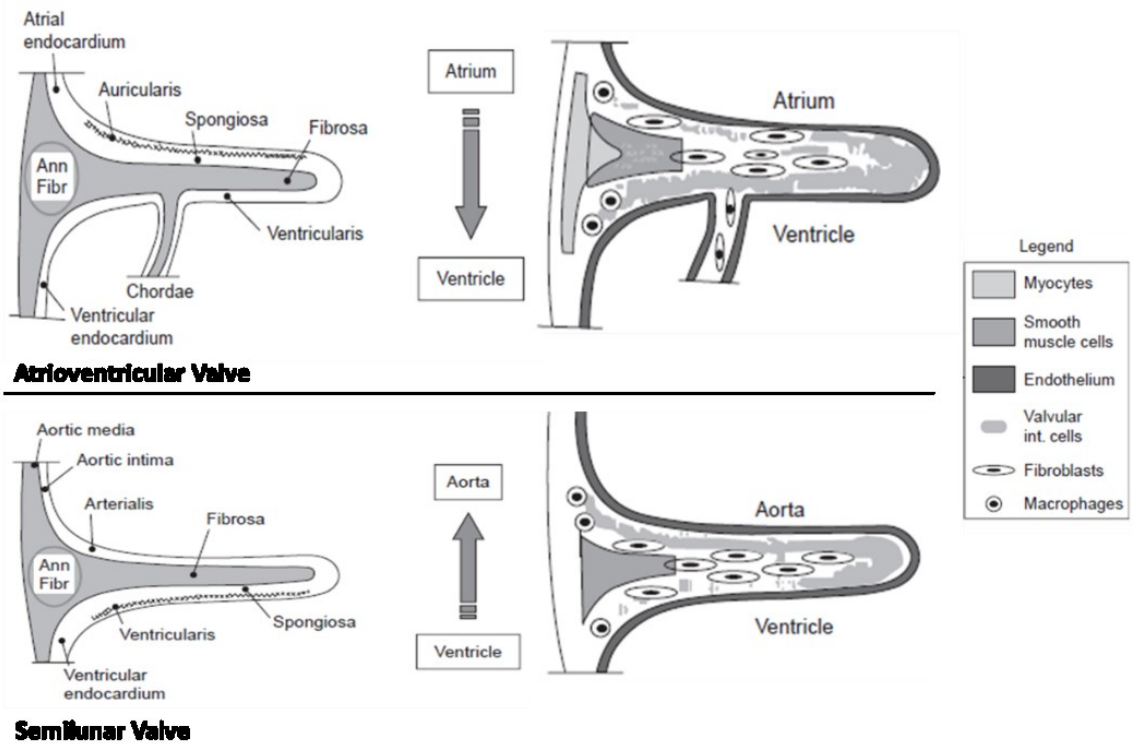

Figure 1.14 General structure of heart valves – ATV and SL. Adapted from (Simionescu 2006).

In order to reduce regurgitation of blood into the ventricle and aid in the complete closure of the valve, each leaflet presents a corpus aranti (or nodulus of Arantus) that is a large collagenous mass located in the coaptation region that allows the complete closure of the valve in the centre. The commissures are the support point of the suspend leaflets to the aortic wall through a fibrous structure. The sinotubular junction is located at the top of the sinus, indicating the transition from the aortic root (AR) to the ascending aorta and functioning as support for the commissures (Figure 1.15). The three bulges formed between the attachment of the leaflets and the sinotubular junction are named sinus of Valsalva. The sinus wall is thinner in comparison with the aortic wall, presenting a small dilatation that forms a skirt pocket shape. In the AV, two of the sinuses give rise to two coronary arteries, in this case usually referred as: right-, left- and non-coronary sinus. The mean diameter for the SL valves was reported as 23.2±3.3 mm for AV while for the PV was 24.3±3.0 mm (Misfeld and Sievers 2007, Waite and Fine 2007).

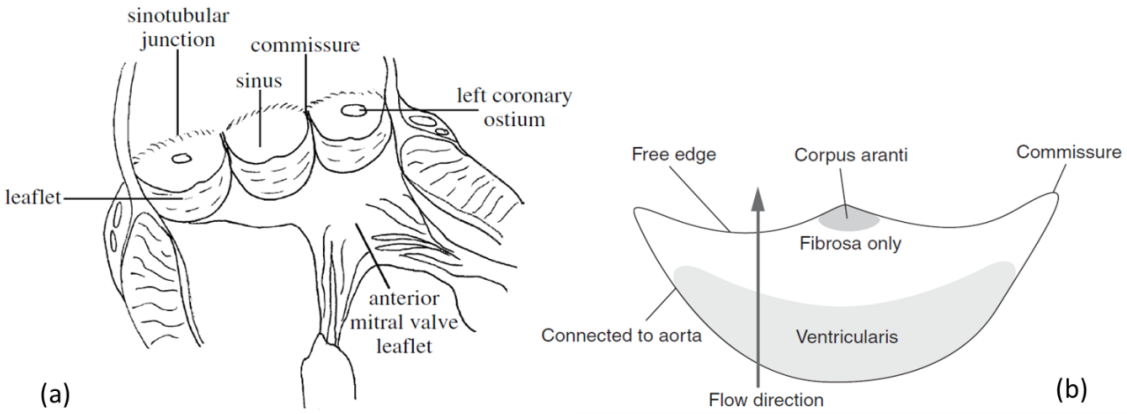

Figure 1.15 (a) Schematic draw of AR structures, (b) Sketch of an AV leaflet. Adapted from (Misfeld and Sievers 2007) and (Waite and Fine 2007).

1.3.3 Function and Structure

Opening and closure of heart valve leaflets are due to the pressure gradient generated during contraction/relaxation of atria and ventricles. The ATV valves are open when ventricles are relaxed, allowing the blood flow from the atria to the ventricles. When the ventricles are filled and start to contract, the internal pressure increases and the blood pressure force the ATV valve to close by pushing the leaflets together and sealing the passage from the ventricle to atria. The ATV valves do not collapse into the atria due to contraction of papillary muscles that pull the chordae tendineae, keeping the ATV valves in the correct position. During the ventricle contraction, the pressure increases as well on the SL valves. When the pressure is higher in the ventricle compared to the pressure in the great arteries, the SL valves open, allowing the blood to flow out of the heart. When the ventricle starts to relax, the pressure drop below that in the arteries. The arterial blood ejected briefly flow back to the heart, filling the pocket-like leaflets of the SL valves. The three leaflets meet in the middle, preventing the regurgitation of blood back to the heart (Saladin 2010, Tate 2012).

In order to withstand repetitive mechanical stress and strain over the years to maintain the unidirectional blood flow, heart valves present a dynamic functional structure. Their macro- and microstructure is able to support the strength and organize according to the variations in the size and shape of valve leaflets during the cardiac cycle (Schoen 2008).

Each ATV and SL valve consists of two or three fibrous leaflets or cusps that are thin sheets of tissue as extensions of the cardiac endocardium. They can be organized in different tissue extracellular matrix (ECM) sections: fibrosa, spongiosa, ventricularis and auricularis. According to the valves (ATV or SL) they are incorporated, they present different organization (Figure 1.14) (Simionescu 2006).

Fibrosa is a hydrophobic, collagenous and load- bearing layer that strengthens the leaflet, located in the central area of both ATV and SL leaflets. Resilience and recoil of the leaflets during systole and diastole are provided by elastic fibres, mainly present in the inflow layers of the heart (auricularis for ATV vales and ventricularis for SL valves). A loose layer of connective tissue (spongiosa) is located between fibrosa and auricularis/ventricularis. It consists of predominantly of hydrophilic and shock-absorbing GAGs, providing a gel-like matrix that acts as a space-filler and lubricant allowing minimal friction during continuous bending, rearranging, straightening and rotating of structural fibres (Figure 1.16) (Simionescu 2006).

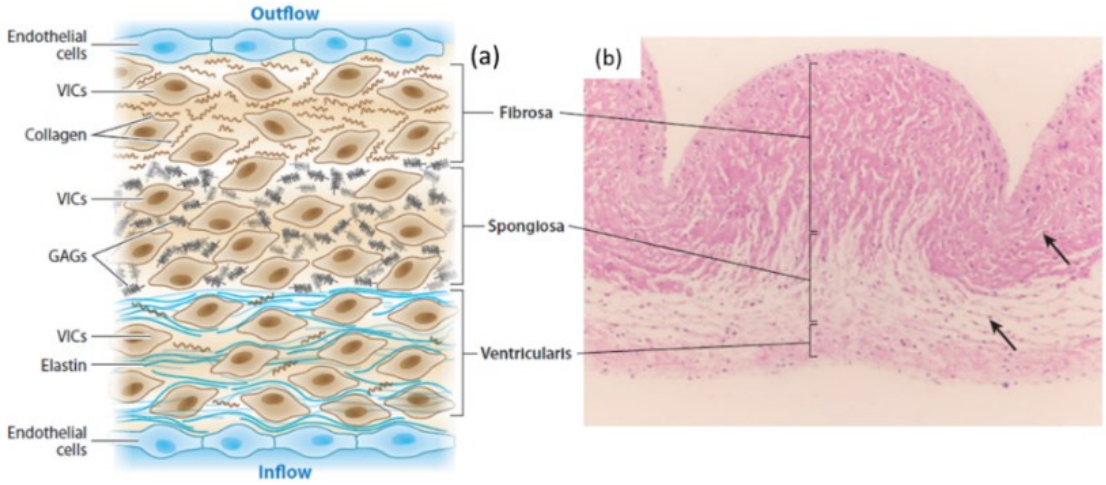

Figure 1.16 (a) Schematic diagram of aortic leaflet in cross section: details of components for fibrosa, spongiosa and ventricularis layers; (b) Photomicrograph of haematoxylin and eosin stain (100x magnification) of aortic leaflet (arrows indicating VIC cells. Adapted from (Schoen 2012).

To allow the continuous adaptation to hemodynamic forces, leaflets contain a multivariate type of cells: myofibroblasts that are matrix-producing cells, active valvular interstitial cells (VICs), valvular endothelial cells and resident macrophages (Figure 1.16). The most abundant cell type in the heart valves are VICs. They are responsible for the synthesis of valvular matrix and regulate remodelling of collagen and other matrix components by matrix degrading enzymes. VICs repair functional damage to matrix ECM and collagen components of the valve, presenting characteristics of fibroblasts in adult heart valve. Valvular cells in general have high metabolic activity related to matrix homeostasis by synthesize and degrade collagen and proteoglycans, having also reactivity with vasoactive compounds as epinephrine and angiotensin. Due to their specific, complex structure and components, heart valves enclose a balanced homeostatic activity essential to achieve their mechanical and biological functions (Simionescu 2006, Sacks, Schoen et al. 2009).

The dynamics of the cardiac cycle during systole and diastole request for rapid and reversible deformations on the ECM structures of the leaflets referred above. Collagen is the major stress-bearing component, able to withstand high tensile forces when taut but cannot be compressed. On the other hand, elastin is able to stretch and contract. During systole and diastole, both collagen and elastin play a major role by stretching and shortening their fibres. During systole, collagen is crimped and unaligned, while elastin is in relaxed state; in contrast, during diastole, collagen presents uncrimped and aligned and elastin in the stretched form (Figure 1.17). Additionally, GAGs present in spongiosa layer assist the rearrangement of collagen and elastin during the cardiac cycle by its high compliance and bond to adjacent layers.

The relative orientation of the collagen fibres determines some properties within the tissue: the greatest compliance is achieved in the orthogonal direction of collagen fibres and greatest tensile stress in parallel to the collagen fibres orientation. Moreover, mechanical properties of the leaflets are different in the radial and circumferential direction, they are referred as anisotropic. They have greater compliance and stretching in radial direction then in the circumferential one (Schoen 2008).

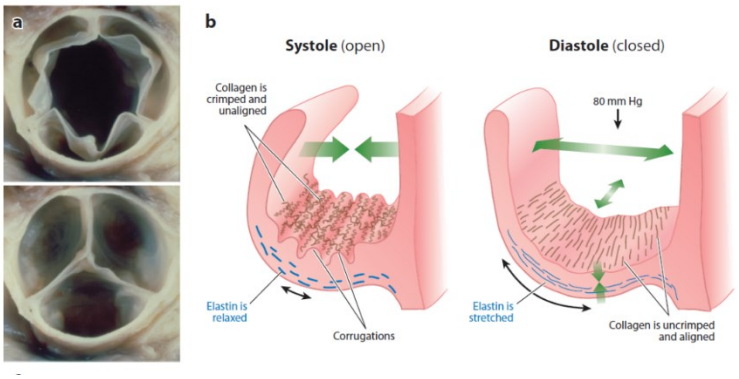

Figure 1.17 (a) Outflow aspect from AR view of AV during systole (top) and diastole (bottom); (b) Schematic representation of aortic leaflet (AL) in cross section during systole and diastole. Adapted from (Schoen 2012).

1.3.4 Pathophysiology of heart valves

Cardiac heart valve pathologies affect mainly aortic and mitral valve, the ones that are subjected to higher pressure and dynamic features during cardiac cycle. Valve dysfunction can be expressed by incompetence/regurgitation (imperfect closure) or stenosis (incomplete opening) of the valve. Still, these complications can be related to congenital, as in the case of bicuspid valve, or acquired causes, as fibrosis, calcification and rheumatic fever (Bateman, Hill et al. 2013). Below are reported the pathophysiology caused by regurgitation, stenosis, bicuspid and myxomatous valve degeneration.

1.3.4.1 Regurgitation

Regurgitation is caused by leaking of heart valves due to the incomplete closure of leaflets, causing heart to overwork to sustain proper blood flow parameters. This results in ventricular hypertrophy, dilatation and associated changes in the ATV and SL valve functions. Dilatation of the AR due to the improper closing of the leaflets of AV is responsible for approximately half of clinical cases of aortic regurgitation, while about one third of the cases are due to congenital bicuspid valve and acquired post-inflammatory responses, with the remaining due to other congenital or endocardial diseases (Bateman, Hill et al. 2013).

1.3.4.2 Stenosis

Stenosis is referred to the narrowing of the valve that causes an incomplete opening of the leaflets. Valve stenosis is usually due to calcific deposits that result in stiffer leaflets with decreased effective valve orifice area. This leads to ventricular hypertrophy to compensate the incomplete open of the valve. Some symptoms can be shortness of breath and generalized weakness due to the reduced blood flow to body and lungs. In the late progression, valve stenosis can cause syncope, angina, sudden cardiac death and chronic heart failure. In general, the most common clinical causes of aortic stenosis are: bicuspid valve with calcium deposits, calcific stenosis and rheumatic valve disease (Figure 1.18) (Bateman, Hill et al. 2013).

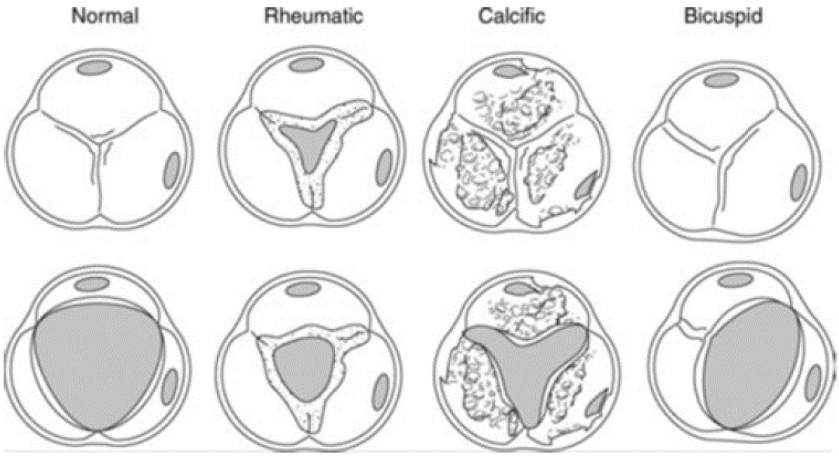

Figure 1.18 Aortic stenosis aetiology: morphology of a normal aortic valve, rheumatic aortic stenosis, calcific aortic stenosis and bicuspid aortic valve. Adapted from (Bateman, Hill et al. 2013).

Valve calcification is characterized as a degenerative and dystrophic mechanism with passive accumulation of hydroxyapatite mineral in dead or damaged cells (Schoen 2012). Calcific deposits usually develop in the attachments of the cusps, place of higher mechanical stress, indicating that mechanical features can potentiate valve calcification.

Rheumatic stenosis is a consequence of acute rheumatic fever, a multisystem inflammatory disease triggered by an autoimmune reaction to a group A streptococcal bacteria. It causes fibrotic thickening of the leaflets. Rheumatic fever is more common in developing countries and in crowded and economically depressed urban areas in the Western world (Schoen 2012).

1.3.4.3 Bicuspid Valve

Bicuspid AV is the most common congenital cardiovascular malformation in humans, with a prevalence of ≈ 1%. Bicuspid AV does not result in major consequences in early life; however, in adult life it can lead to complications such as aortic stenosis or regurgitation, infective endocarditis and aortic dilation. Still, > 67% children and ≈ 50% adults suffer from aortic stenosis related to bicuspid AV (Schoen 2008, Schoen 2012).

1.3.4.4 Myxomatous Valve Degeneration

Myxomatous valve degeneration affects mainly the mitral valve, leading to mitral valve prolapse (MVP). It is characterized by the displacement of mitral valve leaflet(s) into the left atrium during systole. Significant cardiovascular complications are increased by MVP as heart failure, mitral regurgitation, bacterial endocarditis, thromboembolism and atrial fibrillation. Therefore MVP is the most common cause for surgical repair or replacement of the mitral valve (Schoen 2008, Schoen 2012).

The myxomatous degeneration leads to changes in the histology of the normal leaflet. Leaflets present a fibrosa layer with attenuation and/or disorganization of collagen fibres and thickening of spongiosa layer with deposition of myxomatous material rich in proteoglycans (e.g. GAGs). These alterations decrease the stiffness and increase the extensibility of both leaflets and chordae causing mechanical weakening of the valve. Visually, leaflets can present as thick, redundant and with an increased surface area (Grande-Allen, Griffin et al. 2003, Schoen 2012).

1.4 Heart Valve Prostheses

Valvular heart disease is a major health problem worldwide, responsible for high levels of morbidity and deaths. In developing countries, heart valve disease mainly results from persistent burden of rheumatic fever, affecting more paediatric and young patients. Instead, elderly are predominantly affected in industrialized nations by degenerative heart valves pathologies (Weber and Hoerstrup 2011).

As referred, pathophysiology of heart valves is broad and it varies according to the valve that is affected. Still, due to intensive hemodynamic conditions present in systemic circulation, left-sided valves are particularly susceptible to dysfunction. Heart valve disease has a fast progress and may become fatal. The development cannot be prevented by pharmacological treatments since the majority of heart valve disease is irreversible (Simionescu 2006).

Surgical or interventional repair/replacement is the treatment of election for dysfunctional valves. From a clinical point of view and depending on the nature and progression of the pathology, along with patient related factors as age and comorbidities, heart valve repair is preferable to replacement. However, even with the variety of techniques to repair the valves, 70% of diseased valves cannot be repaired. Heart valve replacement is in fact increasing over the years and approximately 290,000 heart valve replacements are performed annually worldwide. This number is expected to triple over the upcoming five decades, having a high social and economic impact (Mol, Smits et al. 2009, Weber and Hoerstrup 2011).

Replacement solutions for diseased heart valves include the use of mechanical prostheses (composed of non-biological material) and bioprostheses (manufactured with biological tissue) implanted via cardiac open heart classic surgery.

1.4.1 Mechanical Prostheses

Mechanical prostheses or mechanical valves offer excellent durability; however, the high risk of thromboembolism events demands use of anticoagulation therapy. Rigid supporting materials and mobile elements are the components of mechanical heart valves. The different designs as a “caged ball” and free-moving tilting discs or flaps with restricted movement allow proper opening and closing of the valves during cyclic blood flow (Figure 1.19 (a) and (b)). The materials used are inert and biocompatible as pyrolytic carbon, polyester (Dacron)-covered polymers and metals. Still, some of these surfaces are not totally antithrombogenic and present non-physiological patterns due to imperfect blood flow through some of the devices that can induce the formation of blood clots. Patients have therefore high risk of haemorrhage complications when

implanted with a mechanical valve due to continuous anticoagulation therapy (Simionescu 2006) (Mol, Smits et al. 2009, Kheradvar, Groves et al. 2014).

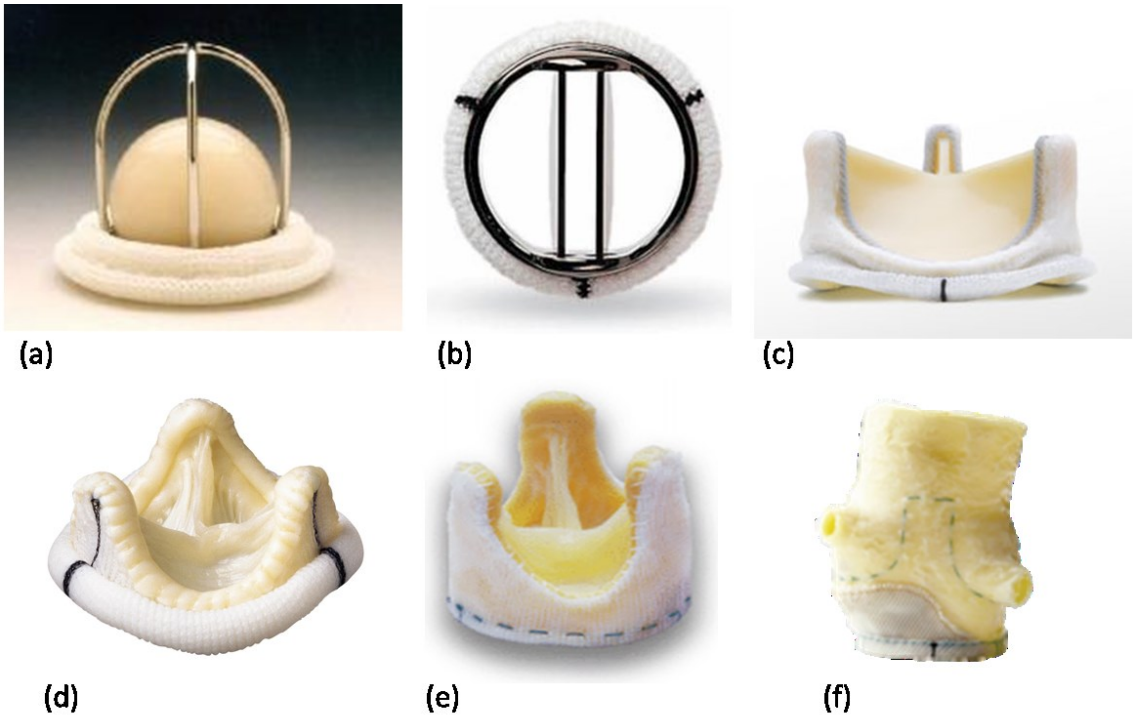

Figure 1.19 Artificial heart valves: mechanical (a) and (b); bioprosthetic (c), (d), (e) and (f); (a) Starr-Edwards Ball Valve®; (b) St Jude Medical® Regent Valve; (c) Carpentier-Edwards PERIMOUNT Magna® Pericardial Bioprosthesis; (d) St Jude Medical® Biocor Aortic; (e) St Jude Medical® Toronto SPV and (f) Edwards Prima Plus® Stentless Bioprosthesis. Adapted from (Simionescu 2006).

1.4.2 Bioprostheses

Cardiac heart valve homografts are cryopreserved donor valves that have been applied in the clinical sector in the last 20 years (de By, Parker et al. 2012) presenting low thrombogenicity and low risk of infection, good mechanical properties and lack of chemical crosslinking that prolongs their lifetime (Mol, Bouten et al. 2004). However, they present disadvantages concerning limited availability and a relative low durability of approximately 15 years. The durability is related with susceptibility of degeneration by calcification or mechanical damage, leading to valve replacement re-interventions (Vesely 2005). Taking this in consideration and associated with the lack of homografts availability due to worldwide shortage of donors, the widespread implementation of

homografts as a cardiac valve replacement concept is limited (Weber and Hoerstrup 2011).

Bioprosthetic heart valves (BHV) can be either from human donors (homografts) or from animal origin (xenografts). They present lower durability when compared with mechanical ones due to their increased risk of calcification and structural degeneration, mainly when implanted in younger patients. For this reason, currently BHV are considered only temporary solution: patients implanted with prosthesis of biological derivation require reoperation within 10-15 years. Indeed, clinical guidelines for implantation of bioprostheses recommend the use of BHV in patients >65 years old. However, the development and research of new design and preservation methods for these prostheses could turn BHV to substitute valves for middle age patients (Mol, Smits et al. 2009, Kheradvar, Groves et al. 2014).

Bioprostheses can be porcine aortic roots or pericardial valves composed of porcine or bovine pericardial sheets. In pericardial valves, pericardium can be mounted on adequate supports - stents - to mimic valve architecture or either manufactured without stent (stentless) (Figure 1.19 (c), (d), (e) and (f)) (Simionescu 2006).

One clinical key pathologic process related to BHV failure is valve calcification. An important step in the pathophysiology of calcification is the presence of devitalized cells and cellular debris in the components of the valve, as the residual devitalized cells resident in the BHV valve after GA treatment. The reaction of calcium-containing extracellular fluid with cell membrane-associated phosphorus represents the mechanism originating calcium phosphate mineral deposits. An accelerated progress of calcification is documented in patients of young age, while valve factors as leaflets GA fixation and increased mechanical stress also play a role. Regulation of inductive and inhibitory factors have been suggested recently to be the putative targets of anti-calcification strategies for the development of new generation BHV, as: binding of calcification inhibitors to GA fixed tissue, modification of GA fixation, removal or modification of components that can lead to calcification and the use of cross linking agents other than GA (Schoen and Levy 2005).

Durability of BHV is increasing due to improvements in stent design and fixative methods. Four major manufacturers of BHV and some examples of their valve replacement solutions are represented in Figure 1.20. The largest product line of bioprosthetic aortic valves (AV) belongs to Edwards Lifesciences. Excellent hemodynamics and durability are outcomes of their bovine pericardial Carpentier-Edwards PERIMOUNT™ Aortic valve. Clinical follow up after valve implantation report that in patients over 60 years of age, 85% were free from valve failure. From Medtronic, stented porcine BHV Hancock II and Mosaic line are implantable in the aortic and mitral positions. Low rates of structural deterioration and low amount of valve related complications were reported for Hancock II, while good durability and hemodynamic were reported for Mosaic, a porcine valve tissue with a flexible stent. Trifecta from St. Jude Medical is composed of pericardial leaflets attached outside of the fatigue resistant titanium stent and a supra-annular sewing ring. It provides large orifice areas and excellent hemodynamic. Sorin Group present several categories of AV: Mitroflow and Soprano Armonia for the stented line and Freedom Solo and Pericarbon Freedom for the stentless line. In a comparison study of Freedom valve with the Carpentier-Edwards PERIMOUNT valve, the Freedom valve implantation provide lower AV gradient immediately post-operatively, at 6 and 12 months (Kheradvar, Groves et al. 2014).

Figure 1.20 Bioprosthetic valves for the major manufacturers: Edwards Lifesciences, Medtronic, St. Jude Medical and Sorin Group. Adapted from (Kheradvar, Groves et al. 2014).

A novel technology that has progressed in the past years consists in the transcatheter aortic valve replacement (TAVR). The innovation of the procedure involves the implantation of a stent-caged bioprosthetic AV through a catheter-based delivery system without requiring open heart surgery. The most promising TAVR valves are depicted in Figure 1.21. The insertion can occur through the apex of the left ventricle, the femoral artery, the subclavian artery or directly through the aorta. Large-scale studies for TAVR implantation include patients with high surgical risk or the ones that cannot undergo surgery. Latest work is also focused on intermediate risk patients. Promising initial results were obtained for therapy treatment of severe aortic stenosis (Kheradvar, Groves et al. 2014).

The current employed BHV, both of human and animal origin, are in summary all presenting shortcomings. As a consequence, tissue engineering (TE) approaches have been taken into account.

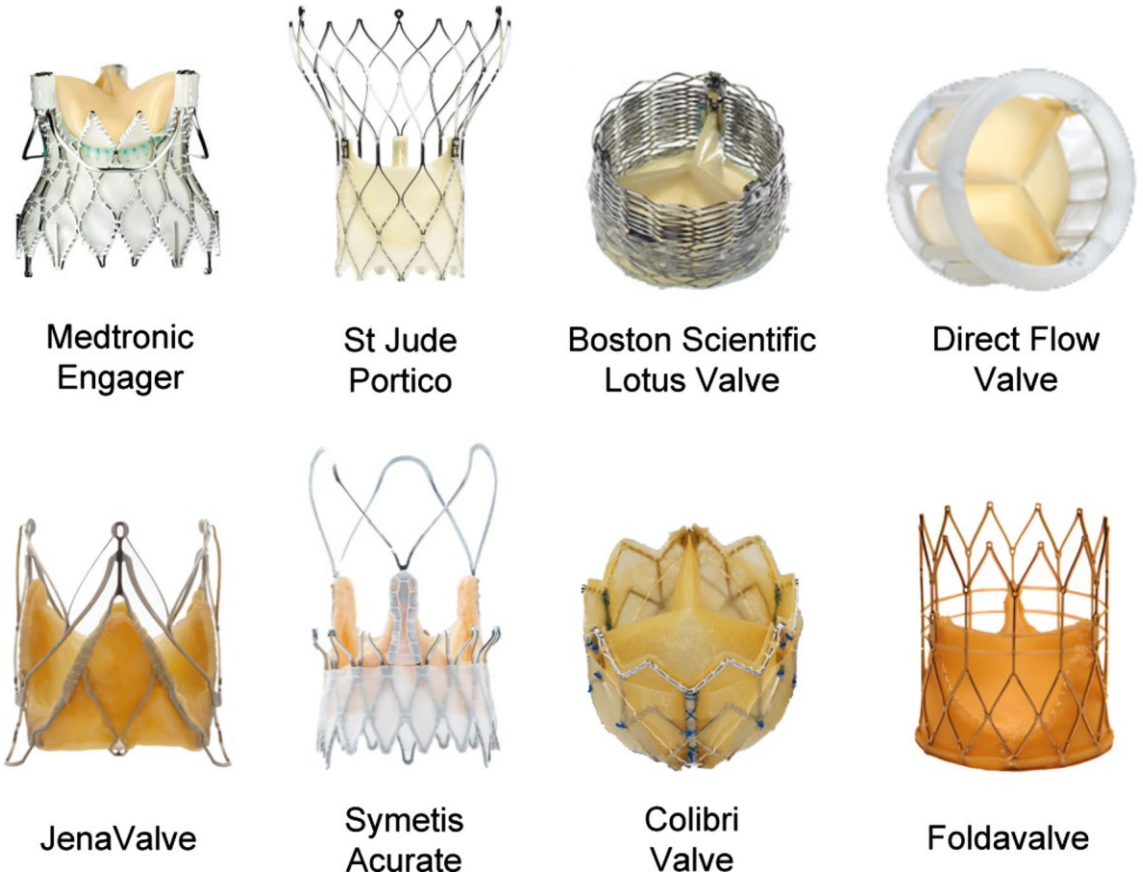

Figure 1.21 TAVR valves developed by several manufacturers. Adapted from (Kheradvar, Groves et al. 2014)

1.5 Scaffolds for Tissue Engineering

The term 'tissue engineering' was first referred by Langer and Vacanti in 1993, as an interdisciplinary field that applies knowledge of both engineering and biology to develop functional substitutes for damaged tissues, providing solutions for tissue creation and repair (Langer and Vacanti 1993). TE approach is based on the growing of living cells (*in vitro* or *in vivo*) in a supporting three-dimensional (3D) structure named scaffold. The scaffold must be biocompatible, enable the proliferation, differentiation and eventually grow into a functional tissue construct (Figure 1.22) (Jana, Tefft et al. 2014).

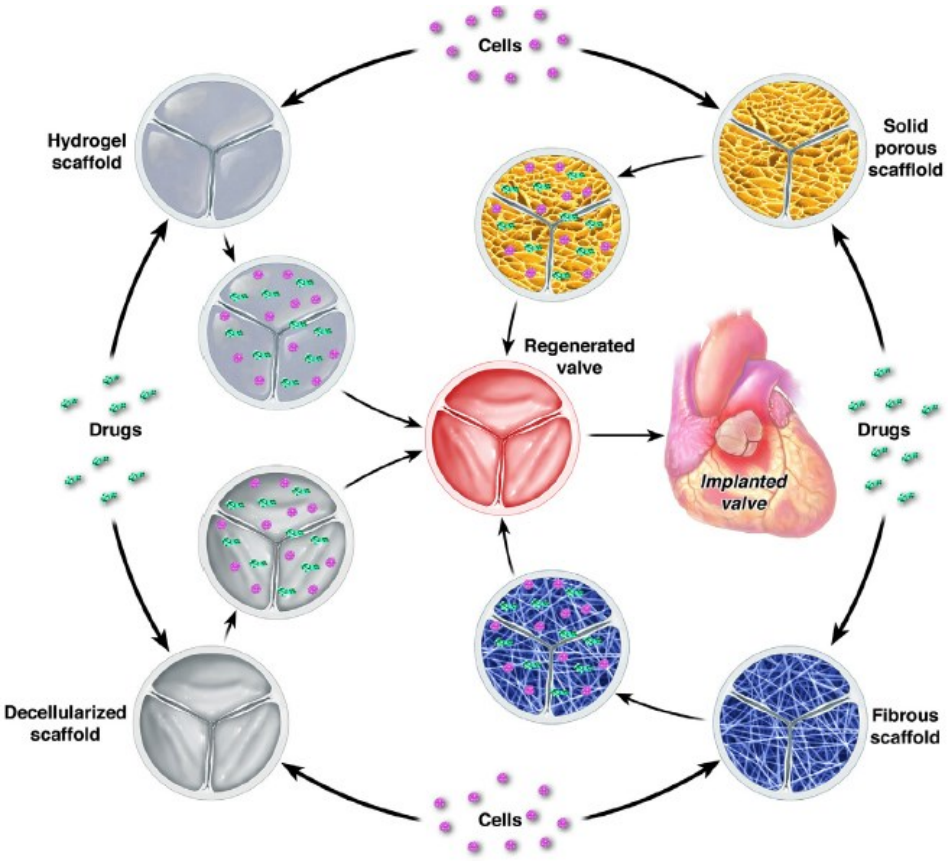

Figure 1.22 Schematic diagram of TE approach for heart valves: tissue culture with several scaffold options to create a regenerated valve viable for implantation. Adapted from (Jana, Tefft et al. 2014).

In general, can be considered two approaches: *in vitro* and *in vivo* TE. *In vitro* TE involves the isolation and expansion of cells from the patient, followed by seeding onto the scaffold and bioreactor conditioning until *in vitro* tissue formation and further implantation in the same patient. On the other hand, *in vivo* TE bypasses the isolation

and seeding of the cells, relying on the regenerative potential of the organism to perform the tissue culture phase *in situ* (Mol, Smits et al. 2009).

The scaffold should possess some important features, as external geometry, surface properties, interface adherence, pore density and size, biocompatibility, degradation, mechanical properties adequate to the purpose and, eventually, be sterile. Tuning and optimization of these parameters plays a major role in the success of tissue viability and functionality post-implantation (Weber and Hoerstrup 2011, Jana, Tefft et al. 2014). For heart valve TE, scaffolds should meet some additional attributes related to resistance to calcification and to thrombosis, due to direct contact with blood (Bouten, Dankers et al. 2011). Also, the hemodynamic pressure and constant flow during cardiac cycle must be considered for the evaluation of material and design selection of scaffold for tissue engineered heart valves (TEHV) retain the proper mechanical function.

As previously described, native heart valves present a complex geometrical and histological structure, challenging to be mimicked during TEHV development. In addition, the ideal prosthetic valve should retain the follow four characteristics: (a) widely available 'off the shelf', (b) regular hemodynamic performance, (c) low risk of calcification, thromboembolism, endocarditis and degeneration and (d) capacity to grow and self-repair. Multiple scaffold design had been developed to obtain a reliable structure of scaffolds to support cell attachment, proliferation and development. The main scaffolds developed so far are based on artificial scaffolds produced from synthetic and natural materials and natural scaffolds based on decellularised tissues from both human and animal origin (Jordan, Williams et al. 2012, Rippel, Ghanbari et al. 2012, Jana, Tefft et al. 2014).

1.5.1 Synthetic Scaffolds

Artificial scaffolds fabrication aims to mimic the structure and function of a heart valve. The common approaches are focused on the use of porous scaffolds, fibrous scaffolds and hydrogels. The advantages of their use include low immunogenicity and thrombogenicity, tailored biodegradability, durability and mechanical properties. As the complex structure and function of a native heart valve is difficult to achieve, variation in

the mechanical properties of fabricated scaffolds are pointed as disadvantages of artificial scaffolds (Dhandayuthapani, Yoshida et al. 2011).

3D porous scaffolds allow a continuous flow of nutrients and metabolic waste due to its interconnected homogeneous pore network and large pore size. This structure promotes growth and vascularization of the scaffold by using also several combinations of synthetic and natural polymers. The most common ones are polyhydroxyalkanoates (PHA), polyglycolic acid (PGA), polylactic acid (PLA), collagen and chitosan. However, pores of irregular size and low interconnectivity are referred as major drawbacks (Mendelson and Schoen 2006).

Fibre aspect of the scaffold and similarities to the ECM structure give characteristics to fibrous scaffolds that promote cell adhesion, migration, proliferation and differentiation. Besides, scaffolds can be conditioned in a bioreactor with cells to improve tissue construct (Figure 1.23). However, a general fibrous and dense structure is still lacking of porosity and mechanical characteristics to be comparable to native heart valves (Hoerstrup, Sodian et al. 2000, Jana, Tefft et al. 2014).

Scaffolds based on hydrogels allow the encapsulation of cells within the network with a high cellular efficiency in TE applications. Hydrogel is a hydrophilic polymeric network with high-water content, which allow permeability of oxygen, nutrients and water-soluble nutrients. The injection of hydrogels through minimally invasive methods, improve cardiac repair by tissue bulking and delivering of bioactive molecules and cells. Weak mechanical properties and absence of a definite structure limit the application of hydrogels as a scaffold for TE of heart valves (Chiu and Radisic 2013).

Figure 1.23 TE heart valve of nonwoven PGA mesh coated with poly-4-hydroxybutyrate after 14 days of conditioning in bioreactor. Adapted from (Hoerstrup, Sodian et al. 2000).

1.5.2 Natural Scaffolds

Natural scaffolds comprise decellularised tissues of human or animal origin and collagen and fibrin based matrices. Even if multi-step static seeding methods have been used in cardiovascular TE, cellular encapsulation in collagen and fibrin gels may be achieved using single step seeding (Mendelson and Schoen 2006).

1.5.2.1 Decellularised Scaffolds

Decellularisation procedure consists on the removal of cells within the tissue while minimizing damages in the original ECM structure to promote subsequent recellularization *in situ*. Besides the native-like geometry, architecture as well as hemodynamic and biomechanical properties are still preserved when compared to the native counterparts. Complete cell removal is essential to minimize immunological response, disease transmission, calcification and thromboembolism. Depending on the decellularisation method applied, the efficiency of cell removal and matrix integrity can be variable (Mendelson and Schoen 2006, Jashari, Faucon et al. 2011, Weber and Hoerstrup 2011).

Scaffolds to be decellularised can be collected from ether human donors (homografts) or animal tissues (xenografts). The tissues from human origin are less antigenic when compared with xenogeneic counterparts; however, homografts present limited availability. Although the development of decellularisation procedures specifically tailored for xenogeneic tissues represents an enormous challenge in terms of

biocompatibility and lack of immunogenicity, tissues from porcine, bovine and sheep origin are the main source of acellular heart valves (Vesely 2005, Jana, Tefft et al. 2014).

The development of tissue engineered valves relying on decellularised scaffolds is addressed to take advantage of the original structure and relies on the maintenance of ECM integrity, avoiding the design of a complex structure for a heart valve as in the case of synthetic scaffolds. ECM can be defined as nature's ideal biologic scaffold material, consisting on a unique, tissue-specific 3D architecture. The ECM composition and structure comprises a complex combination of structural and functional proteins, as collagen, GAGs, elastin, fibronectin, laminin, growth factors and cytokines (Srokowski and Woodhouse 2011, Jana, Tefft et al. 2014). Decellularisation techniques are aimed to eliminate the cell population from the tissue while preserving the ECM characteristic that sustain the functionality, the growth and the homeostasis of the tissues.

1.5.2.2 Decellularisation Techniques

Several decellularisation methodologies have been investigated. Single agents or a combination of agents can be employed, presenting advantages and disadvantages in their application. Methodologies comprising combinations of physical, chemical and enzymatic treatments are more robust and effective in decellularisation protocols (Srokowski and Woodhouse 2011, Keane, Swinehart et al. 2015).

Physical methods as lyophilisation, sonication, freeze-thawing, direct pressure and agitation can provide a direct and rapid decellularisation. In these methods, cell lysis and removal from the tissue is obtained by disruption of cell plasma membrane. Still, in order to increase the efficiency of the decellularisation, chemical treatments are often necessary (Srokowski and Woodhouse 2011).

Chemical methods are based on the use of chemical reagents to remove cellular elements. The selection of the reagents to use is based on the tissue to be decellularised, by focusing on the conservation of the ECM structure and components while all cell components are eliminated. Also, a combination of chemical treatments can be studied to optimize the decellularisation procedure for the tissue in investigation (Srokowski and Woodhouse 2011). Passive diffusion with chemicals followed by several washing steps to remove cell debris and chemical compounds are the usual procedures. Additionally,

factors as composition, thickness and architecture of the tissue must be taken into consideration to select the volume of reagents to use, optimal speed and length of agitation (Keane, Swinehart et al. 2015). For thick tissues, perfusion and convective flow are currently used and reported as an effective decellularisation procedure, as example the cases of human placenta (Flynn, Semple et al. 2006), whole rat heart (Ott, Matthiesen et al. 2008), rat lungs, liver and kidney (Keane, Swinehart et al. 2015).

Solvent extraction is one of the chemical methods that act mainly in the extraction of membrane-bound lipids, as well as removal residual nuclei acids from the tissue. Some examples are ethanol, methanol and butanol (Keane, Swinehart et al. 2015). Tri(*n*-butyl)phosphate (TnBP) is an organic solvent able to disrupt protein-protein interactions, however has also been applied in some decellularisation protocols providing similar results in cell removal ability as sodium dodecyl sulphate (SDS) (Cartmell and Dunn 2000, Woods and Gratzer 2005).

Acid and basic solutions treatments promote the removal of nucleic acids due to disruption of cellular membranes as well as solubilisation of cytoplasmic components of the cells. Alkaline sodium, potassium or calcium salts are used in basic treatments, while acetic acid, PAA, hydrochloric acid (HCl) and sulphuric acid are some examples for acidic treatments (Srokowski and Woodhouse 2011). PAA based treatments are also referred as having a disinfectant potential due to its ability to penetrate into microorganisms and oxidize microbial enzymes (Pruss, Gobel et al. 2003). Still, the use of these treatments is reported to be deleterious for ECM structures, mainly collagen (Dong, Wei et al. 2009).

The utilization of detergents in decellularisation protocols represents the most common treatment. Detergents are water soluble molecules, able to solubilize the lipid membrane of cells by incorporation. Lipid-lipid and lipid-protein interactions are disrupted depending on the detergents used. Non-ionic, ionic, cationic and zwitterionic are the detergents referred for decellularisation techniques (Ingham, Fisher et al. 2008, Srokowski and Woodhouse 2011). Specific characteristics of each detergent such as size, charge and denaturation potential will influence membrane disruption, tissue penetration and interaction with proteins, ultimately having different effects on ECM

structure and biomolecules. The selection of a single or a combination of detergent treatment determines the effectiveness of the decellularisation methodology.

Non-ionic detergents are considered gentle detergents since are able to disrupt lipid-lipid and protein-lipid but not protein-protein interactions. Some examples are Triton X-100 (octylphenol ethoxylate), Tween 20 and Tween 80. On the other hand, ionic detergents are stronger, able to completely disrupt cell membranes and denatured proteins. SDS, sodium deoxycholate and Triton X-200 are ionic detergents commonly used in decellularisation protocols. Zwitterionic detergents present properties of both ionic and non-ionic detergents, more prone to denature proteins when compared to non-ionic ones. They allow the protection of proteins due to net zero electrical charge of hydrophilic groups. Examples include 3-[3-cholamidopropyl)dimethylammonio]-1-propanesulfonate (CHAPS), sulfobetaine-10 (SB-10) and -16 (SB-16) (Ingham, Fisher et al. 2008, Srokowski and Woodhouse 2011, Keane, Swinehart et al. 2015).

An osmotic shock with use of hypotonic and hypertonic solutions can also be included in the decellularisation protocol. Hypotonic solutions will cause cells to swell and burst for high water intake and consequent detergent treatment will also enter in the cellular membrane. The contrary occur in a hypertonic medium: water move outward and cells dehydrate and shrink which aid in cellular death and detachment from ECM. Despite effective cell lysis, residual nucleic acids can remain in the matrix and additional processing such as enzyme digestion are thus required (Ingham, Fisher et al. 2008, Srokowski and Woodhouse 2011).

Enzymatic treatments are included in decellularisation treatments to aid the removal of cellular nuclei residues and proteins. This treatment involves the use of proteases such as trypsin and dispase or nucleases as DNase and RNase. Trypsin detaches cells from tissue surface by disrupting cell adherent proteins on the carboxyl side of the amino acids arginine or lysine. It can damage the collagen matrix if employed with long exposure times, however is effective as a decellularisation adjuvant (Meyer, Chiu et al. 2006). Nucleases are endonucleases capable of hydrolyse deoxyribonucleotide (DNase) and ribonucleotide chains (RNase). They help in the removal of residual DNA when

detergent and chemical treatments are not sufficient to remove nuclear debris (Keane, Swinehart et al. 2015).

Also, chelating agents such as ethylenediaminetetraacetic acid (EDTA) as well as protease inhibitors (PI) can be incorporated in the decellularisation procedure. EDTA can inactivate intracellular proteases capable of degrade ECM components by binding divalent metal cations such as Ca^{2+} and Mg^{2+} at cell-adhesion sites of the ECM. On the other hand, the presence of released proteases from cell disruption during the chemical treatments can damage the ECM ultrastructure. For this, the use of PI such as phenylmethylsulfonylfluoride (PMSF), aprotinin and leupeptin can limit the activity of the proteases (Misfeld and Sievers 2007).

A combination of agents in contrast with a single treatment has been demonstrated to present advantages. In general, the following serial steps are part of a typical decellularisation protocol: (1) physical treatment or ionic solutions to lyse cell membrane, (2) enzymatic treatment to separate cellular components from ECM, (3) detergent treatment to solubilize cytoplasmic and nuclear cell components and, to finalize (4) rising to remove cell remnants from ECM (Srokowski and Woodhouse 2011). Still, decellularisation approaches must be optimized for each tissue. Analyses of the effects on the composition, architecture and function of decellularised ECM will allow the correct selection of concentration and duration of each treatment.

1.5.2.3 Decellularised Heart Valve Scaffolds

The decellularised heart valve scaffolds have been studied as a possible alternative to the heart valve scaffold replacement. Studies have focused on the evaluation and performance of the scaffolds *in vitro* and *in vivo*, with and without cell seeding.

Cell seeding and *in vitro* culturing of cell seeded scaffolds of decellularised heart valve allow endothelialisation of the scaffolds as demonstrated by Schenke-Layland et al., where enzymatically-decellularised porcine PV were successfully reseeded in a hydrodynamic bioreactor with ovine cells and a complete preservation of the ECM integrity was observed (Schenke-Layland 2003).

Further studies foreseen the TE of heart valves repopulated with patient autologous cells as human endothelial cells and human mesenchymal progenitor cells were effectively seeded on decellularised porcine AV (Bader, Schilling et al. 1998) and (Knight, Booth et al. 2005).

Research in cell conditioning with autologous myofibroblasts and endothelial cells followed by implantation in sheep in pulmonary position demonstrated *in vivo* reconstitution of viable heart valve tissue (Steinhoff, Stock et al. 2000).

However, Dohmen et al. evaluate the need of *in vitro* cell seeding on decellularised scaffolds. After implantation of cell seeded and decellularised scaffolds in sheep model, the study conclude that *in vitro* cell conditioning of the scaffolds might not be necessary (Dohmen, da Costa et al. 2006). Indeed, non-preconditioned decellularised porcine AV implanted in a large animal model demonstrate long durability and grow potential after long-term implantation, as demonstrated by Iop et al. (Iop, Bonetti et al. 2014). Besides, repopulation by endothelial and interstitial cells was observed in decellularised heart valve implanted in aortic position in juvenile sheep when compared to non-treated valves (Baraki, Tudorache et al. 2009).

Further studies by Hopkins et al. test the effect of decellularisation after cryopreservation in heart valve performance in juvenile sheep. They demonstrate that decellularisation reduces calcification and promotes durability and functionality of heart valve scaffolds (Hopkins, Jones et al. 2009).

The potential of *in vitro* colonization of hBM-MSC on both porcine and human decellularised valves was demonstrated by Iop et al. (Iop, Renier et al. 2009). *In vivo*, the capacity of matrix-guided regeneration by cell repopulation of valvular matrix after implantation of decellularised pulmonary heart valve allografts in elderly sheep was studied by Theodoridis et al. (Theodoridis, Tudorache et al. 2015).

1.5.2.4 Decellularised Pericardial Scaffolds

Xenogeneic pericardia present good biological and mechanical properties. Currently they are employed for construction of BHV as well as cardiac patches, vascular stents

and staple line reinforcement in cardiovascular and lung surgery (Mavrilas, Sinouris et al. 2005). The development of new pericardium-based BHV for transcatheter implantation is based on the use of porcine and bovine pericardia. BHV manufacturer's preference for these tissues rely on their availability and rigorous quality control of producing farms (Gauvin, Marinov et al. 2013). A further advantage of pericardial scaffolds is the amenability, since there are no anatomic restrictions as the ones associated with homograft valves geometry. Despite the properties of the pericardium currently applied for the construction of the BHV, failure is caused by calcification and mechanical induced fatigue damage, having a limited durability of an average 10-15 years (Mirnajafi, Raymer et al. 2005).

Indeed, bioprostheses for heart valve replacement are composed mainly by GA fixed porcine and bovine pericardium sheets. Fixation with GA improves biomechanical performance of the tissue and reduce biodegradability, while masking immunogenic epitopes that can cause severe immune rejection. However, GA treatment has been associated with acceleration of calcification processes and cytotoxic effects are related with residues of GA in the tissue that prevent cell attachment, migration and proliferation. The cross-linking of the tissue also reduces the ability of regeneration *in vivo*. This drawbacks lead to a long-term failure of GA-fixed pericardial scaffolds (Rémi, Khelil et al. 2011).

Porcine pericardium has the major advantage of lower thickness, while for bovine tissue is pointed the good mechanical properties. Bovine pericardium matrix is composed by 90% of collagen type I, GAGs, proteoglycans, cells and interstitial fluid. An amorphous matrix with collagen fibres and elastin can be observed histologically, while mechanically is characterized by a non-linear and anisotropic behaviour. Porcine pericardium is composed mainly of collagenous proteins, proteoglycans and structural glycoproteins (Aguiari, Fiorese et al. 2016). The clinical application of pericardial scaffolds is mainly in the cardiovascular field as vascular grafts and heart valves (Schmidt and Baier 2000) (Matsagas, Bali et al. 2006) (Vesely 2005). Pericardial patches have also been used for abdominal (D'Ambra, Berti et al. 2012) and vaginal wall reparation (Lazarou, Powers et al. 2005) and tracheoplasty (Dodge-Khatami, Tsang et al. 2000). In Table 1.1 are listed some of the applications of pericardium.

In summary, bovine and porcine pericardial tissues possess the characteristics to manufacture BHV as well as other tissues for applications in the cardiovascular and clinical field. However, the risk of zoonosis is still present. In bovine tissues, questions were raised related with the possible risk of patients developing Creutzfeldt-Jakob disease after implantation of these tissues (Prusiner 1998). Harvesting of material from farms located in “prion free” countries and with rigorous regulations will avoid contaminations from this disease. Furthermore, an open issue is remaining: the durability of devices made from bovine and porcine scaffolds. The durability is dependent on the processing of the tissues as fixation, anticalcification treatments, sterilisation and preservation, that are usually trade secrets of companies (Gauvin, Marinov et al. 2013). Decellularised pericardium demonstrate to maintain mechanical properties, as well as major components of its ECM such as collagen and proteoglycans as GAGs essential for cell attachment and proliferation (Cigliano, Gandaglia et al. 2012) (Rémi, Khelil et al. 2011, Aguiari, Fiorese et al. 2016).

Table 1.1 Applications of pericardial tissues for medical devices. Adapted from (Rémi, Khelil et al. 2011)

Pericardium source	Surgical fields	Product	Company
Bovine or porcine	Soft tissue repair Hernia repair Abdominal & thoracic wall defects	-Peripatch® Implantable surgical tissue -TutoMesh®	Neovasc, Maverick Biosciences PTY Limited, Tutogen medical GmbH, RTI Biologics, Med&Care, Biovascular Inc, Novomedics
	Strip reinforcement	-Veritas Peristrips® Dry	Synovis Life Technology
	Orbital repair	-Tutopatch® -Ocugard®	Tutogen medical GmbH, RTI Biologics, Med&Care, Biovascular Inc, Novomedics
	Dural repair	-Lyolem ®r All BP	National tissue Bank Malaysia
	Perivascular Patch	-Peripatch® biologic vascular patch	Neovac
	Cardiac reconstruction and repair	-Peripatch® Implantable Surgical Tissue	Neovasc, Maverick Biosciences PTY Limited
	Heart valve replacement	-PercevalS® aortic valve -Mitroflow® pericardial aortic valve -Freedom solo® -Carpentier-Edwards PERIMOUNT® Magna EaseAortic Heart Valve -Carpentier-Edwards PERIMOUNT® Magna Mitral Ease Heart Valve -Carpentier-Edwards PERIMOUNT® Theon Aortic Heart Valve -Carpentier-Edwards PERIMOUNT® Theon Mitral Replacement System	Sorin group " " Edwards Life Sciences " " "
Equine	Tendon repair	-OrthADAPT®	Synovis Life Technologies Inc
Human	Valvuloplasty Heart valve	-Xeno or (tissue bank) or autologous grafts	Lausberg et al, 2006 Mirsadaee et al, 2006

1.6 Heart Valve Tissue Banking

Currently, the heart valves stored in tissue banks are cryopreserved homografts from human donors with an age range from new-borns till around 65 years old. In an overview of European Homograft Bank (EHB) activity during 20 years, 8.911 donor valves were evaluated and only 5.258 valves (1.996 aortic, 3.189 pulmonary and 73 mitral) were cryopreserved and stored. From these, 4.516 valves (1.391 aortic, 2.620 pulmonary and 48 mitral) were implanted (Jashari, Goffin et al. 2010).

According to EHB regulations, tissue donors range from heart-beating multi-organ donors (MOD), recipients of heart transplantation (RHT) and non-heart-beating deceased persons (NBHD) (cadavers). The donor medical status is reviewed and several diseases and/or contaminations are exclusion criteria for the donors of the cardiovascular tissues. Screening is focused on transmissible diseases such as HIV (human immunodeficiency virus), AIDS (acquired immune deficiency syndrome), hepatitis B/C, syphilis, enteroviruses, Q fever, malaria, active infection, cancer and West Nile virus among others. Tissue morphology is verified for any malformation, dilatation, atheroma and/or calcification sites. Cardio-vascular or transplant surgeons are responsible for tissue procurement, performed in sterile conditions for the first two tissue donors (MOD and RHT) and clean conditions for the cadaver donors (NBHD). Tissue is transported in sterile triple bag to the tissue bank filled with transporting solution (tissue culture medium (TCM-199), Ringer or saline 0.9% solution) in a box maintained between +2 °C and +8 °C with wet ice. In the tissue bank, two consecutive and independent sets of dissection, morphological evaluation and measurements of valve diameter and length of arterial conduit are performed in sterile conditions. The selected tissues are then incubated in antibiotics cocktail (depending on the tissue bank, the treatment can have a duration between 18-72 h in different formulations of antibiotics cocktail) and then processed for cryopreservation. Following the decontamination with antibiotic cocktails, the valves are cryopreserved with liquid nitrogen to -100 °C. The tissues are then stored in liquid nitrogen vapours below -150 °C for a maximum of 5 years (Jashari, Goffin et al. 2010, Heng, Albrecht et al. 2013). Once cryopreserved, virologic, bacteriologic and histological assessment of the samples

collected from both the patient and the homograft are performed. Donor blood is screened for hepatitis B and C, HIV, HTLV (human T-cell lymphotropic virus), syphilis, malaria, viral myocarditis, enteroviruses and active tuberculosis. The regular microbiological (aerobic and anaerobic bacteria, as well as yeasts and fungi) examination is performed in three solutions employed in the procedure: transport, decontamination and preservation solutions. Finally, histological examination of selected sections of myocardium, aortic and pulmonary trunk and posterior mitral leaflet are performed to quality evaluation and to exclude any disease or evaluate possible infections of the homograft. The tissue approved for implantation is transported to the implantation centre at low temperatures (dry ice at -76 °C or dry shipper at -150 °C) (Jashari, Van Hoeck et al. 2004, Jashari, Goffin et al. 2010, van Kats, van Tricht et al. 2010, de By, Parker et al. 2012).

In heart valve banks, 15% of tissues are rejected due to contamination or are not appropriate for clinical use (Table 1.2) (de By, Parker et al. 2012, Heng, Albrecht et al. 2013). Other reasons for discarding homografts are their unsuitable morphology and positive serology from the donor. In addition, during processing of the biological material, tissues can be contaminated by external factors (Tabaku, Jashari et al. 2004, Eastlund 2006). Indeed, a high rate of contamination in post-mortem retrieval of valves was observed (54%) when compared to multi organ donors (12%) (Gall, Smith et al. 1995). In a recent report by Germain et al. where bioburden analysis performed in cardiac valves determined that *Staphylococci*, *Propionibacterium*, *Streptococci* and *Escherichia coli* were the most commonly contamination bacteria while *Candida* species was the predominant fungi (Germain, Strong et al. 2016).

Table 1.2 Heart valve discards in cardiovascular banks. Adapted from (de By, Parker et al. 2012).

Heart valve discards in 2010, average % of all cardiovascular banks		
Not selected because of:		**% of received hearts**
Medical history		32.7
Serology		4.2
Microbiology	Bacteria	10.7
	Multi resistant bacteria	0.4
	Fungi	3.2
	Not specified	0.1
	Suspected	0.35
	Total microbiology	5.9
Morphology		35.8
Technical		7.3
Other or unknown reasons		7.8

The decontamination methodologies applied in the 17 European cardiovascular tissue banks are variable in terms of decontamination cocktail formulation: 25 antibacterial and antifungal compounds have been reported (de By, Parker et al. 2012). Furthermore, substantial differences were observed for incubation time, a range of 5-72 h and temperature, from 4 °C to 37 °C. However, a study by Germain et al. demonstrate that bioburden reduction was more effective if incubation with antibiotics cocktail was performed at 37 °C (Germain, Thibault et al. 2010).

Among the antibiotic and antimycotic formulations and spectra of activity, the most common ones contained: vancomycin, β-lactams, polymyxin, gentamicin and Amphotericin B. Vancomycin acts specifically against Gram-positive bacteria, β-lactams (e.g. Cefoxitin) have a broad spectrum (Gram-positive and –negative as well as anaerobic bacteria), polymyxin for Gram-negative, gentamicin with broad activity of both Gram-positive and –negative and, finally, antifungal for contaminants as *Candida* and *Aspergillus* spp. (Pitt, Tidey et al. 2014). The use of amphotericin B in the disinfection cocktail was discontinued in some tissue banks after reports of damages in cells and tissue viability were presented (Brockbank and Dawson 1993) (Villalba, Alonso et al. 1995) (Heng, Albrecht et al. 2013).

Other tissues besides heart valve homografts processed by tissue banks were referred: arteries, veins and pericardium. The request of arterial grafts is increasing and also veins

requested for shunts in access surgery and pericardium applied in cardiothoracic operations as patching material for bridge of larger gaps (de By, Parker et al. 2012).

Tissue disinfection and sterilisation are mandatory to improve the safety of both homografts and xenografts to avoid the risk of infectious diseases transmission compromising their application (Eastlund 2006, Heng, Albrecht et al. 2013).

Different disinfection and sterilisation techniques have been used in the field of tissue banking, but the bulk information is currently concerning only effectiveness and consequences associated with storage of native human tissues. A small number of reports have focused on decellularised human and animal tissues and few studies have been reported on decellularised animal heart valves and pericardium. Clinical application of new tissue-engineered scaffolds, especially of xenogeneic origin, requires optimized and rigorous methods (Gilbert, Sellaro et al. 2006, Schmidt, Stock et al. 2007, Delmo Walter, de By et al. 2012).

1.7 Disinfection & Sterilisation Methodologies

1.7.1 Disinfection

Disinfection procedures generally applied for medical devices in contact with mucous membranes or skin aim to reduce the bioburden present in materials, but are ineffective in completely eliminate all microbial forms, as bacterial spores (Qiu, Sun et al. 2011, Rutala and Weber 2013). Methods commonly applied in clinical practice include different cocktails of high-spectrum AA to inactivate the majority of contaminants present in the tissues. For heart valves stored in tissue banks, vancomycin, gentamicin, cefoxitin and amphotericin B are the most commonly used for the decontamination of homografts (Table 1.3) (Heng, Albrecht et al. 2013).

Table 1.3 Types and concentration range of AA used in tissue banks. Adapted from (Heng, Albrecht et al. 2013).

Antibiotics & Antimycotics	**Action**	**Concentration (µg/mL)**
Vancomycin	$Gram^+$ Bacteria	50-500
Gentamicin	$Gram^-$ Bacteria	18-4000
Cefoxitin	$Gram^+$, $Gram^-$ and Anaerobe Bacteria	240
Amphotericin B	Fungi	2.5-50

Antibiotics act on microorganisms by inducing cell death (bactericidal drugs) or by inhibiting cell proliferation (bacteriostatic drugs). Both types operate by inhibiting DNA and RNA synthesis, damaging cell wall integrity or affecting protein synthesis by microorganisms (Kohanski, Dwyer et al. 2010).

Despite the effectiveness and their null effect on the original tissue structure (Gilbert, Sellaro et al. 2006) and function, a critical point in the utilization of antibiotic and antimycotic cocktails is represented by the remaining of potentially toxic chemical residues inside the treated scaffolds (Leeming, Lovering et al. 2005).

1.7.2 Sterilisation

Differently form disinfection, terminal sterilisation provides complete elimination of any microorganisms, including highly resistant bacterial endospores (Qiu, Sun et al. 2011). It represents a mandatory procedure for medical devices since any microbial contamination could potentially result in disease transmission (Rutala and Weber 2013). The effectiveness of a sterilisation process is measured by the sterility assurance level (SAL), which is the probability of a single unit of being non-sterile. For medical devices, SAL should be particularly low (10^{-6} - a chance of one in a million to be not sterile). For biological tissues, since some sterilisation procedures can be harsh and affect their functionality, an higher SAL (10^{-3}) is considered as an adequate sterility level (Qiu, Sun et al. 2011). In fact, most of sterilisation procedures can potentially cause a significant change in the physical and mechanical properties as well as in the structure of the materials, compromising their performance and safety (Matuska and McFetridge 2015).

Sterilisation procedures should also be tailored in order to fulfil the requirements of standards and guidance documents reported for specific sterilisation procedures in European Pharmacopeia, European Agency, Food and Drug Administration (FDA) and ISO (International Organization for Standardization) Standards.

The sterility test of the materials treated with a sterilisation technique permit the evaluation of the effectiveness of the treatment in that material. Furthermore, it is also important the qualification and quantification of the contaminants in the test material since the sterilisation procedure can be tailored specifically according to the microorganisms present in the scaffold (bioburden). Sterility assessment can be tested following European Pharmacopoeia guidelines: 2.6 Biological Tests – 2.6.1 Sterility (Commission 2005). In this test, the sample or the rising solution of the sample are inoculated in two different media (Thioglycolate medium or soya-bean casein digest medium), that promote microorganism growth. If no grow of microorganisms is observed after 14 days of incubation, the sample in test is sterile, otherwise if the medium reveals turbid, the sample is contaminated. For quantification of microorganisms, the MPN method can be applied. This method enable the estimation of the bioburden concentration present in the material using a sample of the rising solution. It is a rapid method, since it does not require counting of colony forming units (CFU) in agar plates. The test is performed by making replicates of the liquid broth in serial ten-fold dilutions. After incubation and record of contaminated/non-contaminated samples, the bioburden concentration is estimated (Sutton 2010). Regarding identification of microorganisms, a simple and reproducible technique can be applied: MALDI-TOF mass spectrometry. This technique is accurate, rapid and permit the identification of bacteria, fungi and mycobacteria in the microbiology field. Commercial databases and interpretive algorithms enable the identification of a wide spectrum of clinically significant microorganisms (Murray 2012).

Terminal sterilisation methods consist mainly of physical and chemical treatments. Physical methods can include the use of ionizing radiation, such as γ-irradiation and E-beam, which act by emission of high-energy photons and electrons that act on the DNA of microorganisms. Chemical methods comprise the use of sterilant solutions, such as PAA, or gases, as ethylene oxide, supercritical CO_2 and gas-plasma treatment. The

procedure comprising these treatments require optimisation in terms of sterilant agent concentration, temperature and pressure, in order to achieve the complete elimination of microorganisms (Qiu, Sun et al. 2011).

1.7.2.1 Peracetic Acid

PAA is a strong oxidizing agent, possessing bactericidal, fungicidal, virucidal and sporicidal properties. PAA allows the elimination of several microorganisms, such as vegetative bacterial cells, endospores, yeasts and mould spores, through the oxidation of their cell membrane or capsid. The rapid penetration of PAA into the microorganisms together with its oxidizing potential, are linked to the PAA sterilisation efficiency (Qiu, Sun et al. 2011). Treatment with PAA has been reported to be compatible with biological tissues, such as skin grafts (Lomas, Huang et al. 2004), tendon grafts (Zhou, Zhang et al. 2014) and small intestine submucosa (SIS) (Freytes, Badylak et al. 2004). Toxic residues are less problematic compared to other treatments, since PAA degrades rapidly into acetic acid, oxygen and water (Qiu, Sun et al. 2011, Delgado, Pandit et al. 2014). Effective sterilisation was achieved in PAA-treated decellularised tendon grafts, with no observable cytotoxic response (Huang, Ingham et al. 2013). Moreover, PAA treatment has been combined with ethanol for skin (Rossner, Smith et al. 2011), bone (Pruss, Gobel et al. 2003) and bladder (Rosario, Reilly et al. 2008) sterilisation. Further studies have focused on the effectiveness and the possible detrimental effects in ECM structure and biocompatibility of soft tissues after treatment with PAA.

A report by Farrington et al. evaluate six treatments on ovine valves: heat, PAA (0.35% and 0.21%), chlorine oxide, a surfactant cleaning agent and a solvent/detergent. PAA 0.21% treatment for 20 minutes provided satisfactory microbial action and no effects on extensibility and minor effects on the elasticity of the valves were observed (Farrington, Wreghitt et al. 2002).

Another study by Lomas et al. treated cryopreserved skin allografts with PAA to achieve high disinfection and tissues were then preserved in high concentration of glycerol or propylene glycol. PAA treatment did not render the grafts cytotoxic and pro-inflammatory (Lomas, Huang et al. 2004).

No pro-inflammatory response and no effects in Young's modulus and ultimate tensile stress were reported by Lomas et al. after treatment with 0.1% PAA in tendons (Lomas, Jennings et al. 2004). Further studies by Huang et al. in decellularised and PAA 0.1% treated tendon scaffolds demonstrated no contact cytotoxicity and no significant denatured collagen increase, while collagen waveform was slightly loosened (Huang, Ingham et al. 2013).

Structure of polymeric scaffolds (poly(D-L lactic-co-glycolic acid) was observed after several sterilisation treatments (ethanol, PAA, UV irradiation and antibiotic solution) by Shearer et al.. Results revealed deformations on the scaffold surface after SEM analysis, whereas little change was observed in breaking stress and insignificant reduction in Young's modulus of PAA and antibiotics treated scaffolds (Shearer, Ellis et al. 2006).

1.7.2.2 γ–Irradiation

γ–irradiation is the most reliable sterilisation method to date due to its high efficiency and the lack of chemical residues and radioactivity that can cause cytotoxicity. In wet specimens, such as biological tissues, γ–irradiation from ^{60}Cobalt source splits polypeptide chains that cause release of free radicals via radiolysis of the water molecules. In addition, this method can be performed with the material in its final packaging representing an advantage for medical materials and devices (Lambert, Mendelson et al. 2011). Nevertheless, it triggers cross-linking reactions in the collagen molecules of the tissue (Nguyen, Morgan et al. 2007, Delgado, Pandit et al. 2014), leading to structural damages and alterations in the biomechanical properties of different tissues, such as tendon allografts (Conrad, Rappe et al. 2013) and bovine pericardium (Hafeez, Zuki et al. 2005). Several studies have been focused on the detrimental effects of γ–irradiation treatment in biological scaffolds.

Decellularised heart valves treated with dosages of 1, 3 and 10 kGy, were reported to present contaminants in the ones treated with low-dosage (1kGy) and decreased strength was observed with increase of radiation (Helder, Hennessy et al. 2016).

γ-irradiation treatment in acellular human tissue matrix cause ECM structural damages as collagen condensation and fragmentation of collagen fibres, while tensile strength and elasticity were also reduced with the increasing of the dosage. However, it did not affect *in vitro* proliferation of fibroblast cells (Gouk, Lim et al. 2008) (Sun and Leung 2008). Allograft tendon treated with 50 kGy was reported to maintain mechanical properties similar to the ones treated with 18 kGy (Grieb, Forng et al. 2006), while strength and stability were reported to increase in 50 kGy treated tendons (Seto, Gatt et al. 2013)

Degradation in collagen bone allografts was observed and decreased mechanical properties were reported for cortical bone above 25 kGy treatment and above 60 kGy for cancellous one. Also, osteoclast activity was reduced when cultured in irradiated bone slices and bacterial products remain after irradiation cause inflammatory bone resorption after macrophage activation (Nguyen, Morgan et al. 2007).

Terminal sterilisation with γ–irradiation is recommended to be performed at a minimum dose of 25 kGy. Although this dosage represents the 'gold standard' for treatment of tissues as bone, cartilage, tendons pericardium, skin and acellular dermis, high dosages of γ-irradiation can evoke several chemical and physical changes that affect the biological quality of tissue allografts, as previously referred. For this reason and to match quality assurance standards and validation procedures, the standard dosage should be reduced, while maintaining a SAL of 10^{-6} (Nguyen, Morgan et al. 2007) (Dziedzic-Goclawska, Kaminski et al. 2005). Reports on bone allografts treated with a lower dose revealed the achievement of the required SAL, whilst maintaining mechanical integrity and biocompatibility (Balsly, Cotter et al. 2008, Nguyen, Morgan et al. 2011, Nguyen, Cassady et al. 2013).

1.7.2.3 Ethylene Oxide

Ethylene oxide (EtO) is a low-temperature sterilant gas that affects the normal cellular metabolism and replication of microorganisms by causing the modification of proteins, DNA and RNA by alkylation. Some disadvantages have been reported, including denaturation of the structural ECM proteins such as collagen and residual toxicity

(Lambert, Mendelson et al. 2011, Qiu, Sun et al. 2011). Removal of EtO and its toxic derivatives, such as ethylene chlorohydrin and ethylene glycol, has been reported to be mandatory to ensure safety of medical devices. Furthermore, during EtO treatment it is important to ensure the appropriate diffusion into the tissues and the proper aeration of the specimen at the end of the procedure in order to guarantee the complete removal of EtO residues (Mendes, Brandao et al. 2007, Matuska and McFetridge 2015).

1.7.2.4 Supercritical CO_2

During supercritical CO_2 (SC-CO_2) sterilisation, CO_2 reaches the supercritical state as a result of a combination of specific temperature and pressure conditions ('critical point') (Figure 1.24). This type of sterilisation has the advantages of a treatment with both gaseous and liquid physical state, such as the viscosity of a liquid and the transport efficiency of a gas. It can be performed at relative low pressure and temperature, which renders it suitable for the sterilisation of biological tissues. However, SC-CO_2 treatment requires well defined conditions of temperature (31.1 °C) and pressure (74 atm) and its effectiveness against some bacterial endospores and virus alone is not sufficient for terminal sterilisation (Qiu, Sun et al. 2011). SC-CO_2 treatment does not result in permanence of toxic residues in the treated materials, since they can be easily removed by depressurization and out-gassing (White, Burns et al. 2006).

The effectiveness of this method can be further enhanced by the utilization of liquid sterilants, such as peracetic acid, hydrogen peroxide and ethanol (Qiu, Sun et al. 2011). Reports in the literature have presented encouraging results with bone allografts treated to terminal sterilisation with SC-CO_2 alone and SC-CO_2 with liquid sterilants; results demonstrated that intrinsic mechanical properties of the allografts were maintained (Russell, Rives et al. 2015).

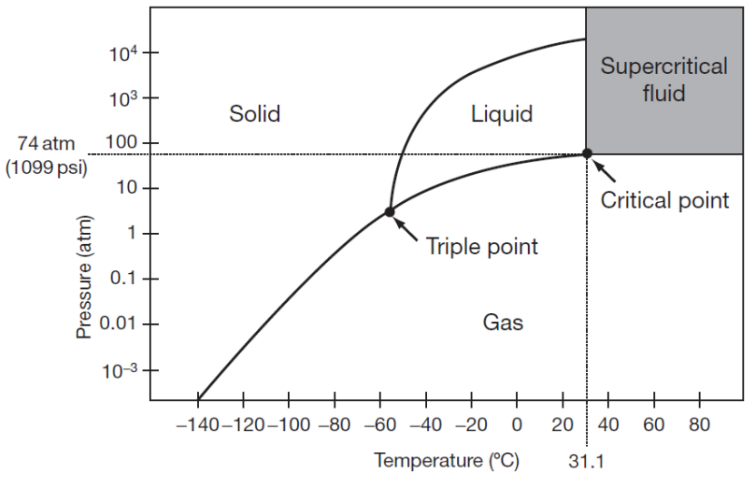

Figure 1.24 Phase diagram of CO_2. Adapted from (Qiu, Sun et al. 2011).

1.7.2.5 Plasma Treatment

Plasma is an ionized gas generated by the application of electric current or electromagnetic radiations on a specimen to produce excited atoms and molecules (radicals). Ultraviolet (UV) irradiation, generated from excited molecules, causes damages on the DNA strands of microorganisms, followed by intrinsic photo desorption and etching of pathogens due to atomic and molecular radicals and excited molecules within the plasma field (Figure 1.25) (Qiu, Sun et al. 2011).

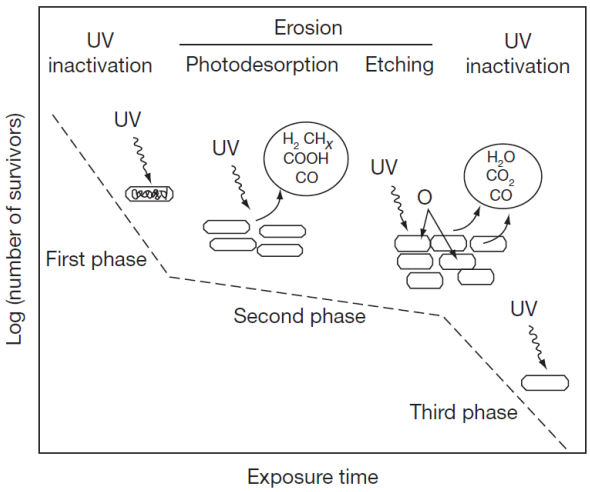

Figure 1.25 Schematic representation of the elimination of the microorganisms during the plasma treatment. Adapted from (Qiu, Sun et al. 2011).

Although the effective elimination of the microorganisms with plasma treatment requires further investigations, the products of the treatment are non-toxic elements, such as CO_2 and water. Besides, it can be performed at low pressure and temperatures. Human and animal skin tissues for wound and burn treatment have been sterilised in hospital facilities with non-thermal (low temperature) plasma discharges with minimal tissue damage (De Geyter and Morent 2012, Isbary, Zimmermann et al. 2013). Thus, this procedure could potentially be a viable alternative to the classical sterilisation techniques (Moisan, Barbeau et al. 2001, Tendero, Tixier et al. 2006, Qiu, Sun et al. 2011). However, the technique has been reported to be efficient only with thin materials, whereas it involves a complex process for moist materials (Delgado, Pandit et al. 2014) and presents difficulties for perform the process in packaged items (Moisan, Barbeau et al. 2001).

1.8 Summary

The utilization and consequences of the above-mentioned disinfection and sterilisation methods have been extensively described in the literature for the treatment of some native cardiovascular tissues. Up to date, few studies could be on the contrary tracked regarding their effects on decellularised scaffolds. However, the application of such methods on xenogeneic decellularised scaffold to employed in the construction of cardiovascular substitutes can be well assumed to have the same drawbacks observed on native tissues, including partial/ineffective sterilisation, toxic chemical residues and damages in the ECM proteins. These drawbacks can potentially lead to cytotoxicity of the implanted graft, the onset of calcification, tissue degeneration and graft rupture, leading to poor durability and hemodynamic performance and eventually failure of the graft (Heng, Albrecht et al. 2013).

The development of off-the-shelf, safe and functional cardiovascular substitutes composed of decellularised human or animal tissue is largely dependent on the development of optimised sterilisation procedures.

1.9 Aims and Objectives

This PhD project aims to investigate novel and/or optimise conventional disinfection and sterilisation methods for decellularised scaffolds. The aim is to identify optimal technologies that will ensure the safe clinical translation of decellularised pericardium (porcine, bovine). The developed technologies can also be used with human tissues and scaffolds. The work focused on disinfection methods with AA, possessing a high spectrum of action able to inactivate the most types of contaminants, as well as terminal sterilisation treatments, including PAA and γ-irradiation treatment. The establishment of the most favourable methods will take in consideration the effectiveness of disinfection and sterilisation together with the minimum effect on the biomechanical, biochemical and biological properties of the tissues and the practicality in tissue banks. The results outline the optimal procedures for treating the different tissues, as well as specific differences between species.

The major goal of this PhD project is the development/optimisation of appropriate disinfection/sterilisation methods for porcine and bovine decellularised scaffolds. The work conducted in the project focused on the following objectives:

- Decellularisation of different tissues, including porcine and bovine pericardium (in-house TRICOL protocol (Spina, Ortolani et al. 2003));
- Assessment of decellularised scaffolds in terms of ECM integrity (histological, biochemical, biomechanical and surface analysis) and biocompatibility (cytotoxicity evaluation);
- Development/optimisation of disinfection and sterilisation methods tailored for decellularised tissue scaffolds;
- Evaluation of the sterility level of each sterilisation method;
- Qualification and quantification of contaminants;
- Assessment of the effects of the sterilisation treatments on the scaffolds in terms of ECM integrity (histological, biochemical, biomechanical and surface analysis) and biocompatibility (cytotoxicity and cytocompatibility evaluation);

CHAPTER II

MATERIALS & METHODS

2.1 Animal Tissues

Porcine pericardia were obtained from local slaughterhouse (Macello F.lli Guerriero, Villafranca Padovana, Padua), from 9-11 months old animals (Duroc pigs) with weight ranging 165-175 kg. Bovine pericardia were obtained from 8 months old animals (Piebald calves) in a local slaughterhouse (Bugin S.r.L, S. Maria di Sala, Venice) within 2h after animal slaughter (≈170 kg). Tissues were immersed in phosphate-buffered saline (PBS) until arrival in laboratory. Follow dissection and isolation of tissue and further rinsing in PBS for blood washout was performed on both tissues (Figure 2.1). Fat adherences were removed with help of scissors and tweezers and the tissue kept wet during all the processing time.

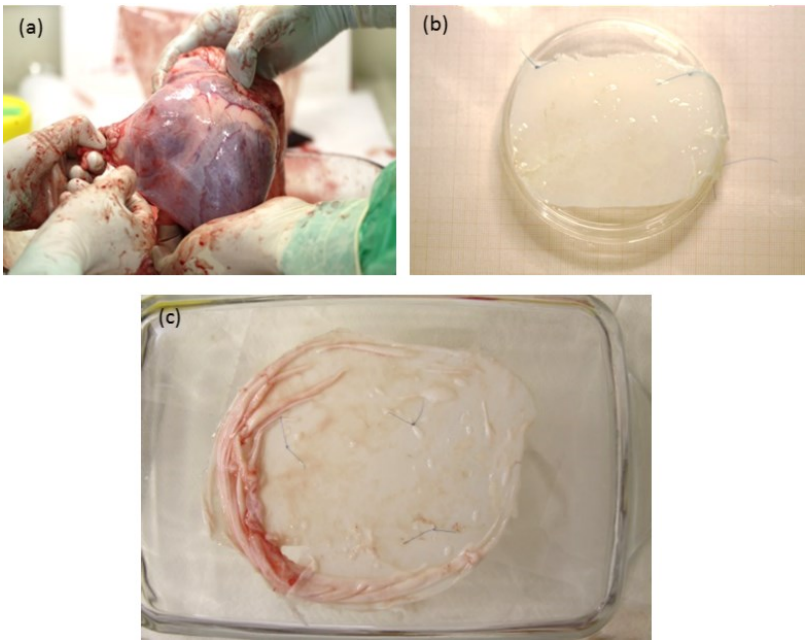

Figure 2.1 (a) Dissection and isolation of porcine pericardia from porcine heart; (b) isolated porcine tissue; (c) native bovine pericardia with reference of interest area by suture points.

2.2 Decellularisation Protocol

Porcine and bovine pericardia were decellularised with a decellularisation procedure developed in Professor Gerosa's Cardiovascular Regenerative Medicine Group, called TRICOL and based on TRITON x100 and cholate) (Spina, Ortolani et al. 2003). Isolated pericardia were kept in bottles of 200 mL or 400 mL according to the amount of tissue to be decellularised (≈ 100 cm^2/400 mL). Briefly, pericardial patches have been treated

with alternated hypo- or hypertonic solutions, TRITON X-100 (0.1 – 1%) and 10 mM sodium cholate. All the extractions were carried out in a degassed solution containing 10 mM sodium ascorbate and 5 mM EDTA under N_2 atmosphere and continuous stirring. Residual nucleic acids have been digested using 330 U/cm^2 of the non-specific endonuclease Benzonase™ at 37 °C twice for 24 h. All the solutions were sterilized by filtration across Filtropur filters of 0.20 µm pore size (Sarstedt, Numbrecht, Germany).

The decellularised bovine (BPD) and porcine (PPD) pericardial patches were sectioned differently according to the experiment to be performed:

- Isolation with 12 mm-diameter circular biopsy punches (disinfection and sterilisation tests, histological analyses and SEM);
- 6 cm^2 rectangles (biochemical and biomechanical assays);
- Isolation with 5 mm-diameter circular biopsy punches (cytotoxicity tests).

2.3 Sterilisation Assessment Methodology

To the aim of assessing the sterility effectiveness of the protocols in development as well as identifying and quantifying the residual bioburden, a sterility assessment protocol was developed. This protocol comprises the verification of the sterility and the identification and quantification of the residual bioburden, achieved through the methodologies herein described.

2.3.1 Sterility Test and Quali/Quantification of Contaminants

Sterility was evaluated according to guidelines of the European Pharmacopoeia 2.6.1 for biological specimens (Commission 2005). Samples were inoculated in two different bacteria media: Thioglycolate (Thio) medium and Tryptone soya broth (TSB). Thio medium is intended for the detection of anaerobic bacteria, while TSB is suitable for culture of both aerobic bacteria and fungi (Commission 2005). Both media were prepared and sterilised by autoclaving at 121 °C for 20 min. Media were stored at 4 °C for maximum 1 month. Samples were immersed in Thio and TSB and incubated at 30-

35°C and 20-25 °C, respectively. After 14 days of incubation, turbid medium was indicative of contaminated samples, while sterile samples resulted in clear medium.

On contaminated (turbid) samples, identification of contaminants was carried out by aseptic inoculation of positive Thio and TSB media on chocolate agar plates. Chocolate agar is an enriched medium, recommended for growth of fastidious microorganisms that require specific supplemented media. After inoculation with inoculation-loop of the contaminated sample, the chocolate agar was incubated between 24-48 h at 37 °C until bacteria growth was observed.

Chocolate agar plates were incubated at 37 °C between 24-48 h. After bacteria grow, plates were brought to Department of Microbiology and Virology of the University of Padua where pathogen identification was performed by MALDI-TOF mass spectrometry. MALDI-TOF is a technology capable of identify specific biomolecules of each bacterium, comparing the spectra of the tested sample to a dedicated database.

2.3.1.1 Most Probable Number Method

Estimation of residual bioburden concentration was performed on a sampling the last washing step solution, through the MPN method (Sutton 2010). This method is based on serial ten-fold dilutions of the contaminated sample to be tested, as shown in Figure 2.2. As the number of dilutions increases, the number of microorganisms is so low that the possibility of inoculation with microorganisms' decreases. The degree of dilution at which absence of contaminants begins indicates that the contaminants are diluted so much that the medium ultimately fails to be inoculated with any microorganism. Effective estimation of bioburden is obtained checking the positivity (turbidity) on triplicate samples for each dilution (Sutton 2010).

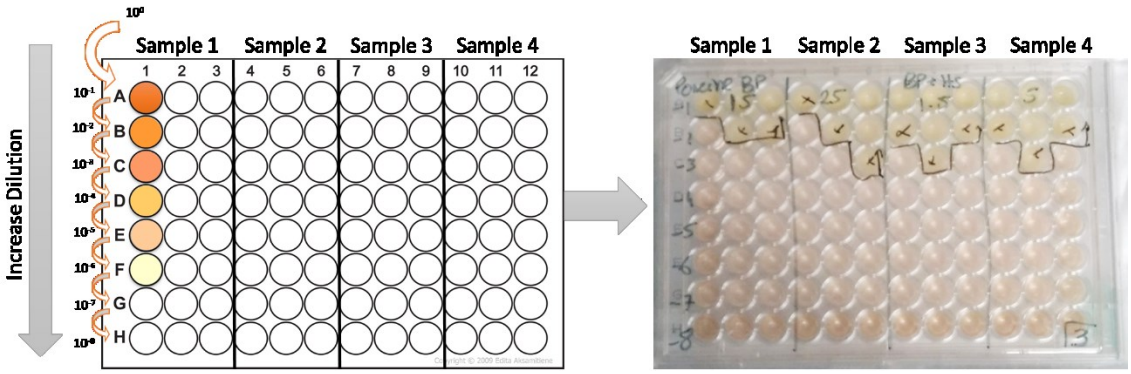

Figure 2.2 MPN method plate with serial tenfold dilutions.

US FDA Bacterial Analytical Manual (BAM) (U.S. FDA BAM Appendix 2) provides a MPN table (Table 2.1) that could be employed for the estimation of the MPN when employing three dilutions in sequence (10^{-1}, 10^{-2}, 10^{-3}). To increase the accuracy of the estimation, we performed a wider set of ten-folds dilution (10^{-1} - 10^{-8}) and the MPN calculations were performed using a dedicated Excel spreadsheet, as described in Jarvis, et al. (Jarvis, Wilrich et al. 2010).

Table 2.1 MPN table for a three-replicate design test of a sample where "positive tubes" indicate the number of positive samples for each dilution in triplicates that can be 0, 1, 2 or 3. Adapted from (Sutton 2010).

Positive Tubes				
0.1	0.01	0.001	MPN	95% Confidence Range
0	0	0	<3.0	0-9.5
0	0	1	3	0.15-9.6
0	1	0	3	0.15-11
0	1	1	6.1	1.2-18
0	2	0	6.2	1.2-18
0	3	0	9.4	3.6-38
1	0	0	3.6	0.17-18
1	0	1	7.2	1.3-18
1	0	2	11	3.6-38
1	1	0	7.4	1.3-20
1	1	1	11	3.6-38
1	2	0	11	3.6-42
1	2	1	15	4.5-42
1	3	0	16	4.5-42
2	0	0	9.2	1.4-38
2	0	1	14	3.6-42
2	0	2	20	4.5-42
2	1	0	15	3.7-42
2	1	1	20	4.5-42
2	1	2	27	8.7-94

Positive Tubes				
0.1	0.01	0.001	MPN	95% Confidence Range
2	2	0	21	4.5-42
2	2	1	28	8.7-94
2	2	2	35	8.7-94
2	3	0	29	8.7-94
2	3	1	36	8.7-94
3	0	0	23	4.6-94
3	0	1	38	8.7-110
3	0	2	64	17-180
3	1	0	43	9-180
3	1	1	75	17-200
3	1	2	120	37-420
3	1	3	160	40-420
3	2	0	93	18-420
3	2	1	150	37-420
3	2	2	210	40-430
3	2	3	290	90-1000
3	3	0	240	42-1000
3	3	1	460	90-2000
3	3	2	1100	180-4100
3	3	3	>1100	420-4000

Decellularised scaffolds in study were inoculated directly in Thio and TSB medium, while the rinsing solution (usually PBS) in which the tissues were stored analysed for bioburden quantification by inoculation in Thio medium. A sample of the rising solution was inoculated in Thio medium and serial tenfold dilutions were performed (Figure 2.2). Positivity was recorded by turbidity of the media after incubation between 24-48 h at 37 °C. The serial ten-fold dilutions performed in the 96 well plate, dilution factor, volume inoculated and number of replicates used were introduced in the Excel spreadsheet. With this input data was obtained the MPN value and the relative 95% confidence interval (CI) (Figure 2.3).

Calculations for the MPN value follow the general formula $\sum_{j-1}^{k}\left(\frac{g_j m_j}{1-\exp(-\lambda m_j)}\right) = \sum_{j-1}^{k} t_j m_j$, where exp(x) means e^x and λ denotes the estimated concentration (MPN value), k the number of dilutions, g_j number of positive (or growth) tubes in the j dilution, m_j the amount of the original sample put in each tube in the j dilution and t_j the number of tubes in the j dilution. This equation can be then solved by iteration (U.S. Food and Drug Administration, BAM Appendix 2).

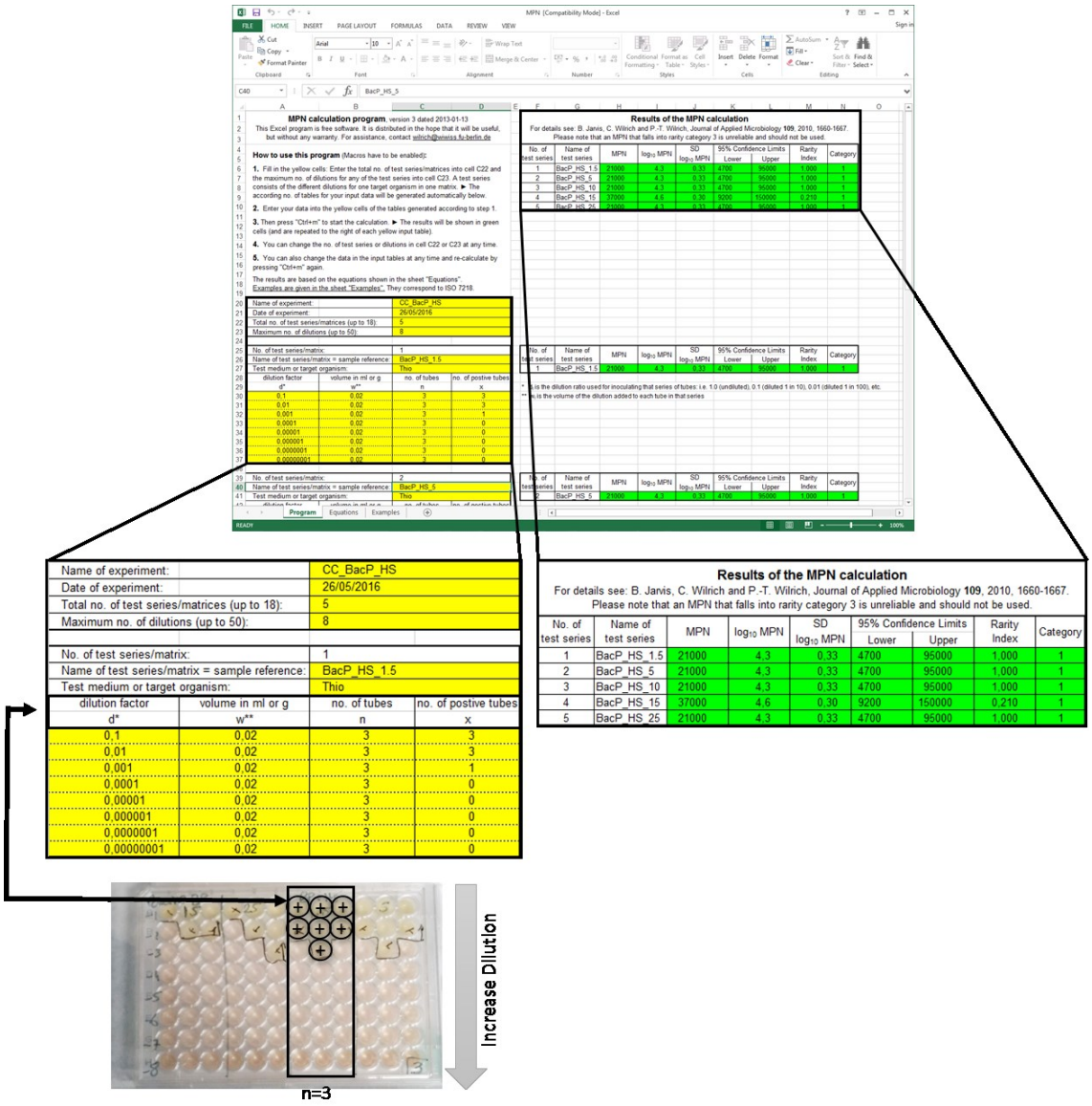

Figure 2.3 General Excel file for the MPN calculation.

2.3.2 Controlled Contamination

In order to prove the effectiveness of the sterilisation protocols developed, a controlled contamination (CC) method with known pathogens was established.

The bacterial strains used for the CC of the scaffolds were obtained from the Department of Microbiology and Virology of the University of Padua or from ATCC. Strains of *Enterococcus faecalis* (Gram$^+$, ATCC® 29212™), *Escherichia coli* (Gram$^-$, ATCC® 35218™) and *Staphylococcus aureus* (Gram$^+$, ATCC® 29213™) were collected in agar plates after overnight (ON) grow and brought to the laboratory. Strain of *Bacillus*

Pumilus (*BacP* - ATCC® 27142™) was obtained freeze dried. TSB medium was used to rehydrate the pellet while mixing. Following, aseptically transfer of this aliquot to sterile TSB and further mix of the suspension was performed. Expansion of bacteria was performed ON at 37 °C.

Quantification of bacteria was performed by spectrophotometer analysis of turbidity. McFarland Standards can be used to approximate the concentration of cells or bacteria in a suspension as can be observed in Table 2.2 (Acharya 2016).

Table 2.2 McFarland Standards table. Adapted from (Acharya 2016).

McFarland Standard No.	Approx. cell density ($1x10^8$ CFU/mL)
0.5	1.5
1	3.0
2	6.0
3	9.0
4	12.0

Bacterial strains were inoculated in Thio medium and incubated ON at 37 °C to support the growth of the bacteria. After 24 h, bacteria had been quantified by measuring the absorbance at 600 nm on spectrophotometer; a sample of each suspension was collected and absorbance was read in individual cuvette, with Thio medium as blank. Final absorbance values were collected and an approximation of the CFU/mL of bacteria present in the solution were calculated following the McFarland Standards. The bacterial strains above mentioned were preserved at -20 °C as 1:1 solution (bacterial strain suspension after ON growth and glycerol tryptose broth). Reactivation of the strains was achieved by ON growth in Thio medium at 37 °C of small amount of stock solution collected with an inoculation loop.

For one set of samples, bacterial strains of *Staphylococcus aureus*, *Enterococcus faecalis* and *Escherichia coli* were selected. These strains are commonly isolated from cardiovascular homografts and are referred as high virulence and opportunistic pathogens (Villalba, Solis et al. 2012). Contamination was performed by incubation of the scaffolds with $\approx 10^9$ CFU/mL for each bacteria type during 2 h at 37 °C. Three washes with sterile PBS in agitation for 30 min each were performed to remove non-adherent

contaminants. To verify the effective contamination, a sample of the last wash step was collected and inoculated in Thio and TSB medium.

For the samples treated with Sterilisation Protocol 2, a further specific bacteria strain, *BacP*, was added to the CC. In this case, the concentration of *BacP* was ≈10^5 CFU/ml. In addition, the endospore form of *BacP* (*BacP*+HS) was obtained performing a heat shock (HS) by treatment of inoculate at 48 °C for 30 min (Merkli, Heller et al. 1994) (Movahedi and Waites 2000). Following, washes were performed as referred previously.

After CC, porcine and bovine decellularised pericardia were processed for histology as described in section 2.5.1 and Gram staining was performed to observe adherence and distribution of the microorganisms to the surface of the tissues.

2.4 Disinfection & Sterilisation Methods

2.4.1 Sterilisation Protocol 1

2.4.1.1 Antibiotics & Antimycotics (AA) Treatment

An AA cocktail comprising three types of antibiotics and one antimycotic was prepared in PBS (Table 2.3). The cocktail was employed immediately for tissue treatment. Vancomycin, Gentamicin and Cefoxitin are antibiotics currently applied in tissue banks with a high spectrum activity; Vancomycin acts against Gram-positive bacteria, Gentamicin on both Gram-positive and –negative and Cefoxitin has a broad spectrum-activity and acts on Gram-positive and –negative as well as anaerobic. For fungi, Amphotericin B is the most common antifungal used (Pitt, Tidey et al. 2014). The concentrations of AAs applied were the lower applied in tissue banks for cardiovascular tissues (Table 2.3) (Heng, Albrecht et al. 2013). In order to increase the efficacy of the AA treatment, the treatment was performed at 37 °C, as previously reported (Germain, Thibault et al. 2010). Briefly, 1 cm^2 of tissue was treated with 1 mL AA cocktail at 37 °C for 24 h in agitation (400 rpm) on a plate shaker. Then, two washes with sterile PBS (first 30 min, second wash ON) were performed to wash out antibiotic and antimycotic residues. The treated tissues were then tested for sterility and quantification using the MPN method.

Table 2.3 AA cocktail concentration.

Type	Concentration
Vancomycin	50 mg/L
Gentamicin	80mg/L
Cefoxitin	240mg/L
Amphotericin B	250mg/L

2.4.1.2 Peracetic Acid Treatment

PAA solutions of 0.1% (v/v) and 0.05% (v/v) were prepared in PBS and adjusted to pH 7.3 with sodium hydroxide (NaOH). The solutions were sterilised by filtration and used within 1 h after preparation. Treatment with PAA at both concentrations was performed on samples previously treated with AA (2 mL/cm2) at 27 °C for 3 h in constant agitation (300 rpm) (Wilshaw, Kearney et al. 2008). Three washes with sterile PBS (two for 30 min and third wash ON) were performed to wash out any PAA residues. Following sterility assessment, quantification of the microorganisms was carried out as described above. All sample groups were tested in triplicates.

2.4.2 Sterilisation Protocol 2

The second sterilisation protocol was developed testing γ-irradiation in different dosages. γ-irradiation procedure was performed in collaboration with the company Gammatom based in Como, Italy. The γ-irradiation dosage acquired by materials in test is proportional to the exposition time. As consequence, as higher is the exposition time, higher will be the dosage obtained by the materials.

PPD and BPD samples to be γ-irradiated were sectioned as referred previously and delivered to the company in 50 or 15 mL tubes with ≈ 10 cm^2 of tissue per tube in sterile PBS in double plastic bags. 25 kGy is the 'gold standard' dosage in the clinical practice for sterilisation of medical devices. This dosage often results in damages of the ECM and for this reason lower γ-irradiation dosages were tested: 15, 10, 5 and 1.5 kGy. 25 kGy

was employed as negative control. Except for the treatment that was performed at RT, all samples were kept or shipped at refrigerated conditions.

2.5 Tissue Assessment

Since sterilisation procedures are known to cause structural damages and interfere with biocompatibility of tissues, besides the verification of sterility and quali/quantification of contaminants, AA + PAA-treated and γ-irradiated PPD and BPD samples were subsequently assessed in terms of ECM structure and organization, surface topology and in vitro cytocompatibility and cytotoxicity. Histological and SEM analyses provided an overview of the general ECM histoarchitecture of the tissues, while the biochemical quantification of the major components of the tissue as collagen and GAGs reveal the possible susceptibility of these components to the treatments that were furthermore investigated through mechanical assessment of the scaffolds under uniaxial tensile tests. Finally, cytotoxic and cytocompatibility were investigated through in vitro cell seeding experiments to the aim of unravel the biological features of the scaffolds after the selected sterilisation procedures.

2.5.1 Histological Staining and Immunofluorescence

Decellularised scaffolds 12 mm-diameter circular biopsy punches were isolated as referred previously. Mild aldehyde fixation of tissues was performed with 4 % paraformaldehyde (PFA) for 20 min at room temperature (RT) in the dark. To avoid crystals formation during the freezing procedure, samples were kept in 20% sucrose ON at 4 °C and subsequently embedded in a solution 1:1 of Tissue-Tek® Optimum Cutting Temperature (OCT) compound and 20% sucrose and snap-frozen with isopentane in nitrogen vapours. Frozen samples were stored at -80 °C until further processing.

Frozen samples were sectioned in cryostat at 5-7 µm thickness and kept in -20 °C until staining. Haematoxylin & Eosin (HE), Mallory Trichrome (MT) and Alcian Blue (AB) staining were performed while immunofluorescence was carried out as reported by Iop et al. (Iop, Renier et al. 2009). Images of the stained sections were acquired with light

microscope Nikon Eclipse 50i equipped with NIS-Elements D 3.2 Software (Nikon Corporation Shinagawa, Tokyo, Japan), while immunofluorescence sections were acquired in fluorescence microscope equipped with LAS-AF lite Leica software (Leica Microsystems CMS TCS SP8, Mannheim, Germany).

2.5.1.1 Haematoxylin & Eosin

In this staining, general ECM is stained in pink by eosin, while nuclei are stained in blue/purple by haematoxylin. Sections were stained following the following protocol, as a modification of the manufacturer's instructions:

- 30 sec in haematoxylin and wash in tap water;
- 1 min of incubation in basic buffer and wash in tap water;
- 30-40 secs in eosin;
- 10 dips in ethanol 95% for two times;
- 10 dips in absolute ethanol for two times;
- Clear in xylene and mount with mounting medium.

2.5.1.2 Mallory Trichrome

With MT staining, nuclei can be visualized in red, collagen fibrils in deep blue and elastic fibrils can be unstained or stained in pale pink or yellow. The staining was performed as follows:

- 10 min in carbolfuchsin solution (reagent A) and wash in distilled water;
- 2 min in acid differentiating buffer (reagent B) and quick wash in distilled water;
- 5 min in phosphomolibdic acid solution (reagent C) and, without washing, 1 min in polychrome solution according to Mallory (reagent D) and wash in distilled water;
- Dehydration in ascending alcohols (70%, 95% and 100%), leaving 1 min in the last one;
- Clear in xylene and mount with mounting medium.

2.5.1.3 Alcian Blue

Acid mucopolysaccharides (GAGs) can be observed in AB staining. In this case, sections were processed as follows:

- 30 min in alcian blue pH 2,5 solution (reagent A) followed by drain of the slide and 10 min in sodium tetraborate hydroalcoholic solution (reagent B);
- Washing the slide and dehydrate in ascending alcohols (70%, 95% and 100%);
- Clear in xylene and mount with mounting medium.

2.5.1.4 Immunofluorescence

Indirect double-immunofluorescence staining was performed to visualize specific components of the ECM of the treated pericardial scaffolds. A combination of specific primary antibodies that form an immune complex to mark desired molecules of the tissue with fluorochromes (secondary antibodies) that couple to the immunocomplexes permit the visualisation of the target structure under fluorescence microscope. The antibodies, dilution and supplier used for immunohistochemistry are described in Table 2.4.

Table 2.4 Primary and secondary antibodies.

Primary Antibodies		
Antibody	**Dilution**	**Supplier**
Collagen I (Mouse)	1:100	Sigma-Aldrich (C2456)
Collagen IV (Rabbit)	1:100	Abcam (ab6586)
Laminin (Rabbit)	1:500	Dako (Z0097)
Elastin (Rabbit)	1:50	Abcam (ab21610)
Heparan sulphate (Rat)	1:100	Millipore (MAB1948P)
Secondary Antibodies		
Fluorescein (FITC) (Anti-Mouse)	1:100	Millipore (12-506)
Rhodamine (Anti-Rabbit)	1:100	Millipore (AP132R)
Rhodamine (Anti-Rat)	1:100	Millipore (AP136R)

The slides were washed in PBS for totally remove OCT followed by incubation during 10 min with bovine serum albumin (BSA). Since it is a double-immunofluorescence, the primary antibodies were incubated for 1 h at 37 °C in a humidified atmosphere and slides were washed three times with PBS for 5 min each, followed, the secondary antibodies

incubation was performed protected from light during 30 min at 37 °C and another three washes with PBS for 5 min each were performed. Finally, DAPI (4',6-diamidino-2-phenylindole) staining was carried out during 10 min at 37 °C and washes with were followed for the mounting of the slides with aqueous mounting medium.

2.5.2 Biochemical Assays

Quantitative biochemical analysis of hydroxyproline (HYP) and GAGs was performed on decellularised and treated samples. Samples for biochemical analyses were dissected in rectangles with 6 cm^2 and washed with distilled water twice for 1 h. Treated and decellularised samples were frozen first at -20 °C ON and then -80 °C over day (OD) followed by lyophilisation at -60 °C during two days under vacuum (Modulyo® Freeze Dryers, Edwards).

2.5.2.1 Hydroxyproline Assay

HYP is a major component of the collagen protein, accounting for approximately 14% of collagen in mammals. The quantification of this protein can be therefore indicative of the collagen content of samples. Since some sterilisation methods can reduce the amount or denature the collagen present in the scaffolds by impair the integrity of collagen molecules, the HYP content can be indicative of the extension of the damages caused. HYP content of the samples was determined as described by Edwards et al. (Edwards and O'Brien 1980). Samples of 3-4 mg were weight and kept in glass test tubes. Assay buffer was prepared with 50 g/L citric acid monohydrate, 120 g/L sodium acetate trihydrate, 34 g/L sodium hydroxide, 0.8% (v/v) glacial acetic acid and 20% (v/v) 1-propanol, at pH 6-6.5. Standard curve was obtained with dilutions of 2.5 µg/mL trans-4-hydroxy-L-proline: 0, 2, 4, 6, 8, 10, 15, 20, 25, 30, 40, 50 and 100 µg/ml. Other solutions were prepared such as Ehrlich reagent and oxidizing solution: Ehrlich's reagent was prepared with 200 g/L 4-(dimethylamino) benzaldehyde, 60% (v/v) 1-propanol and 26% (v/v) perchloric acid and oxidizing solution was prepared with 14.1 mg/mL of chloramine-T.

The protocol was carried out by hydrolysis of tissue samples with 6N HCl at 121°C ON. The hydrolysate was neutralized at 96°C for 90 min and assay buffer was added in dried samples (1:15 dilution). Standard solutions and neutralized samples (triplicated for each) were placed in a 96 well plate and the oxidizing solution was added and the plate was mildly shaken for 5 min. After incubate with Ehrlich reagent for 45 min at 60°C, the optical density at 570 nm was read at a microplate reader spectrophotometer. Finally, HYP content in tested samples was calculated by interpolation with the calibration curve and plotted as µg/mg of dry tissue.

2.5.2.2 Glycosaminoglycan Assay

The GAGs content on the samples was carried out as referred by Barbosa, et al. (Barbosa, Garcia et al. 2003). Samples of 3-4 mg were weight dry and digested using papain digestion buffer, containing 5 mM L-cysteine, 5 mM EDTA and 7 U/ml of papain in PBS. Assay buffer, primary standard and dye solution were prepared. Assay buffer was prepared with sodium di-hydrogen phosphate (0.1 M), di-sodium hydrogen phosphate (0.1 M) at pH 6.8. Primary standard was obtained with 0.1% (w/v) of chondroitin sulphate in assay buffer and standard solutions were prepared: 0, 2, 4, 6, 8, 10, 15, 20, 25, 30, 40, 50 and 100 µg/ml. The dye solution contains 16 mg/L 1,9-dimethylene-methylene blue zinc, 2 g/L sodium formate, 0.5% (v/v) ethanol (99.5%) and 0.2% (v/v) formic acid, with pH range of 3.0-3.1.

The samples were digested with papain digestion buffer at 60 °C for 24 h. Standard solutions and digested samples (triplicated for each) were placed in a 96 well plate and the dye solution was added. Optical density at 525 nm was read at a microplate reader spectrophotometer and GAGs content in tested samples was calculated by interpolation with the calibration curve and plotted as µg/mg of dry tissue.

2.5.3 Biomechanical Testing

Biomechanical properties of the scaffolds were investigated by uniaxial tensile test. Samples were isolated form left anterior area of both pericardial tissue. After each treatment, samples were kept in PBS. The day before mechanical test, samples were sectioned using an in-house cutter in order to obtain strips of 2 cm x 3 mm. For obtain the sectional area, the thickness of each sample was obtained with a thickness gauge and the values recorded.

2.5.3.1 Test Procedure

Mechanical test was performed on Bose Electroforce System equipped with one loading cell of 220 N and two linear actuators of 200 N each (Figure 2.4). Samples were uniaxially deformed at a speed of v = 0.5 mm/s until tissue rupture and the test was performed at RT. All samples were kept wet with PBS to prevent dehydration during the procedure.

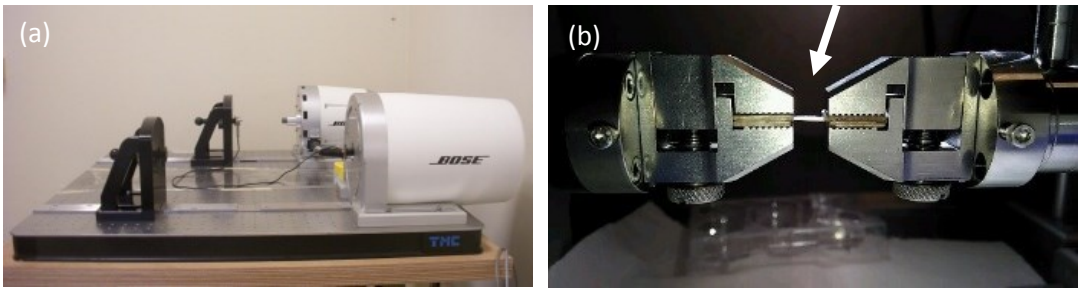

Figure 2.4 (a) Bose equipment; (b) sample (arrow) mounted on grips.

2.5.3.2 Data Analysis

The data obtained for each sample were: change in distance and subsequent stress generated. From this, elongation strain (%) and stress (MPa) were plotted. Elongation strain (ε, in %) was obtained by the formula $\varepsilon = \frac{\Delta l}{l_0}$, where Δl the change in length and l_0 the initial length, while stress (σ, in MPa) was obtained by $\sigma = \frac{F}{A}$, where F force and A cross-sectional area. Young's modulus (E, in MPa) was calculated as the slope of the stress-strain curve in the collagen phase. Cross sectional area was calculated using the measured thickness and the width of sample (3 mm). Ultimate tensile strength (UTS) was obtained by $UTS = \frac{F_{max}}{A}$, where F_{max} is the maximum load of sample rupture.

Failure strain was obtained for the correspondent strain at UTS. Plot of stress-strain graphs was done for each sample and UTS, failure strain and Young's modulus were calculated.

2.5.4 Scanning Electron Microscopy

For surface analysis of the tissues, SEM was carried out. An equipment JEOL JSM-6490 was employed for the assessment. Decellularised and treated samples were fixed and maintained in Karnovsky solution [8% (w/v) paraformaldehyde, 10% (v/v) glutaraldehyde (50%) and 40% (v/v) cacodylate buffer (0.2 M). pH range 7.2-7.4] at 4 °C in the dark. Before performing SEM analysis, Karnovsky solution was removed and the samples washed in physiologic solution (0.9 % NaCl) and dehydrated with 10 min for serial gradients of ethanol (50%, 60%, 70%, 80% and 90%). Samples were then placed in 100% ethanol and dried in critical point dryer under vacuum to substitute ethanol for CO_2 in a liquid state to reduce damages in the materials. After gold palladium coating to create a conductive layer of metal on the scaffolds, samples were observed at SEM microscope. Image acquisition was performed using low vacuum mode 20 kV of the equipment and images were obtained wit magnifications from 1000 – 20000x.

2.5.5 Cell Seeding Experiments

For cell seeding experiments hBM-MSC (PromoCell) were employed. Complete cell culture medium was prepared with alpha Minimum Essential Medium Eagle (MEMα) supplemented with 1% Penicillin Streptomycin (PS), 1% L- Glutamine and 10% of foetal bovine serum (FBS) and cultured at 37 °C in a 5% CO_2 humidified atmosphere. Cell seeding was performed (passage 10) at a density of 15.000 cells/cm^2 on the test biomaterials in a 96 well plate, with the plastic bottom of the well (polystyrene) as control. Medium was changed every 2 days.

2.5.5.1 Cytotoxicity Test – LDH

Lactate dehydrogenase (LDH) is an enzyme present in cells leaked when plasma membrane is damaged. It catalyses the conversion of lactate to pyruvic acid, as it converts NAD^+ to NADH. Its presence in cell culture supernatant is indicative of cell damage and, subsequently, can be related to the cytotoxic effect of the biomaterial. LDH activity is measured by NADH production from NAD and quantified using a colorimetric assay (LDH activity assay kit, Sigma Aldrich) according to manufacturer's instructions. Cell medium was collected at 24 h, 72 h, 7 days and 14 days and stored at -80 °C until further analysis. The follow solutions were prepared and used: LDH assay buffer, LDH substrate mix, 1.25 mM NADH standard, LDH positive control, master reaction mix prepared with LDH assay buffer and LDH substrate mix and the NADH standards for the calibration curve (0, 2.5, 5, 7.5 and 12.5 (nmole/well)).

Supernatant of samples and complete medium were thaw at RT and 10 µL were placed in the well plate. LDH Assay Buffer and Master Reaction Mix were added in each well (samples and standards) and the plate gently agitated in a plate shaker at 37 °C protected from light. After 2 min of incubation, the initial measurement ($t_{initial}$) was read at absorbance 450 nm (A_{450}). At this point, the plate was incubated at 37 °C and measurements were performed each 5 min until the value of the most active sample is higher compared to the value of the highest standard (12.5 nmole/well). Background absorbance from complete medium was subtracted to each measurement and the last reading (t_{final}) was used. Difference was calculated by $\Delta A_{450} = (A_{450})_{final} - (A_{450})_{initial}$. The follow equation was used to obtain the LDH activity: $LDH\ Activity = \frac{B\ x\ Sample\ Dilution\ Factor}{Reaction\ Time\ x\ V}$, where B is NADH amount (nmole) calculated by interpolation with the calibration curve; $Sample\ Dilution\ Factor$ in case the medium sample was diluted (in this case is 1); $Reaction\ Time = t_{final} - t_{initial}$ (in minutes) and V the volume of sample used (in this case 0.010 mL). LDH activity is reported as mU/ml.

2.5.5.2 Proliferation Test - MTS

Proliferation test was carried out using CellTiter 96®AQ_{ueous} One Solution Cell Proliferation Assay that contains MTS (tetrazolium compound [3-(4,5-dimethylthiazol-2-yl)-5-(3-carboxymethoxyphenyl)-2-(4-sulfophenyl)-2H-tetrazolium, inner salt]). This

colorimetric test enables the quantification of proliferating cells by reduction of MTS tetrazolium compound operated by cellular oxidoreductase enzymes of viable/proliferating cells to generate formazan product, a purple soluble reagent released in the culture media. The number of living cells in culture is directly proportional to the quantity of formazan product measured by absorbance.

For this experiment, 6 samples of each condition were tested for all timepoints. At 24h, 72h, 7 days and 14 days cell culture medium of each cell seeded sample was replaced with a mixture of 20 µL CellTiter 96® with 100 µL of complete fresh medium. The plate was incubated in the dark for 3 h at 37 °C in a humidified 5% CO_2 atmosphere. After, scaffold samples were removed from the plate and optical absorbance of the supernatant was read at 490 nm in a plate reader spectrophotometer. Two readings were performed and the mean value subtracted by the absorbance of the medium was plotted.

After 7 days and 14 days of culture with hBM-MSC, 3 samples of each condition were collected for histological analyses to investigate cell adhesion. Sample preparation and HE histological staining was performed as previously referred.

2.5.6 Statistical Analysis

Data processing was carried out using Excel spreadsheets and OriginPro 2016 programs while GraphPad was used for statistical analysis. Two-way ANOVA and one-way ANOVA tests were performed with Bonferroni as post-test. Data are plotted by mean ± 95% confidence intervals (CI).

CHAPTER III

RESULTS

3.1 Sterilisation Assessment Methodology

A method to confirm the effectiveness of sterilisation methods for biological tissues was established. It comprehends a CC tailored for each method to be applied, the confirmation of sterility/contamination (by turbidity check), the quantification performed by MPN method and qualification (by MALDI-TOF) of the residual bioburden, as can be observed in schematization in Figure 3.1, Figure 3.2 and Figure 3.3.

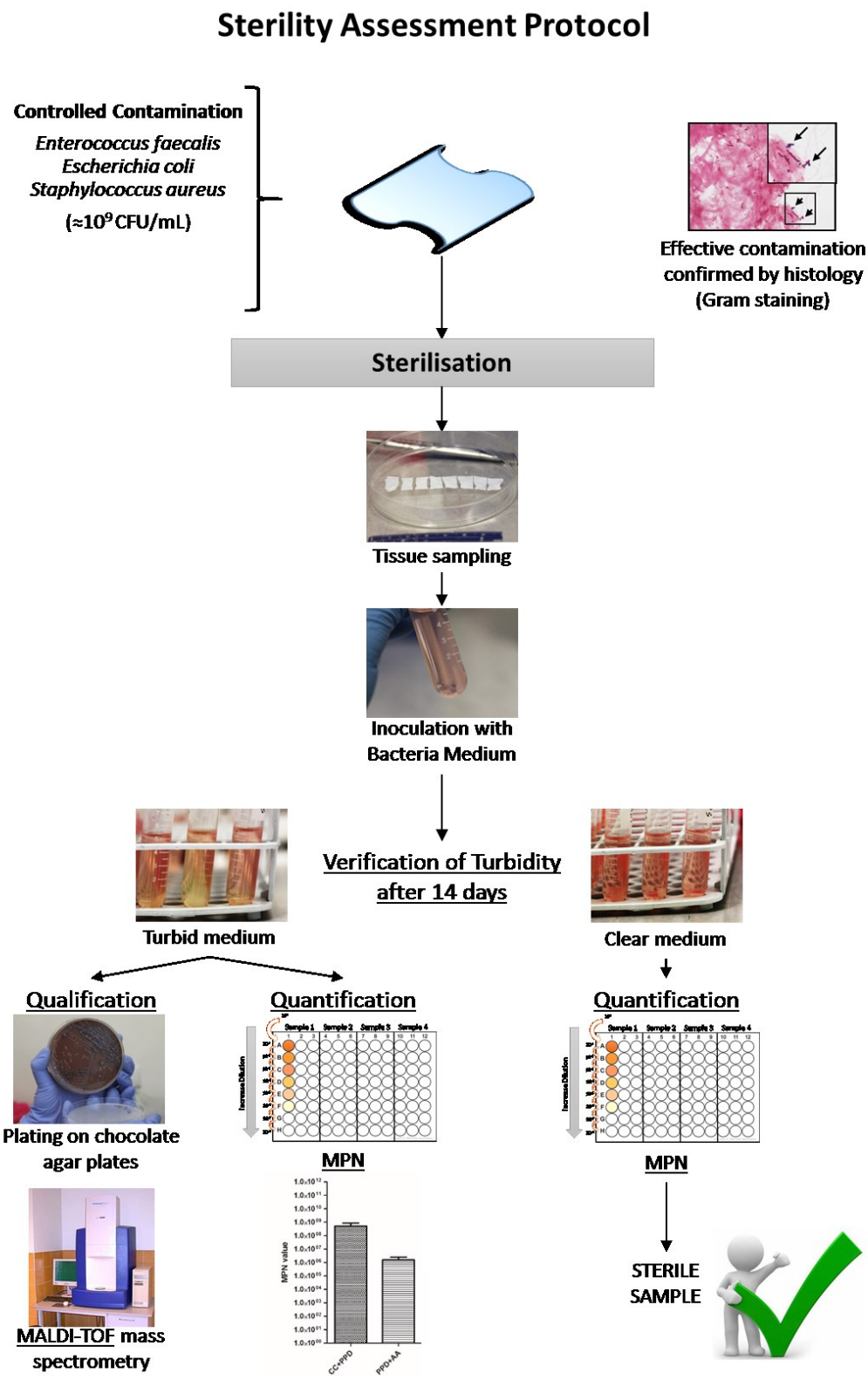

Figure 3.1 Schematization of the Sterilisation Assessment Methodology.

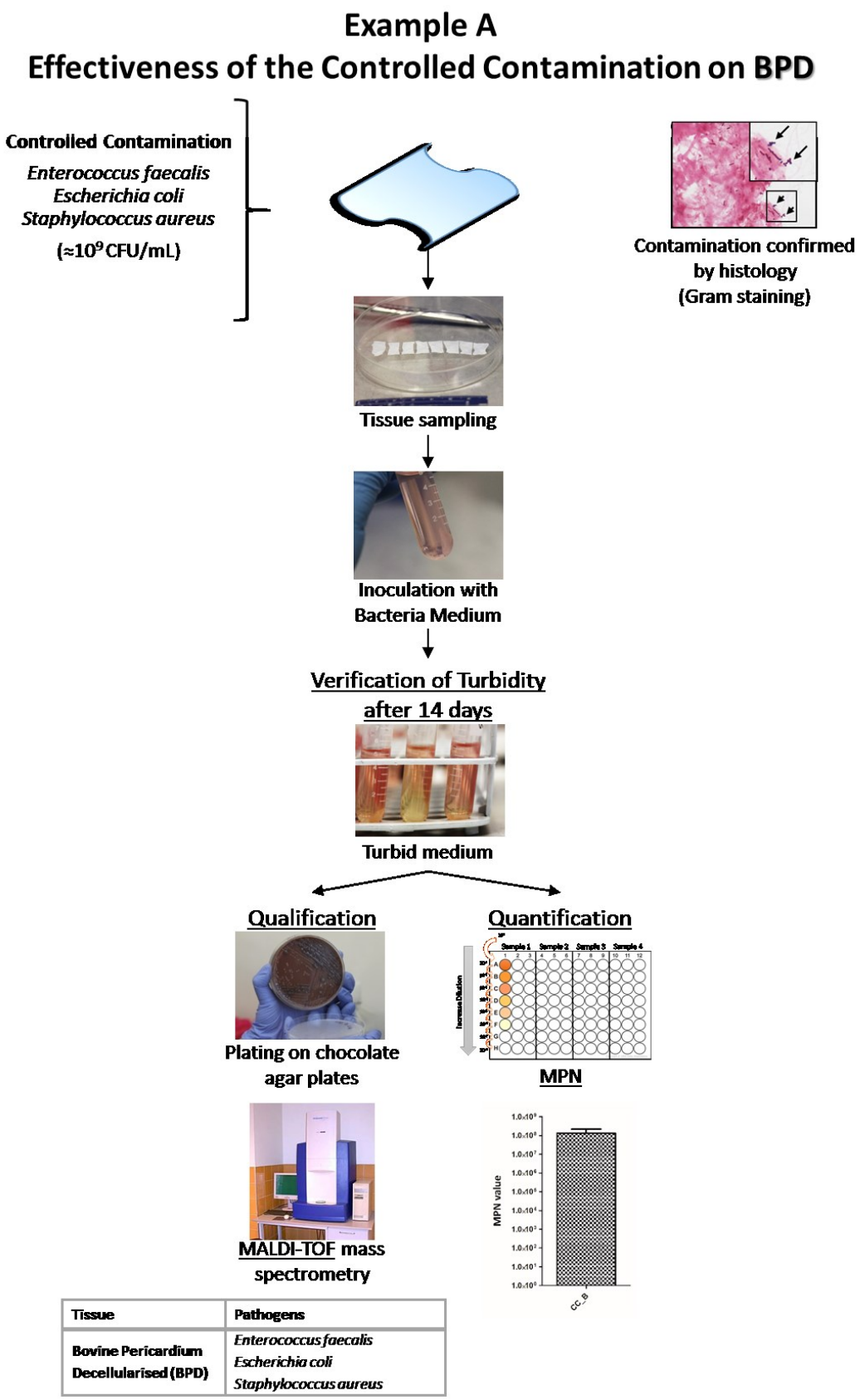

Figure 3.2 Example (A) - Application of the Sterility Assessment Methodology to a pericardial bovine decellularised scaffold exposed to CC.

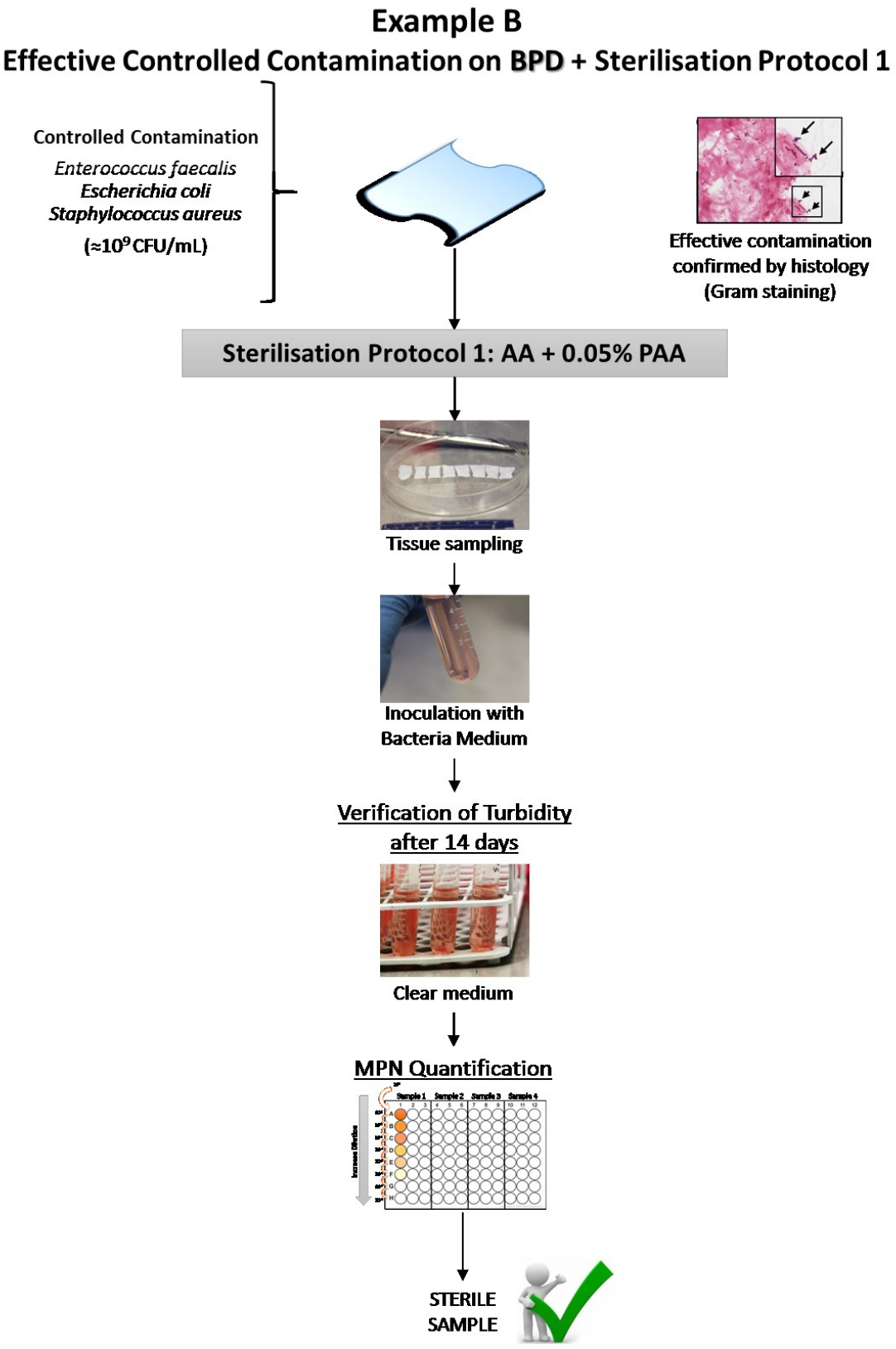

Figure 3.3 Example (B) - Application of the Sterilisation Assessment Methodology to a sample of bovine pericardium treated with the sterilisation protocol 1 (AA+0.05% PAA) after CC.

3.1.1 Controlled Contamination

Preliminary analyses were performed to verify the effectiveness of the protocol for CC employed, which was proven successful for PPD and BPD since both the scaffolds were found to be contaminated after inoculation with bacteria. Turbidity of the medium after CC reveal the effective contamination, as can be observed in Figure 3.4. MALDI-TOF analysis after CC confirm that the contaminants inoculated were the only strains of bacteria present in the tissues (Table 3.1). MPN method on the contaminated samples reveal the high-level of contamination inoculated in both scaffolds. Gram staining of PPD and BPD after contamination with all bacteria (*Staphylococcus aureus, Enterococcus faecalis*, *Escherichia coli* and *BacP*) or with *BacP* for samples treated with γ-irradiation was performed. Bacteria seem to present a preferential adhesion on fibrosa: as can be observed in (Figure 3.5) both porcine and bovine pericardia presented positive Gram staining only in the fibrosa surface, while the pathogens were not observed to attach on the serosa.

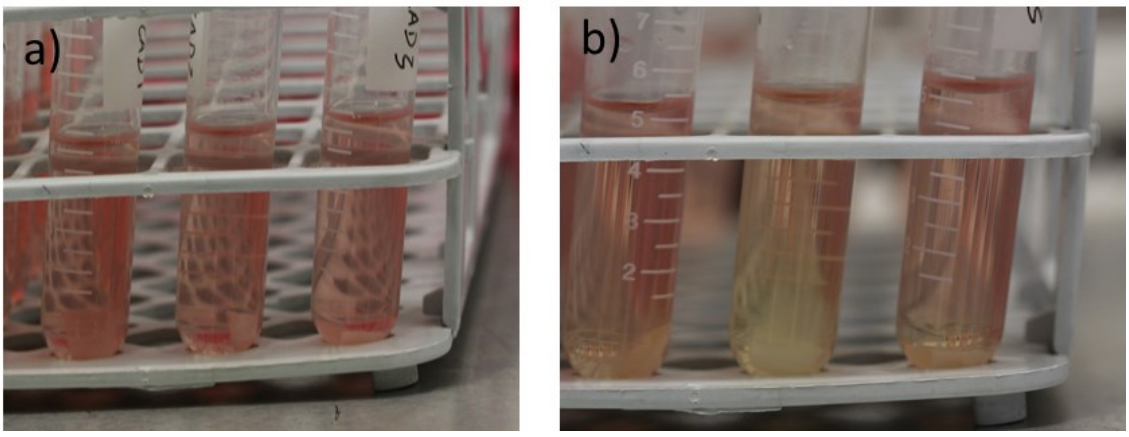

Figure 3.4 PPD and BPD inoculated with bacteria (a) before and (b) after CC.

Table 3.1 MALDI-TOF analysis after CC on PPD and BPD.

Tissue	Pathogens		
	Decellularised	**After CC**	**After CC with *Bacillus pumilus***
PP	—	***Staphylococcus aureus, Enterococcus faecalis, Escherichia coli***	***Bacillus pumilus***
BP	—	***Staphylococcus aureus, Enterococcus faecalis, Escherichia coli***	***Bacillus pumilus***

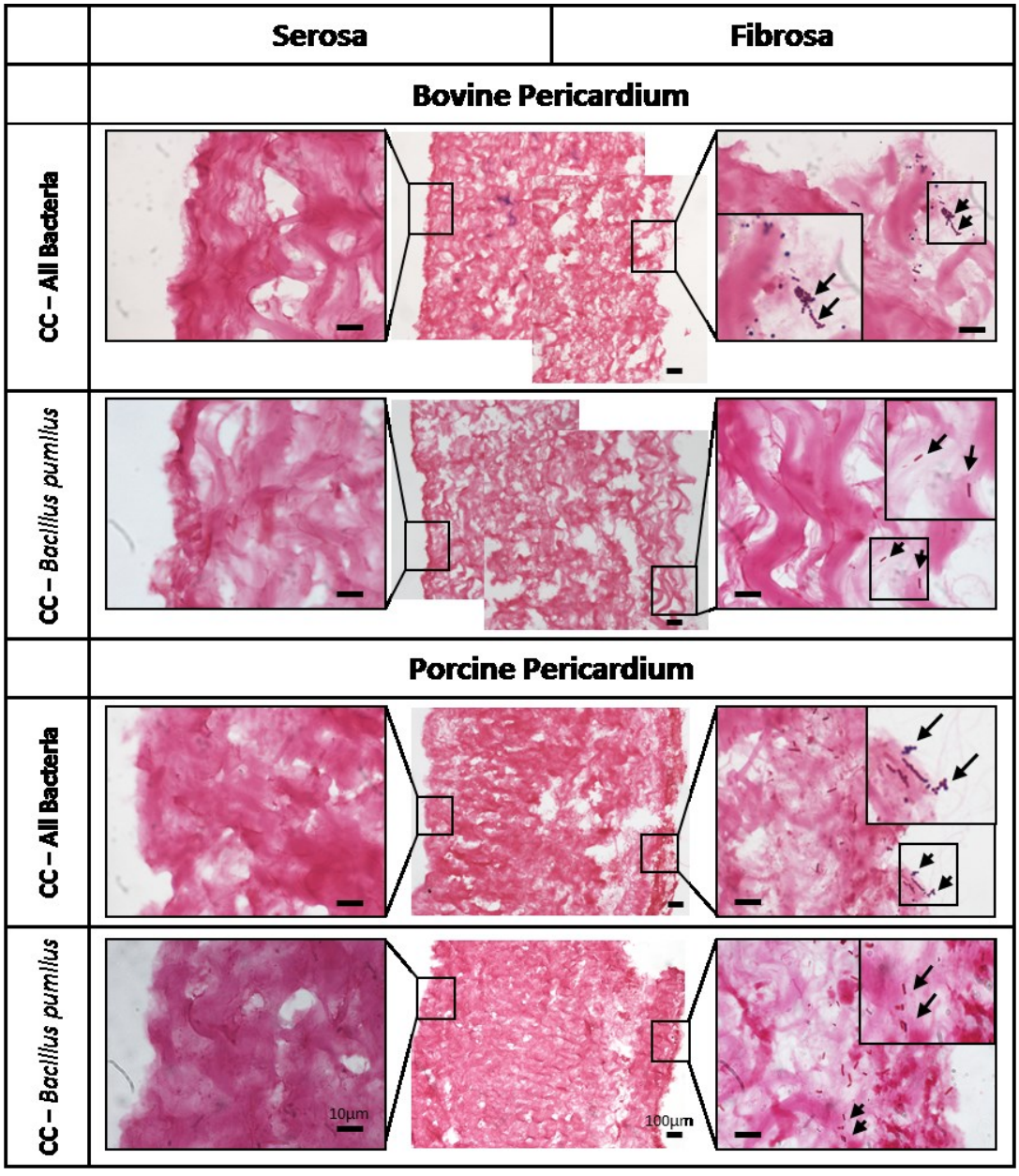

Figure 3.5 Gram staining of BPD and PPD. Scale bar 10 and 100 µm.

3.2 Assessment of Decellularised Tissue

3.2.1 Tissue Assessment

PP and BP after decellularisation presented gross structure similar to the native, having a whitish aspect in comparison to the native, as can be observed in Figure 3.6. Following decellularisation, the produced scaffolds were sectioned and divided according to the experiment to perform.

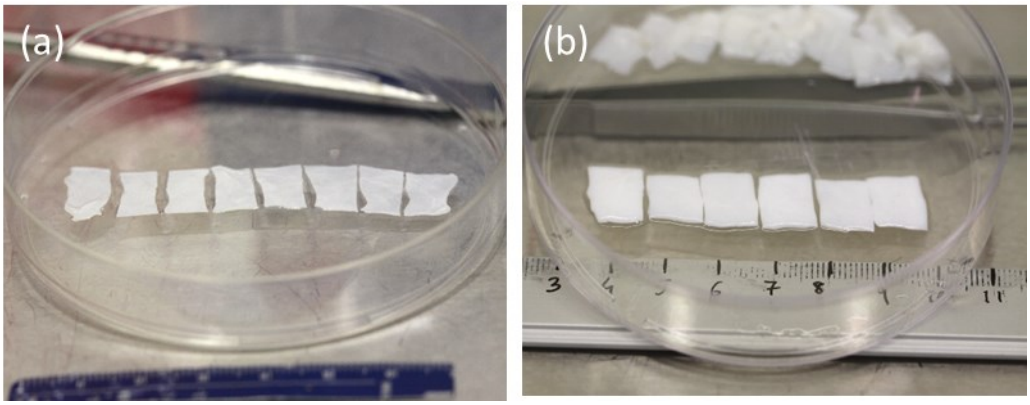

Figure 3.6 Decellularised pericardia: (a) porcine and (b) bovine.

The effective decellularisation of both bovine and porcine pericardia was assessed by HE and MT staining (Figure 3.7). Complete removal of nuclei and collagen structure preservation can be observed on decellularised scaffolds.

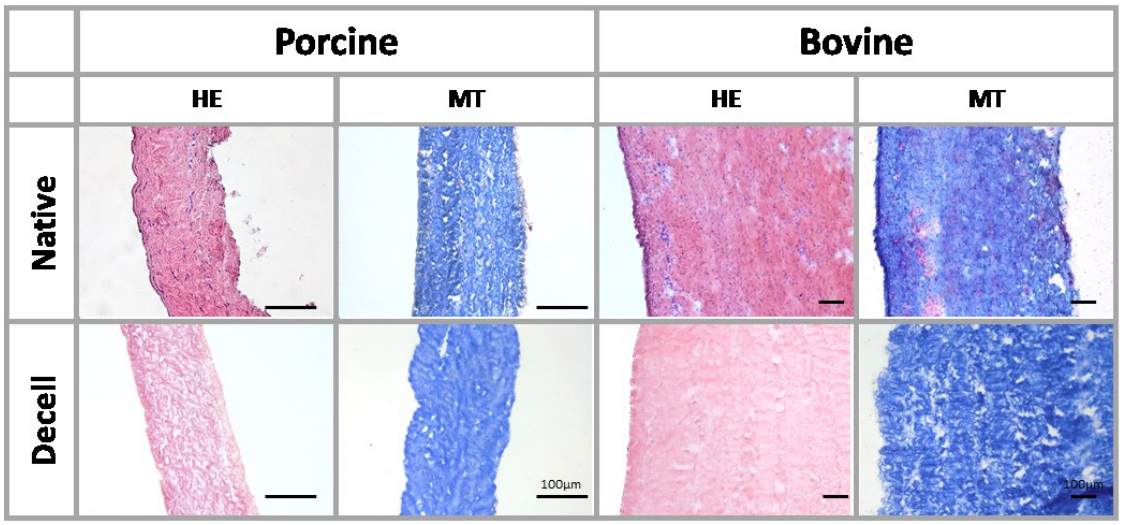

Figure 3.7 HE and MT staining of native and decellularised porcine and bovine pericardium. Scale bar 100 µm.

3.2.2 Resident Pathogens

The resident pathogens found in native PP and BP are presented in Table 3.2. Despite the high variability observed, the contaminants found on native tissues were found to be Gram$^+$ rather than Gram$^-$, with variability depending on the sample source. The contaminants belong to the species commonly present in the animal environment: *Streptococcus hyointestinalis* can be found on intestines of pigs (Devriese 1988), while *Streptococcus uberis* has been reported to be present in manure and organic matter in contact with animals (Currin 2012).

It is important to emphasize that the type of pathogens recorded can differ depending on the season of the year when the tissue is collected; e.g. during spring, there is a higher amount and variability of pathogens in the animal surrounding environment in comparison to the wintertime. The analyses here described were performed in different times of the year, providing a more complete description of the resident microorganisms and a wider indication of the target bioburden to be addressed.

Table 3.2 Identification of resident pathogens for pericardia and valves.

Tissue	**Pathogens**	
	Native	**Decellularised**
PP	*Pseudomonas aeruginosa* (Gram$^-$) *Enterococcus faecalis* (Gram$^+$) *Streptococcus uberis* (Gram$^+$) *Streptococcus hyointestinalis* (Gram$^+$) *Enterococcus faecium* (Gram$^+$)	----
BP	*Streptococcus infantarius ssp infantarius* (Gram$^+$) *Streptococcus hyointestinalis* (Gram$^+$) *Streptococcus infantarius ssp coli (str. Lutetiensis)* (Gram$^+$) *Staphylococcus vitulinus* (Gram$^+$) *Staphylococcus cohnii ssp cohnii* (Gram$^+$) *Aerococcus viridans* (Gram$^+$)	----

Sterility assessment of decellularised bovine and porcine pericardium with TRICOL protocol resulted in no growth of microorganisms after 14 days of incubation, indicating the disinfection potential of TRICOL decellularisation procedure. However, in a test experiment, the TRICOL decellularisation procedure alone was not sufficient to produce sterile scaffolds after the CC of the native tissues with ≈10^9 CFU/mL of *Staphylococcus*

aureus, *Enterococcus faecalis* and *Escherichia coli*. In fact, *Enterococcus faecalis* and *Staphylococcus aureus* were detected on decellularised PPD, while *Enterococcus faecalis* and *Escherichia coli* were found on BPD (Figure 3.8). This suggested that the TRICOL decellularisation procedure was effective as a disinfection method for tissues with a lower bioburden and that the effectiveness of a sterilisation treatment is dependent on the initial bioburden present in the tissues.

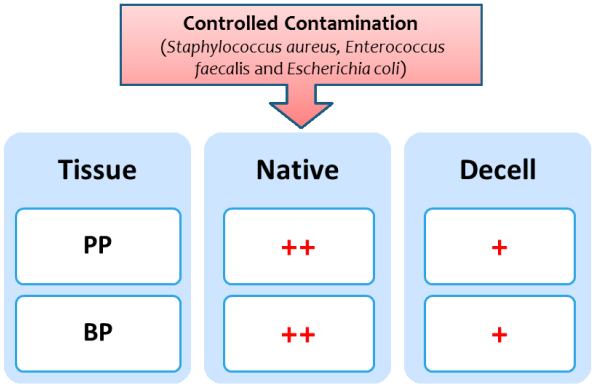

Tissue	Pathogens
Porcine Pericardium Decellularised (PPD)	*Enterococcus faecalis* and *Staphylococcus aureus*
Bovine Pericardium Decellularised (BPD)	*Enterococcus faecalis* and *Escherichia coli*

Figure 3.8 Effectiveness of TRICOL protocol in high bioburden contaminated bovine and porcine native pericardia.

3.3 Sterilisation Protocol 1: AA + PAA

3.3.1 Sterility Assessment

Sterility was assessed after AA treatment and PAA treatment on controlled contaminated scaffolds with high bioburden (Figure 3.9). As revealed by the turbidity of the medium, contaminants were detected in all samples after AA treatment (Figure 3.10) while PAA treatment at both concentrations (0.05% and 0.1%) resulted in no growth of microorganisms observed for PPD and BPD after 14 days of incubation.

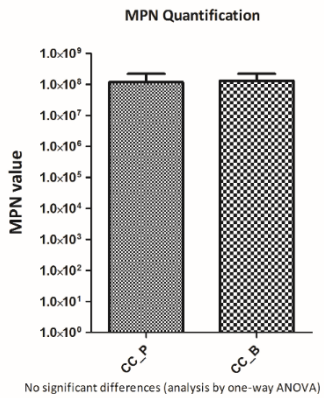

Figure 3.9 MPN quantification of CC in PPD and BPD.

In summary, the treatment with the both concentrations of PAA (0.1% and 0.05%) has been proven effective in the complete elimination of a high bioburden of microorganisms in several decellularised tissues: pericardia from bovine and porcine origin.

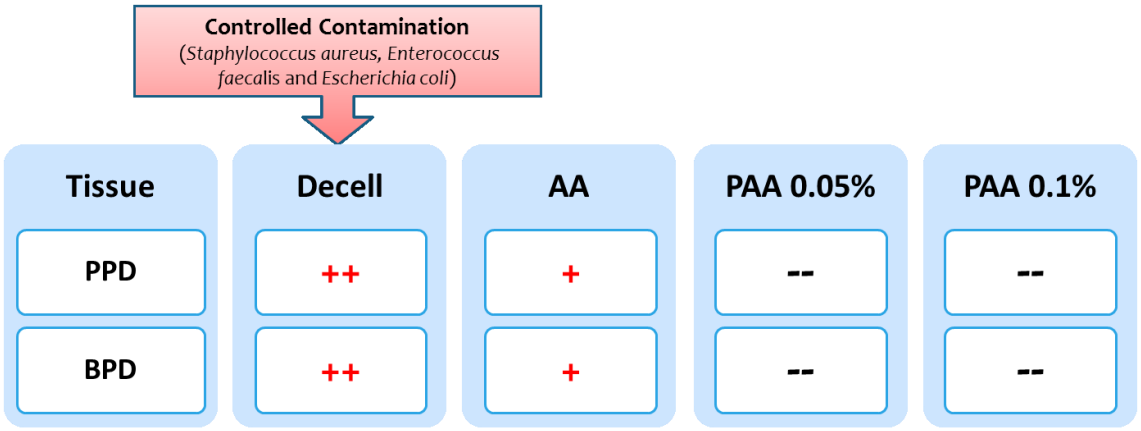

Figure 3.10 Sterility assessment of inoculated media for decellularised scaffolds after Sterilisation Protocol 1.

The quantification of the microorganisms by the MPN method (Figure 3.11 (a)) confirmed the results observed after the 14-days inoculation: no contaminants were detected after treatment with PAA at both concentrations. AA treatment resulted in a decrease of microorganisms for the analysed tissues, in a significant manner for bovine pericardium.

Qualification of residual bioburden after AA treatment was performed by MALDI-TOF (Figure 3.11 (b)). Bacteria identification of the tissues under test revealed that the most common microorganisms were *Enterococcus faecalis* and *Escherichia coli.* These bacteria can produce pili to improve attachment to surfaces, therefore elimination can be more difficult.

a)

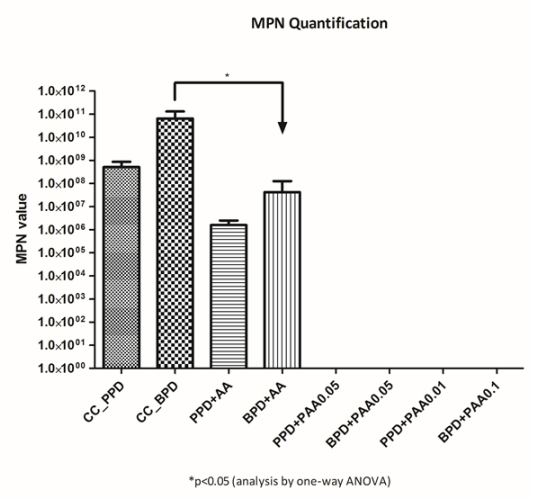

b)

Tissue	Pathogens
Porcine Pericardium Decellularised (PPD)	*Enterococcus faecalis, Staphylococcus aureus, Escherichia coli*
Bovine Pericardium Decellularised (BPD)	*Enterococcus faecalis, Escherichia coli*

Figure 3.11 Sterility assessment of Protocol 2: (a) MPN quantification and (b) bioburden after AA treatment for PPD and BPD.

3.3.2 Histological and Immunofluorescence Assessment

The ECM structure of pericardial scaffolds was assessed by histological staining following AA and PAA treatment (Figure 3.12 and Figure 3.13). HE, MT and AB staining were performed to visualize the structure of collagen fibres and GAGs, as well as the general appearance of the matrix.

As expected, AA treatment maintained the ECM histoarchitecture for all tissues analysed. On the contrary, the treatment with 0.1% PAA induced harsh effects on the ECM structure of porcine pericardium. In these cases, the ECM of the tissue appears damaged, as fragmented collagen network and large spaces can be observed.

Regarding the immunofluorescence, the components collagen I and IV, elastin, laminin and heparin sulphate of the both scaffolds were analysed (Figure 3.14 and Figure 3.15). All components were present in both porcine and bovine scaffolds after the Sterilisation Protocol 1. The signal was similar for all tissues tested and a general well preserved ECM was observed.

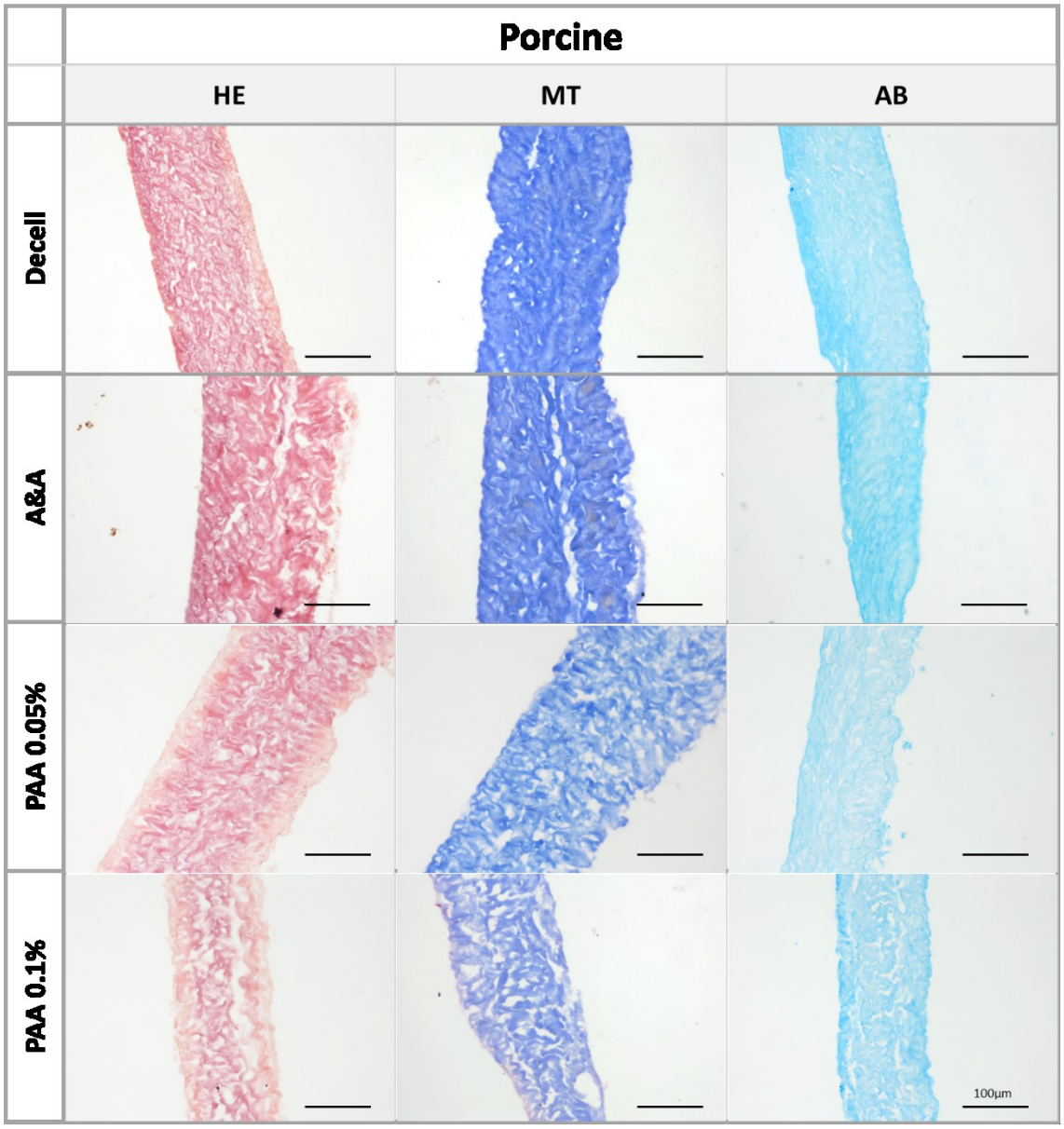

Figure 3.12 HE, MT and AB staining of PPD after Sterilisation Protocol 1 treatments. Scale bar 100 µm.

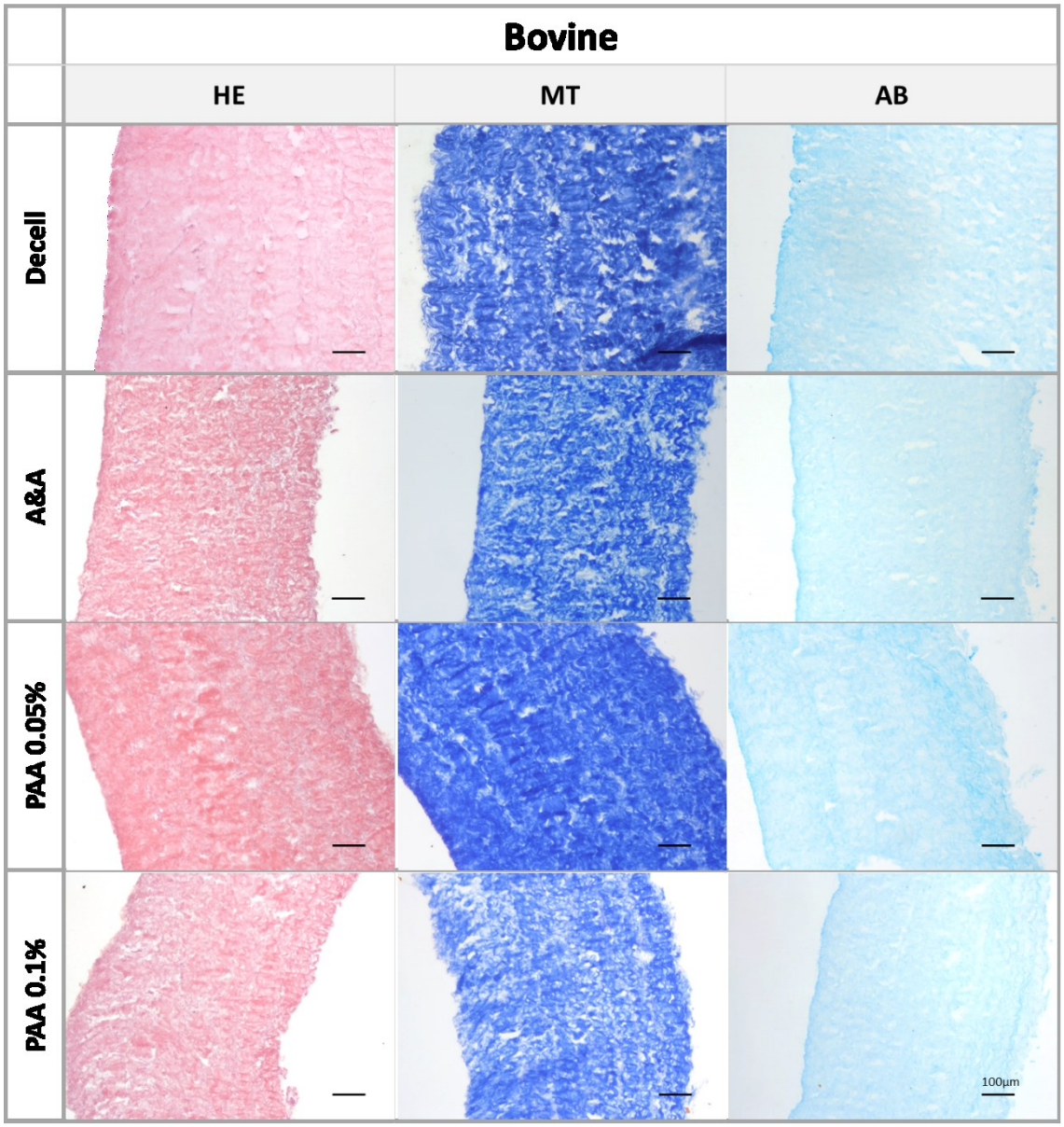

Figure 3.13 HE, MT and AB staining of BPD after Sterilisation Protocol 1 treatments. Scale bar 100 µm.

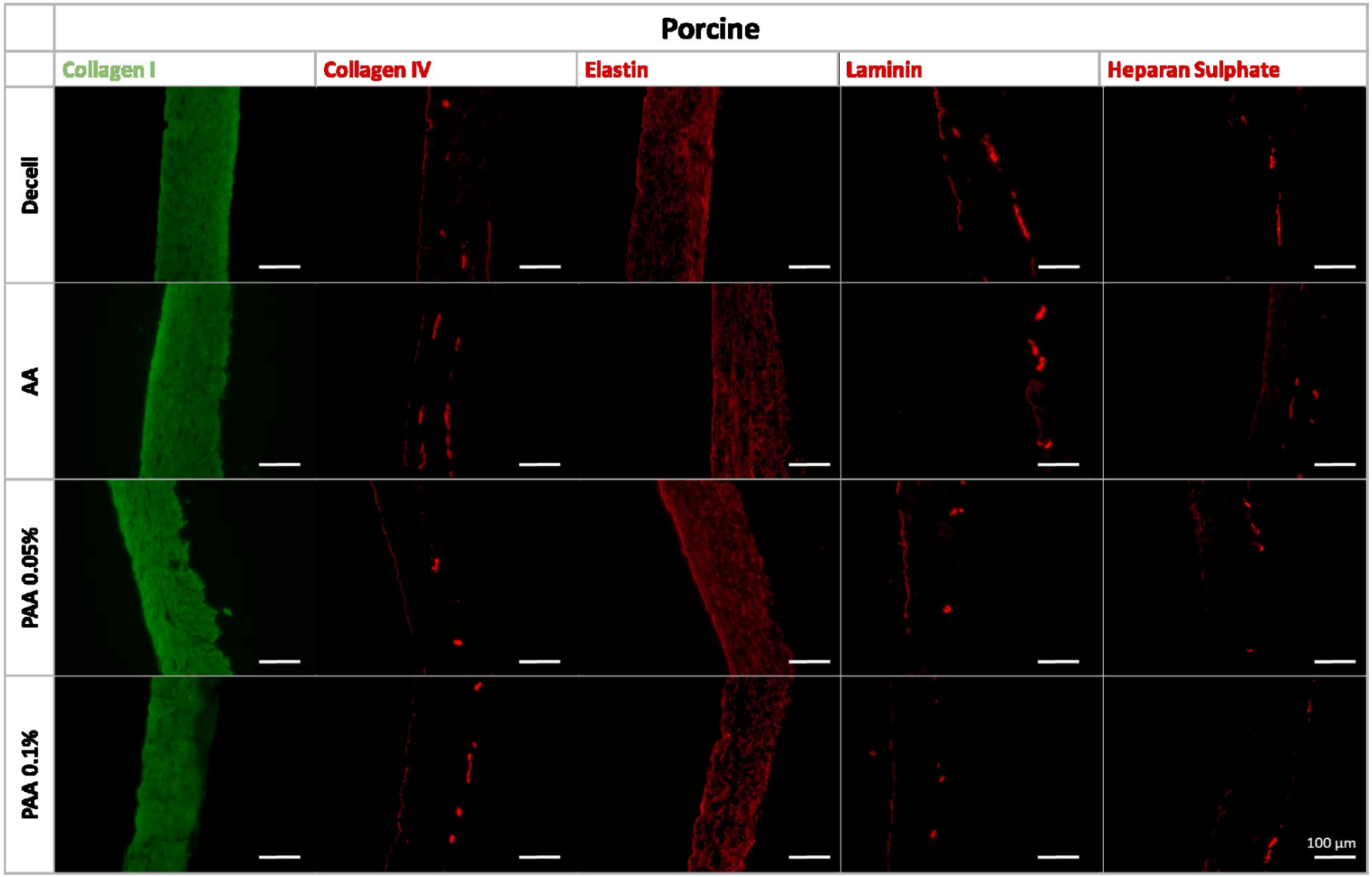

Figure 3.14 Immunofluorescence of PPD after Sterilisation Protocol 1 treatments. Scale bar 100 µm.

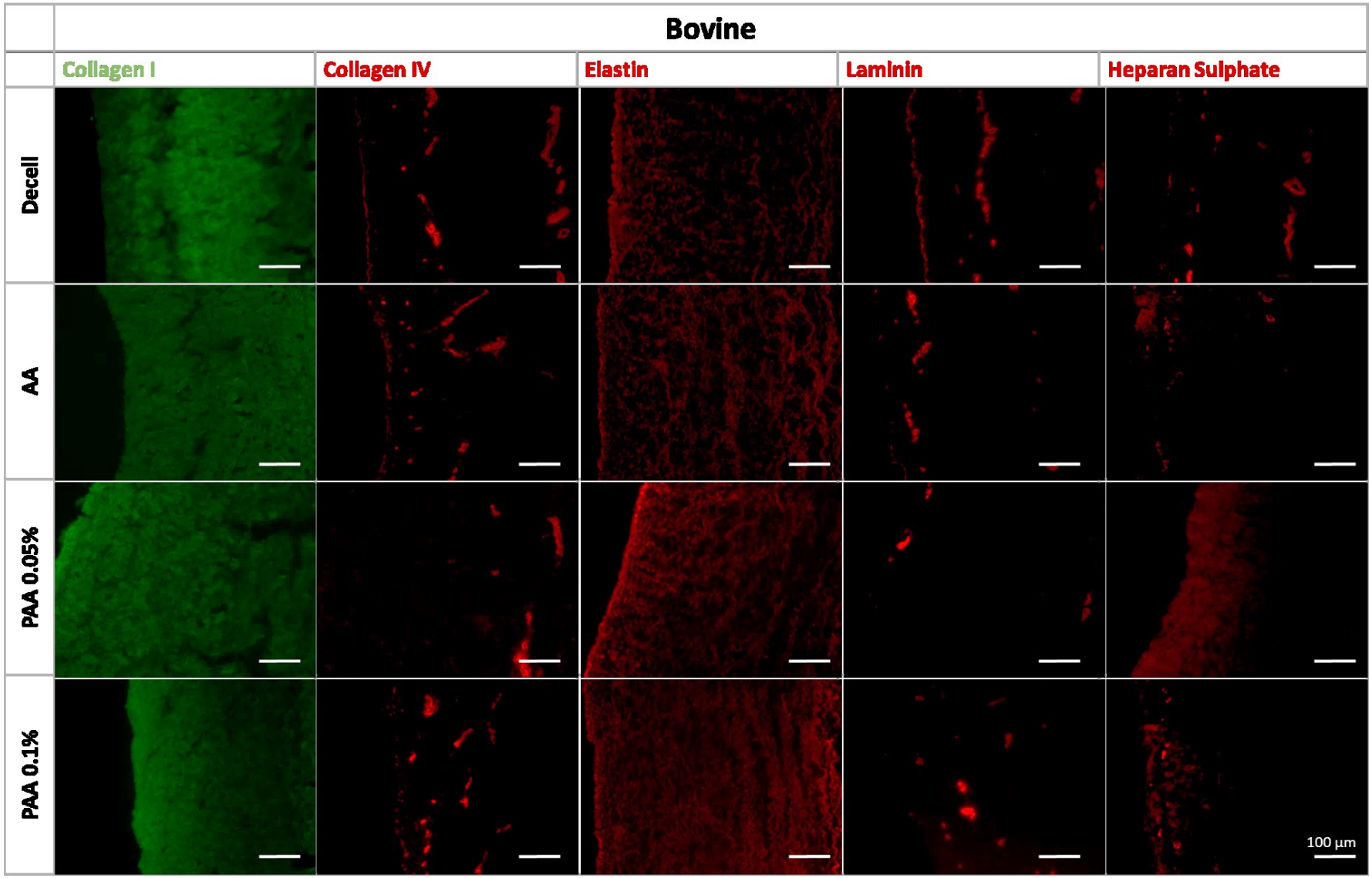

Figure 3.15 Immunofluorescence of BPD after Sterilisation Protocol 1 treatments. Scale bar 100 µm.

3.3.3 Biochemical Assessment

Collagen and GAGs are two of the major components of the pericardial scaffolds. Quantification of these components after each treatment can be indicative of the extension of the possible damages caused by the treatment performed. Collagen content is estimated by the quantification of HYP, one of the major proteins of collagen. HYP and GAGs were quantified before and after the treatments with AA and PAA (0.05% and 0.1%). In Figure 3.16 (a) are represented values of HYP quantification. No significant differences were observed in the HYP content before and after the treatments on porcine tissue, while the PAA 0.05% treatment on bovine tissue seems to induce an increase in HYP content. Depletion of ECM components other that HYP by the sterilisation treatments could be accounted for the increase of the relative proportion of HYP on dry weight in sterilized tissues. However, no significant differences were observed in the GAGs content after each treatment of both bovine and porcine pericardia, as depicted in Figure 3.16 (b).

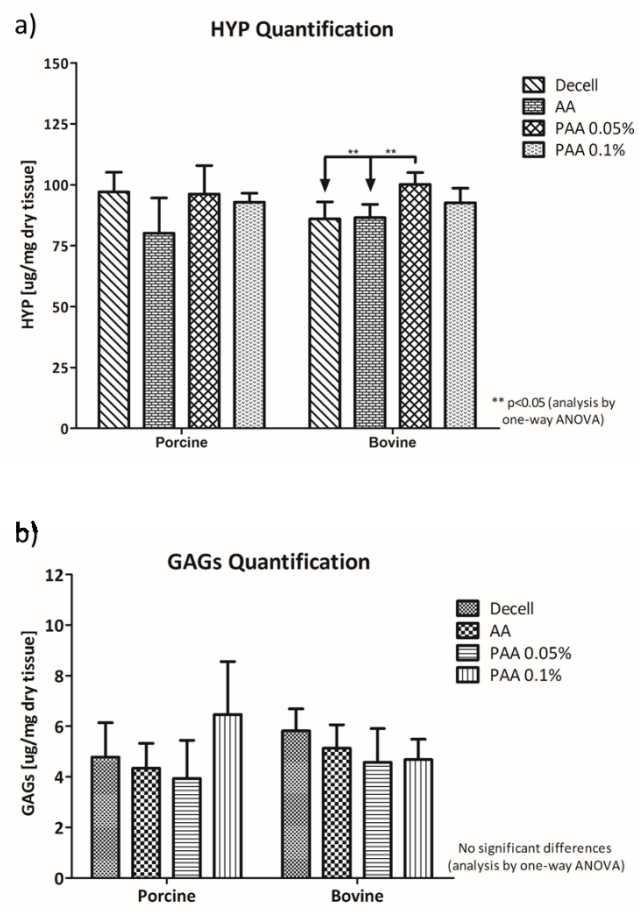

Figure 3.16 (a) HYP quantification and (b) GAGs of PPD and BPD.

3.3.4 Biomechanical Assessment

Biomechanical properties of the decellularised pericardia were assessed by uniaxial tensile test. After biomechanical test, stress-strain curves were plotted for each sample and a representative curve can be observed in Figure 3.17. All the tested samples are behaving biomechanically in agreement with previous observations by Radjeman, et al. (Radjeman, Liew et al. 1985). Calculation of UTS, failure strain and Young's modulus of the collagen slope were performed.

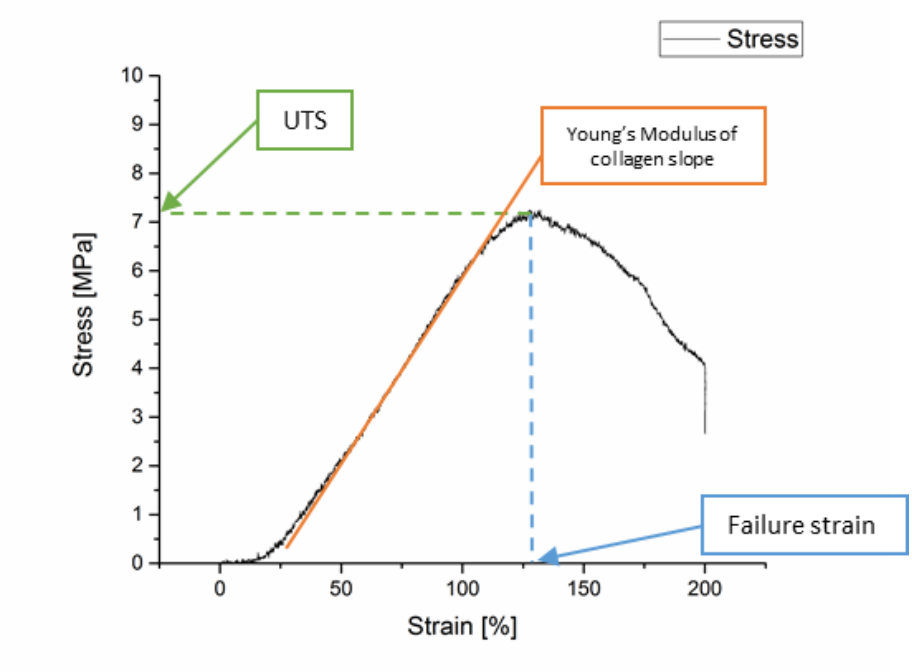

Figure 3.17 Example of stress-strain curve obtained with biomechanical test.

Failure strain, UTS and Young's modulus are presented in Figure 3.18 (a), (b) and (c) respectively. In case of porcine tissue, AA and 0.1% PAA treatment induced a significant decrease in failure strain, while PAA 0.05% treatment produced an increase of the UTS. For the bovine scaffolds, the treatments did not result in any significant differences of the failure strain and UTS as scaffolds in all groups presented a more uniform behaviour in comparison with porcine. On the other hand, the Young's modulus of both porcine and bovine scaffolds was not modified after the different treatments (Figure 3.18 (c)).

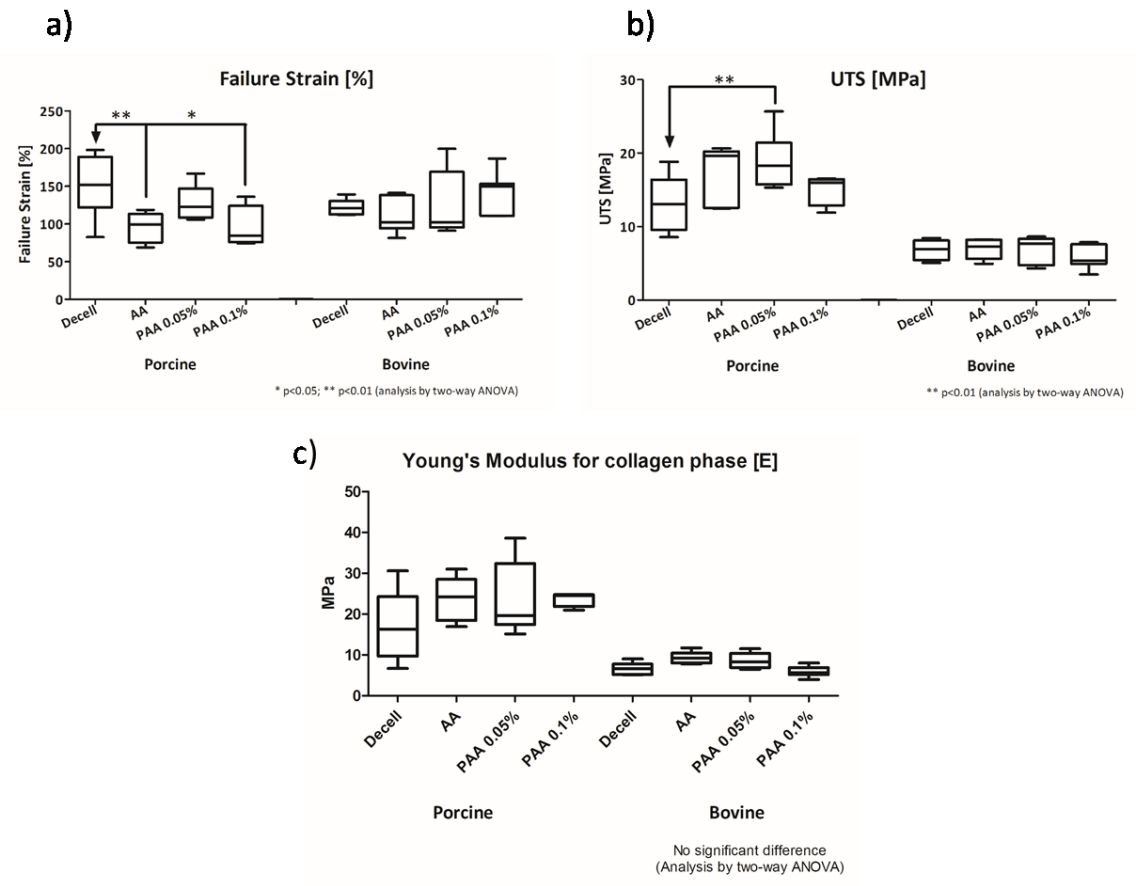

Figure 3.18 (a) Failure strain, (b) UTS and (c) Young's modulus of collagen phase of PPD and BPD.

3.3.5 SEM

Surface of the scaffolds was observed by SEM. This technique permits the observation in detail of surface of scaffolds where damages can be reported by disruption of tissue fibres. SEM analysis of both serosa and fibrosa surface of porcine and bovine pericardial scaffolds are presented in Figure 3.19 and Figure 3.20. It can be observed a cobblestone-like morphology more evident in the bovine scaffolds. For porcine scaffolds, a smoothing of both fibrosa and serosa surface after PAA treatment was detected. However, in the case of the bovine scaffolds, this effect was not observed at the same extension.

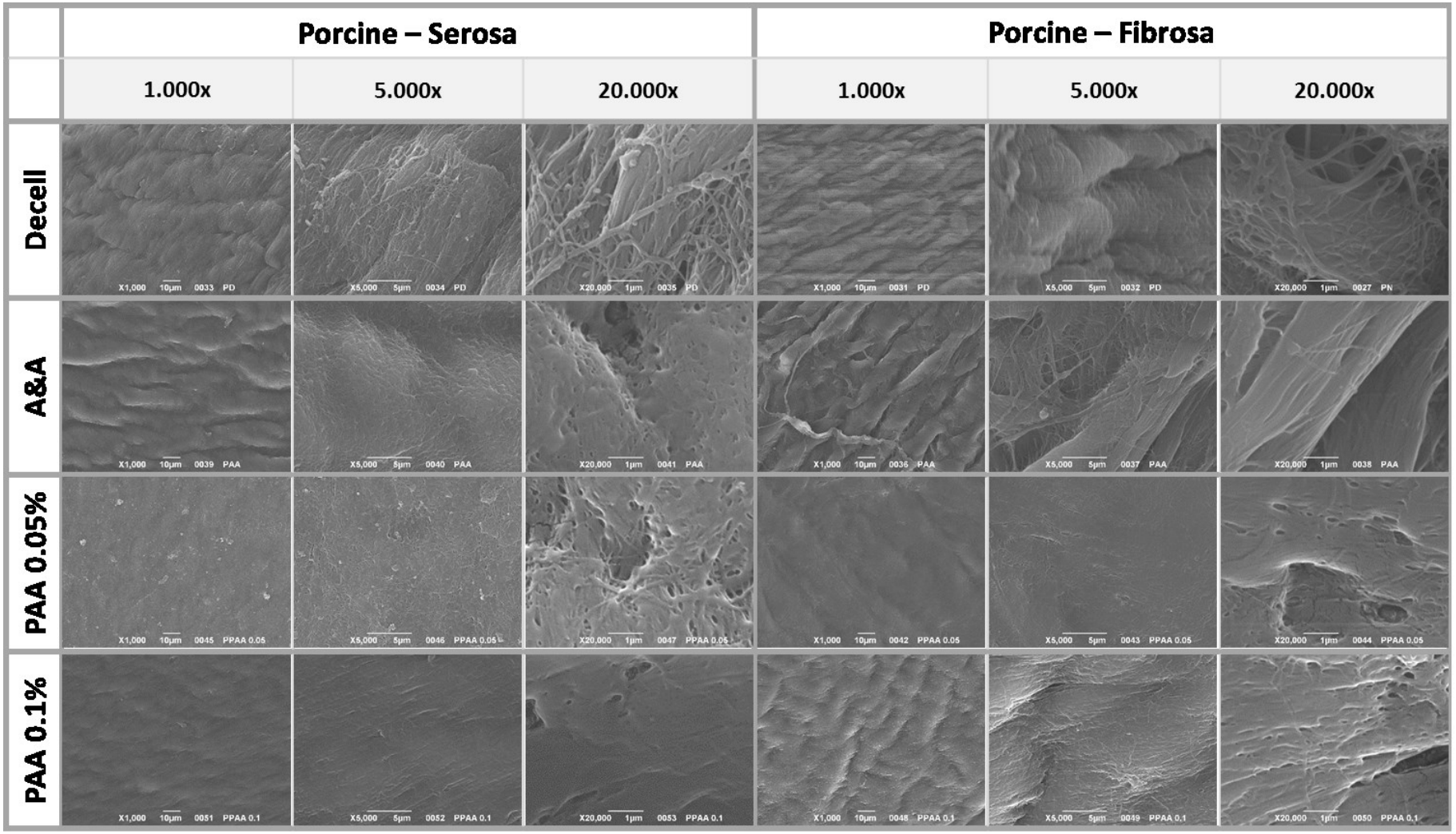

Figure 3.19 SEM analysis of PPD (fibrosa and serosa). Scale bar 10, 5 and 1 µm.

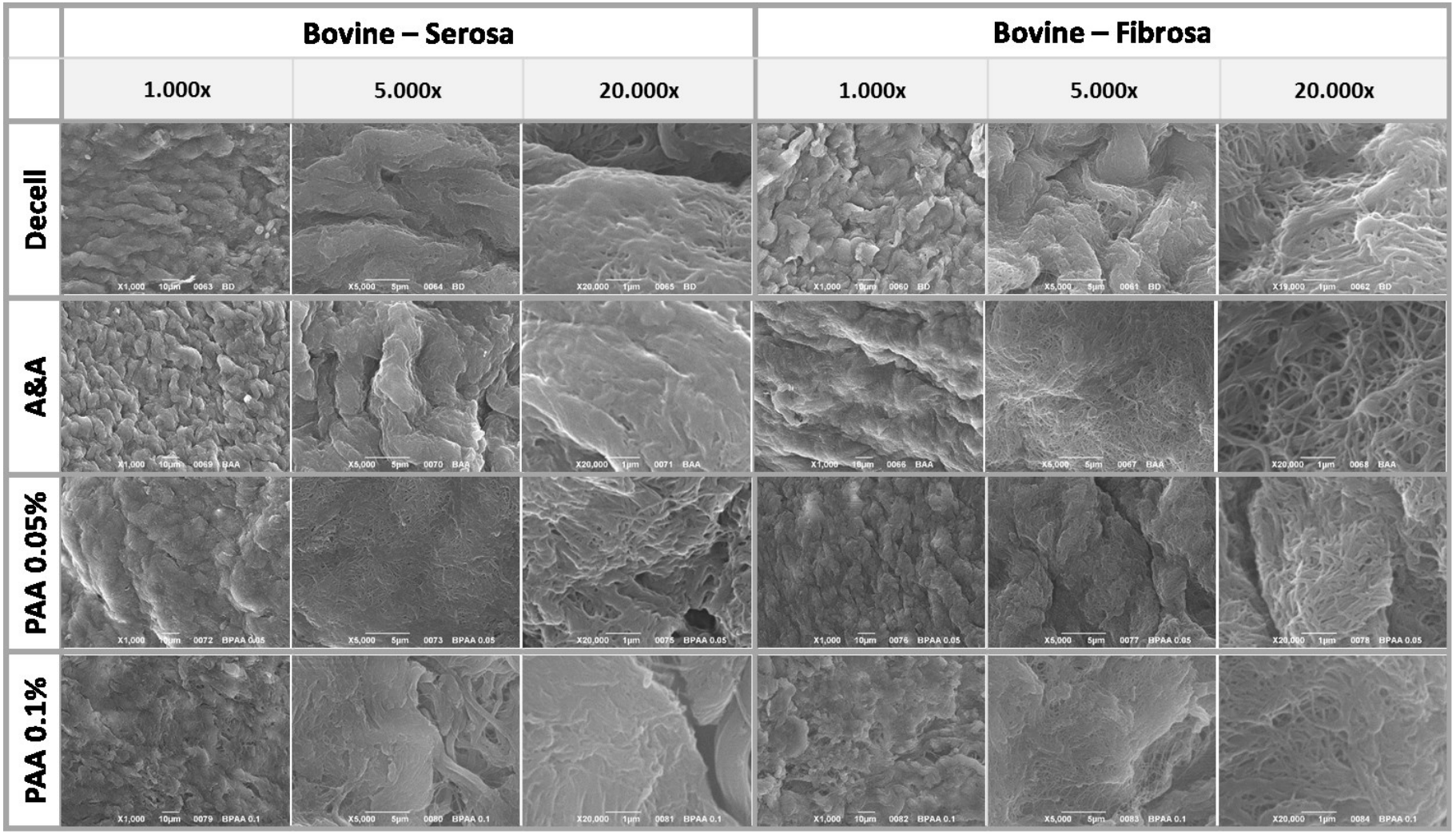

Figure 3.20 SEM analysis of BPD (fibrosa and serosa). Scale bar 10, 5 and 1 µm.

3.3.6 Cell Seeding Experiments

Sterilisation of biological tissues could induce modifications that could potentially affect their compatibility. For this reason, biocompatibility of the sterilized scaffolds was assessed through cell seeding experiments with hBM-MSCs. Cytotoxicity was evaluated by LDH quantification of the cell culture supernatant, while cell proliferation was investigated by MTS assay.

The results obtained for LDH analysis are plotted in Figure 3.21 (a) and (b) for porcine and bovine tissues, respectively. Cytotoxicity of the decellularised scaffolds after sterilisation treatment was surprisingly found to be lower compared to unsterilized ones, indicating that the sterilisation treatment enhanced biocompatibility of the tissue. This improvement in compatibility might be related with the effect of the treatments that exposed more the cues in the ECM responsible for cellular attachment and growth.

Cell proliferation after sterilisation of porcine and bovine pericardium is presented in Figure 3.22 (a) and (b). As confirmed by the trend showed by the cells seeded onto the polystyrene bottom of the well and on the biomaterials tested, hBM-MSCs proliferation is increasing during time. No differences in cell proliferation rates were observed among the treated porcine scaffolds, while for bovine tissues PAA at both concentrations was found to significant decrease the number of cells compared to AA-treated scaffold at 7 days. However, this difference was completely recovered at 14 days of cell seeding.

The results obtained for both LHD and MTS tests provide evidence that the treatments applied do not appear to lead to cytotoxic scaffolds or interfere with cell attachment and proliferation on the scaffold sterilized with the proposed method.

To the aim of further assess the cell adhesion to pericardial sterilized scaffolds, cell seeded samples were processed for histology and stained with HE (Figure 3.23 and Figure 3.24). As it can be observed, a cell monolayer is present on both bovine and porcine pericardial scaffolds, more uniform and continue after 14 days of hBM-MSC seeding.

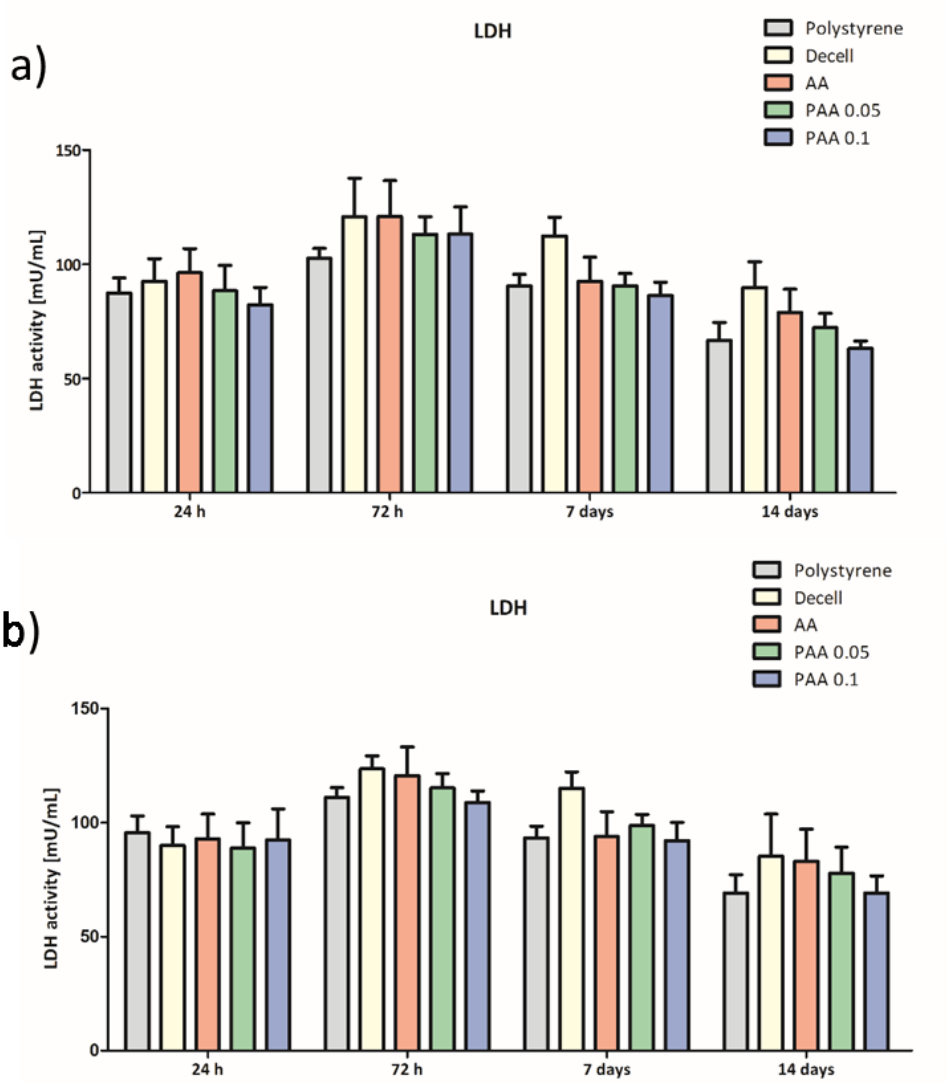

Analysis by two-way ANOVA	24h	72h	7d	14d
Porcine	AA vs PAA0.1*	Polystyrene vs Decell** Polystyrene vs AA**	Decell vs AA** Polystyrene vs Decell*** Decell vs PAA0.05*** Decell vs PAA0.1***	Decell vs PAA 0.05** Polystyrene vs Decell*** Decell vs PAA 0.1*** AA vs PAA0.1*
Bovine		Decell vs PAA0.1*	Decell vs PAA0.05** Polystyrene vs Decell*** Decell vs AA*** Decell vs PAA0.1***	Polystyrene vs Decell* Polystyrene vs AA* Decell vs PAA0.1* AA vs PAA0.1*
*p<0.05; **p<0.01; ***p<0.001				

Figure 3.21 LDH quantification of (a) PPD and (b) BPD after 24h, 72h, 7d and 14d of hBM-MSC seeding.

a)

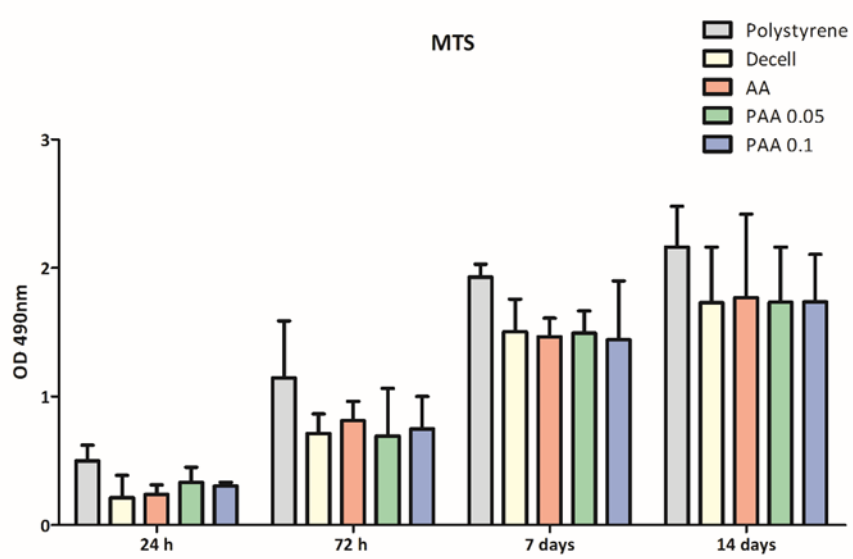

b)

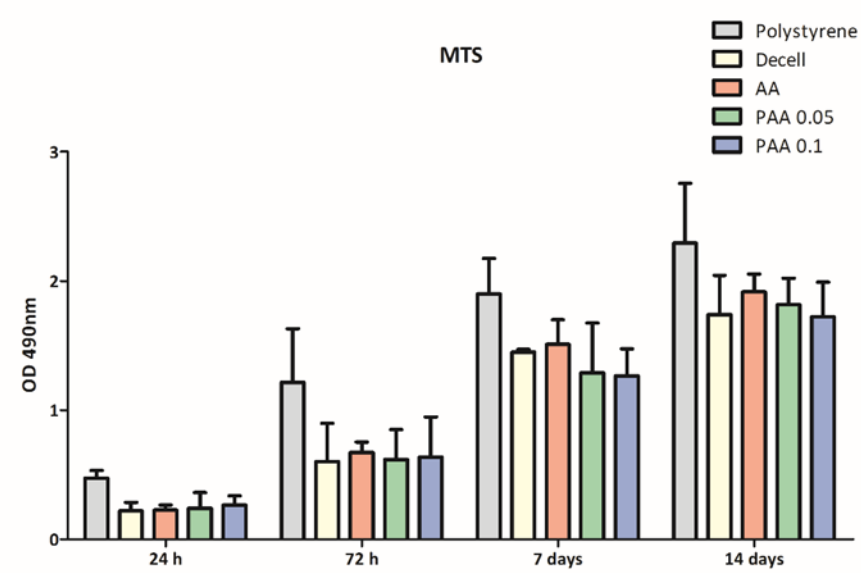

Analysis by two-way ANOVA	24h	72h	7d	14d
Porcine	Polystyrene vs Decell*	Polystyrene vs AA** Polystyrene vs PAA 0.1** Polystyrene vs Decell*** Polystyrene vs PAA0.05***	Polystyrene vs Decell*** Polystyrene vs AA*** Polystyrene vs PAA0.05*** Polystyrene vs PAA 0.1***	Polystyrene vs AA** Polystyrene vs Decell*** Polystyrene vs PAA0.05*** Polystyrene vs PAA 0.1***
Bovine	Polystyrene vs Decell* Polystyrene vs AA* Polystyrene vs PAA0.05*	Polystyrene vs Decell*** Polystyrene vs AA*** Polystyrene vs PAA0.05*** Polystyrene vs PAA0.1***	Polystyrene vs Decell*** Polystyrene vs AA*** Polystyrene vs PAA0.05*** Polystyrene vs PAA0.1*** AA_PAA0.05* AA vs PAA0.1*	Polystyrene vs Decell*** Polystyrene vs AA*** Polystyrene vs PAA0.05*** Polystyrene vs PAA0.1***
*p<0.05; **p<0.01; ***p<0.001				

Figure 3.22 MTS quantification of (a) PPD and (b) BPD after 24h, 72h, 7d and 14d of hBM-MSC seeding.

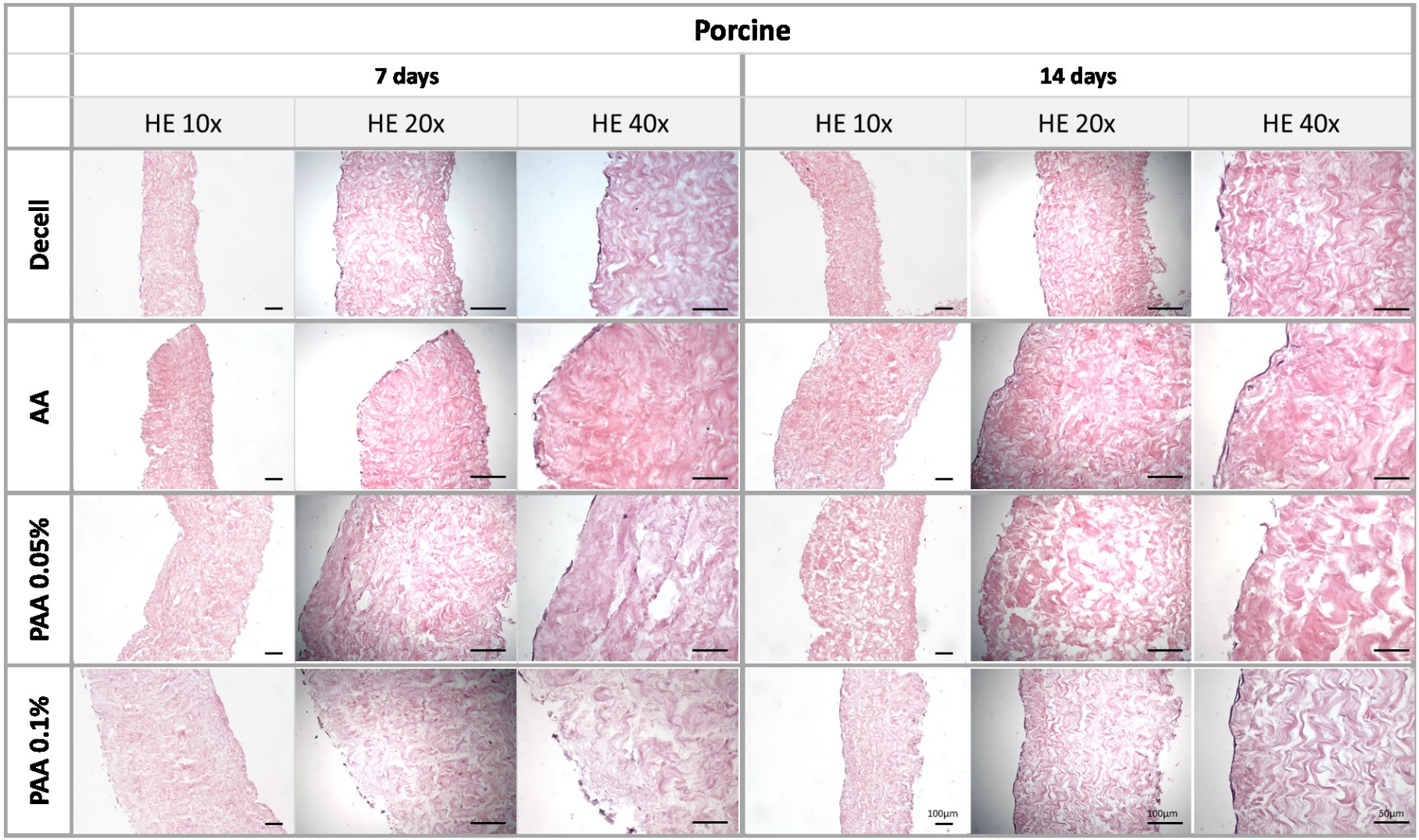

Figure 3.23 HE staining of PPD after 7d and 14d of hBM-MSC cell seeding. Scale bar 100 and 50 µm.

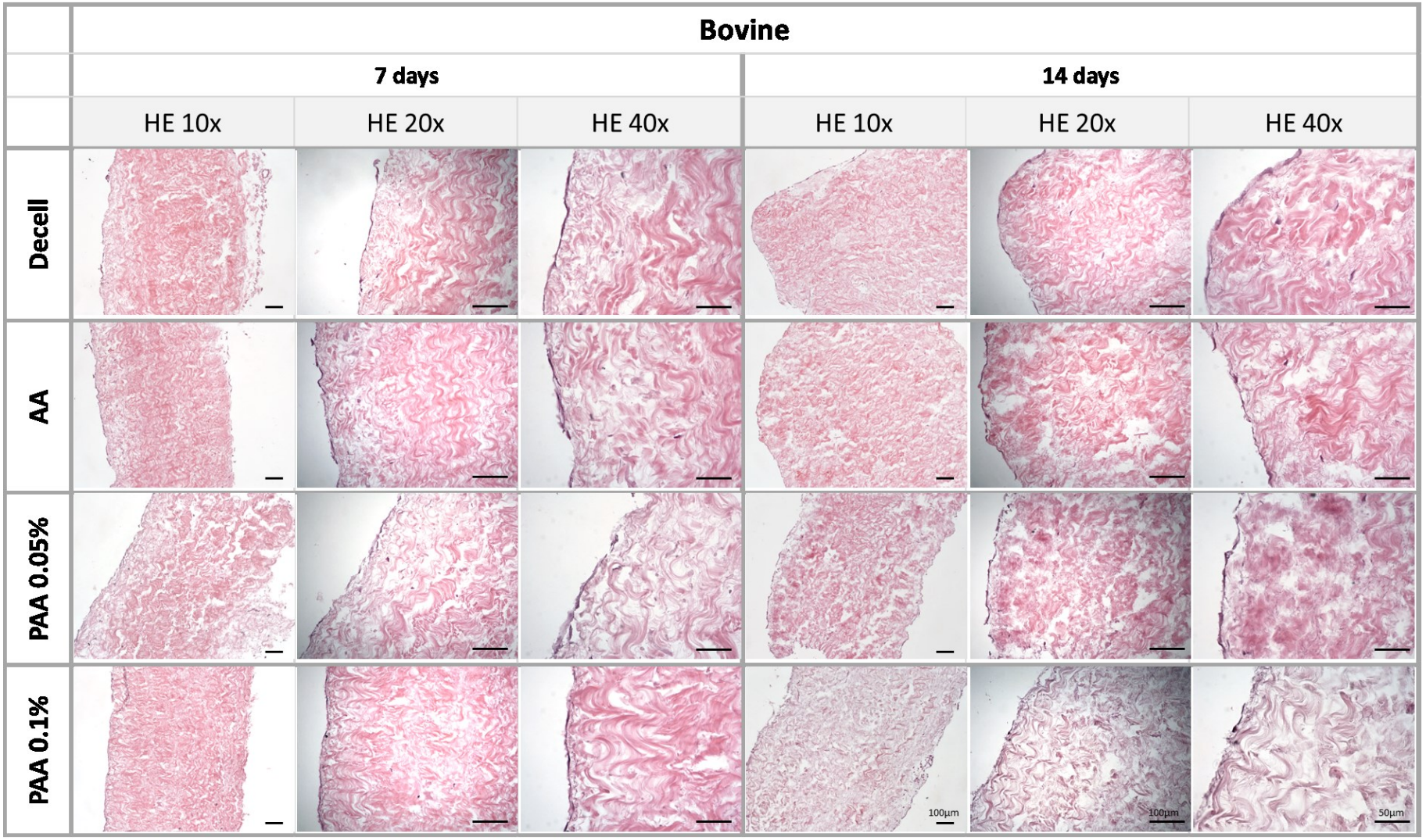

Figure 3.24 HE staining of BPD after 7d and 14d of hBM-MSC cell seeding. Scale bar 100 and 50 µm.

3.4 Sterilisation Protocol 2: γ-irradiation

The second protocol is based on the utilization of γ-irradiation. Tissues underwent to the sterilisation protocol were subsequently evaluated in terms of sterility and histological, biochemical and SEM analyses.

3.4.1 Sterility Assessment

Sterility assessment was performed on the scaffolds after the treatment applying five different dosages: 1.5, 5, 10, 15 and 25 kGy. Three types of CC were performed on decellularised pericardial scaffolds: 'standard' CC comprising *Staphylococcus aureus, Enterococcus faecalis* and *Escherichia coli*; only *BacP*; *BacP* in spore form induced by heat shock (*BacP*+HS). Quantification of contaminants by MPN method confirmed the effective contamination of both the pericardial scaffolds in study (Figure 3.25) where CC was proven to induce a higher concentration of contaminants than *BacP*.

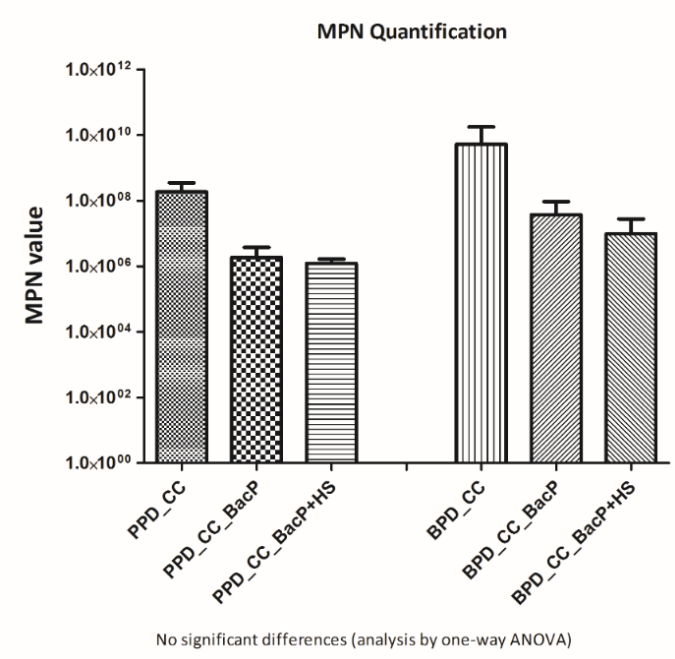

Figure 3.25 MPN quantification of CC in PPD and BPD.

The results obtained from turbidity assessment following γ-irradiation for PPD and BPD are presented in Figure 3.26. Even with the lower dosages applied, all contaminants were eliminated including the spore form (*BacP*+HS) of the biological indicator (the more resistant form of bacteria) for the γ-irradiation treatment.

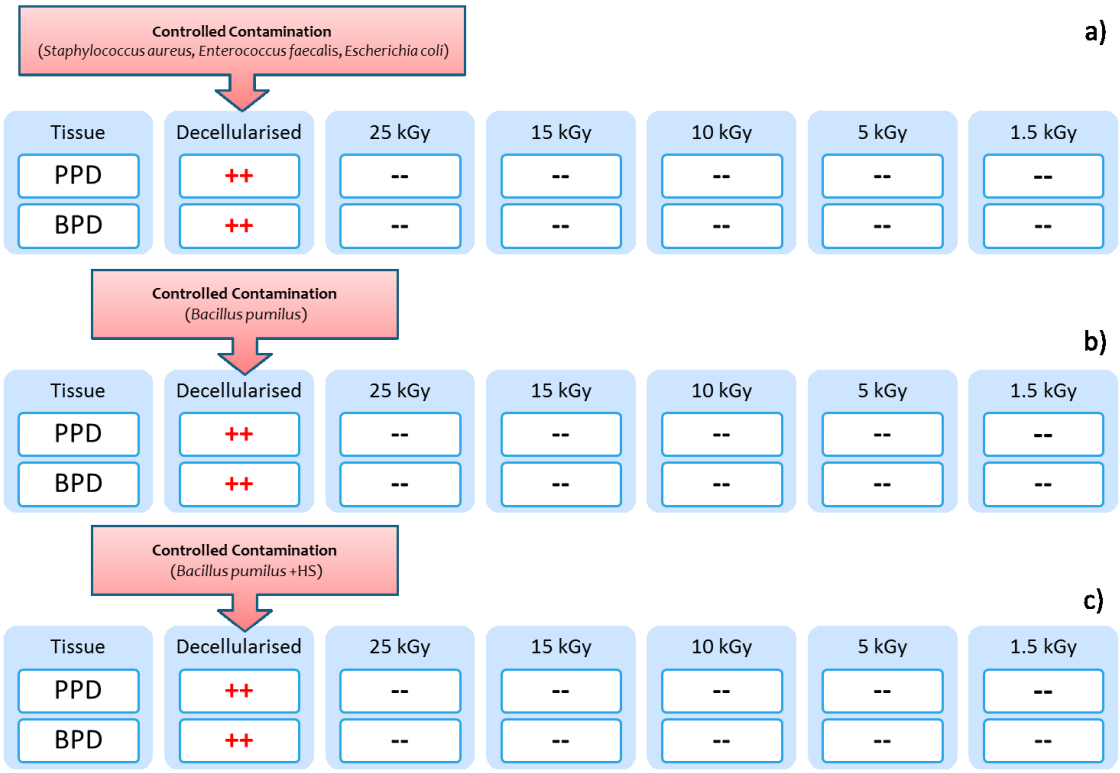

Figure 3.26 Sterility assessment of turbid and clear bacteria media of bovine and porcine scaffolds after CC with: (a) Staphylococcus aureus, Enterococcus faecalis and Escherichia coli; (b) BacP and (c) BacP+HS.

3.4.2 Histological and Immunofluorescence Assessment

ECM structure of PPD and BPD after γ-irradiation treatment was assessed by histological staining with HE, MT and AB (Figure 3.27 and Figure 3.28). Results indicated that tissues treated with low dosages maintained the ECM gross histoarchitecture. Apparently, no conclusive differences of the ECM structure and components distribution can be detected in all the dosages applied, even after the exposure to the higher dosage (25 kGy). Further quantification of the components of the matrix (HYP and GAGs) can provide an insight of these observations in histological sections.

Regarding the detection of specific components of the matrix, the immunofluorescence images obtained can be observed in Figure 3.29 and Figure 3.30. The components collagen I and IV, elastin, laminin and heparan sulphate were present in all sections except for the heparin sulphate in bovine tissue treated with 15 kGy, where no signal was detected. In general, both scaffolds treated with γ–irradiation preserved the main components of the ECM.

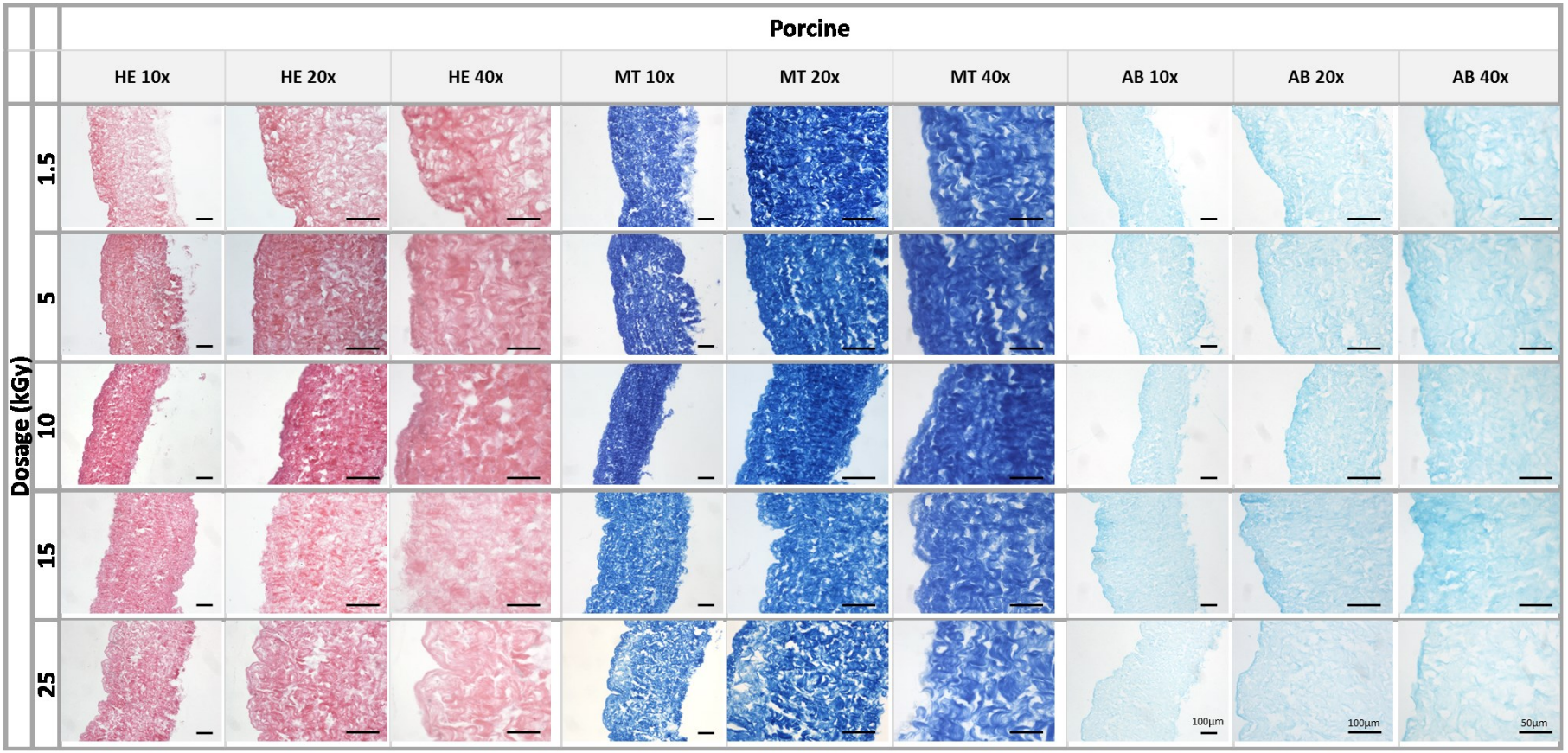

Figure 3.27 HE, MT and AB staining of PPD after γ-irradiation treatment. Scale bar 100 and 50 µm.

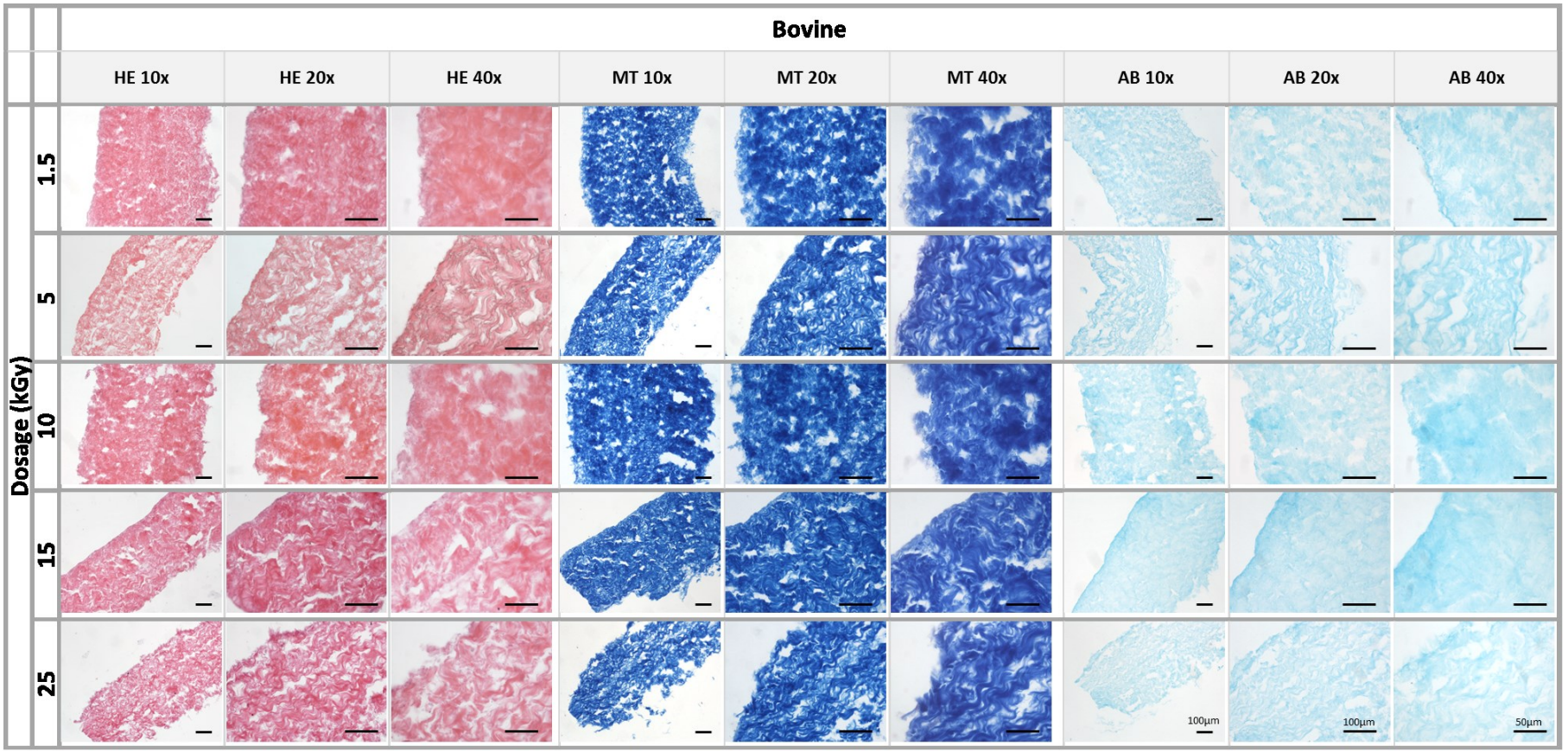

Figure 3.28 HE, MT and AB staining of BPD after γ-irradiation treatment. Scale bar 100 and 50 µm.

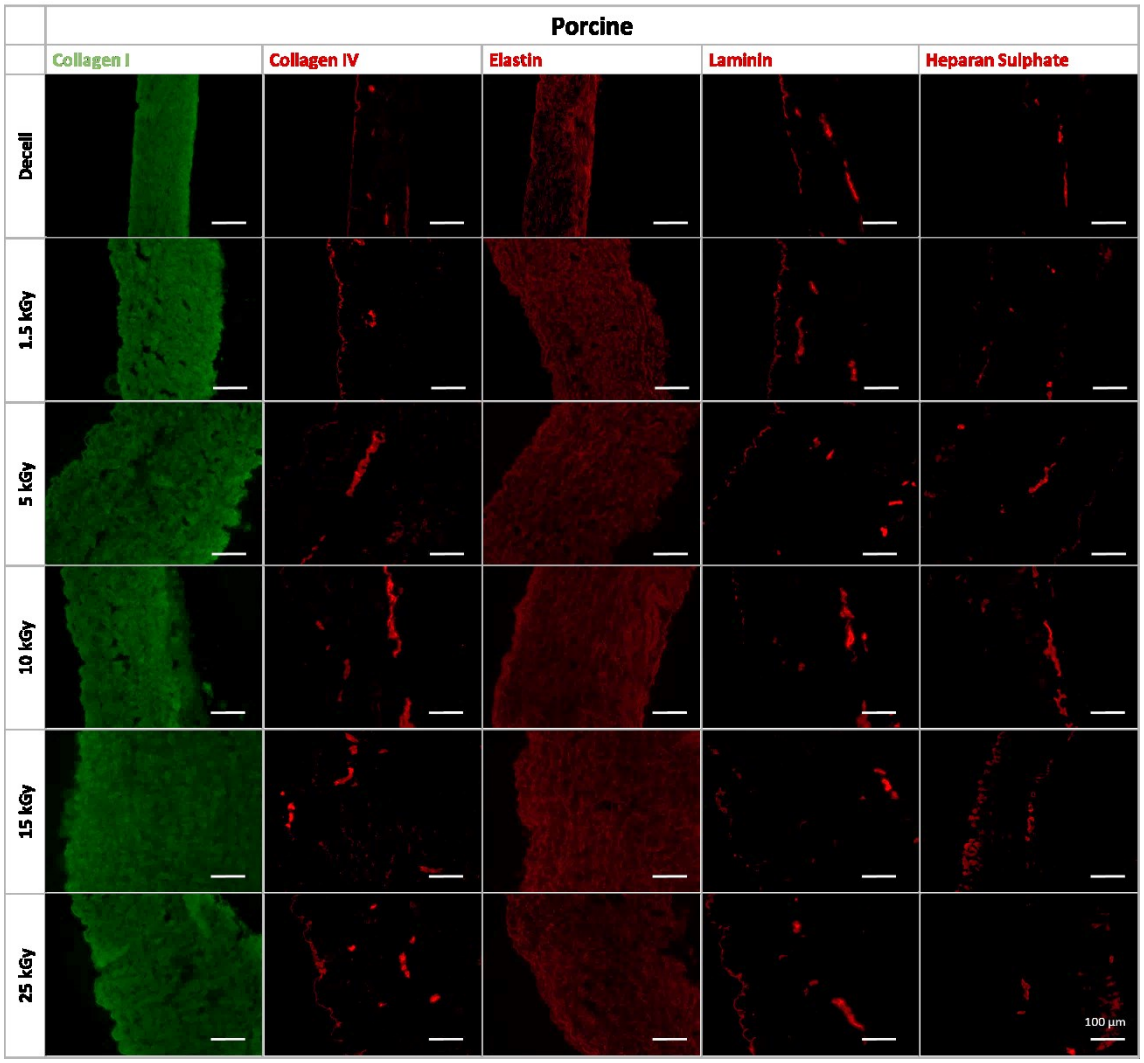

Figure 3.29 Immunofluorescence PPD after γ-irradiation treatment. Scale bar 100 µm.

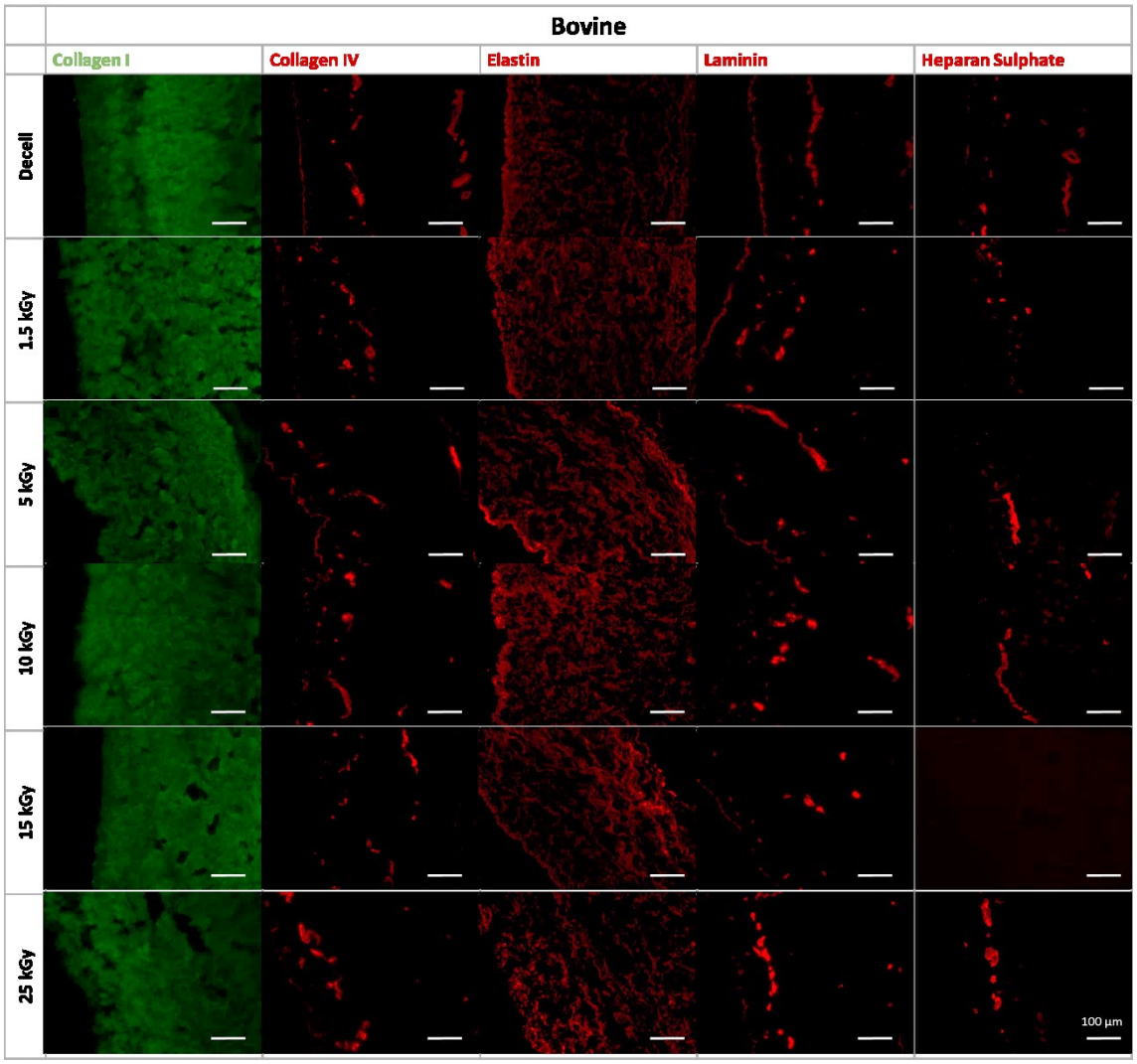

Figure 3.30 Immunofluorescence BPD after γ-irradiation treatment. Scale bar 100 µm.

3.4.3 Biochemical Assessment

In order to deeply investigate the extension of the damages after γ-irradiation treatment in several dosages, major components of the matrix, HYP and GAGs were quantified. In Figure 3.31 (a) are plotted the values obtained from HYP quantification of porcine and bovine untreated and sterilized scaffolds. γ-irradiation treatment was proven to not reduce the total amount of HYP present in the tissues. However, it was observed an increase of HYP content in bovine pericardial decellularised scaffold after 15 and 25 kGy treatment. As previously observed during HYP quantification after the application of the sterilisation protocol 1, other components of the ECM components could be affected by

the sterilisation treatment, thus inducing an increase of the relative proportion of HYP on dry weight in treated tissues.

As in the case of the Protocol with AA and PAA and represented in Figure 3.31 (b), GAGs content of the decellularised scaffolds resulted to not be affected by γ-irradiation for both bovine and porcine pericardia.

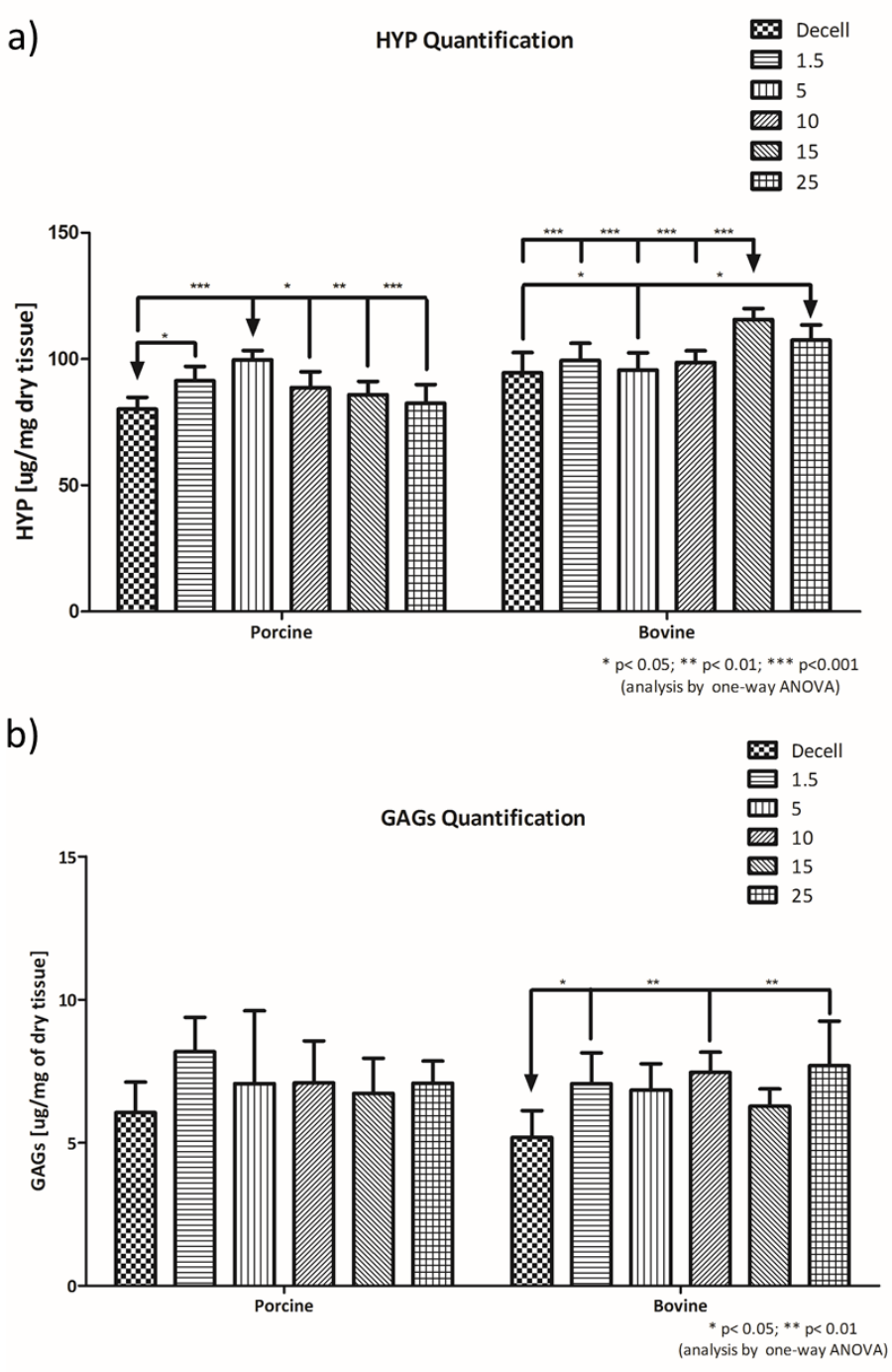

Figure 3.31 (a) HYP quantification and (b) GAGs quantification of PPD and BPD: Decellularised, 1.5, 5, 10, 15 and 25 kGy treatment.

3.4.4 SEM

SEM analysis of both serosa and fibrosa surface of porcine and bovine pericardial γ-irradiated scaffolds are presented in Figure 3.32. In comparison with the decellularised control, the treated scaffolds present more evident fibres and a less smooth - wavier surface appearance. This can be related to condensation of collagen fibres or rupture of hydrogen bonds during the γ-irradiation treatment. However, no major damages on the continuity of the fibres were observed in fibrosa and serosa surfaces of the treated scaffolds with the different dosages in study.

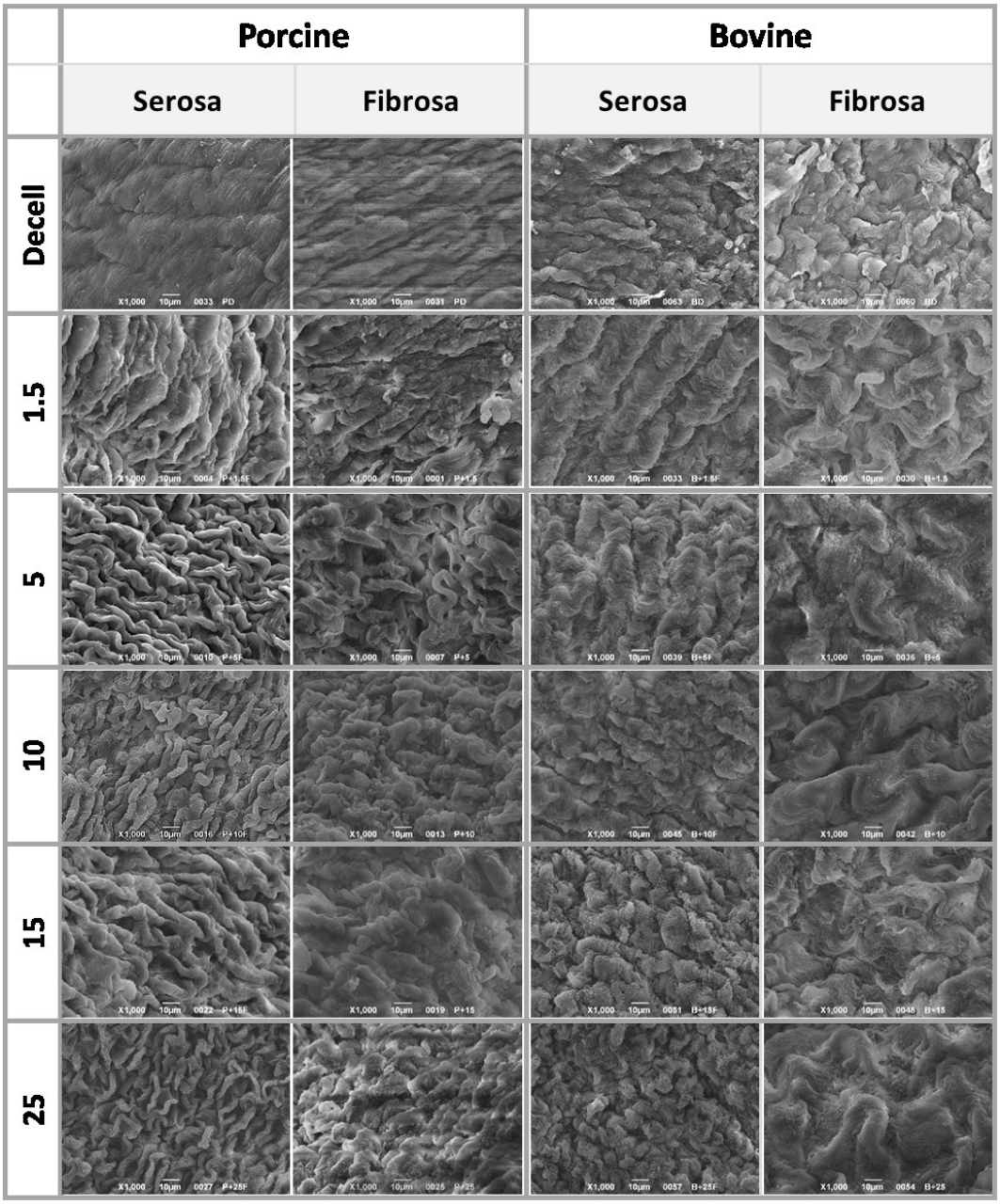

Figure 3.32 SEM analysis of PPD and BPD (fibrosa and serosa). Scale bar 10 µm.

CHAPTER IV

DISCUSSION, CONCLUSIONS & FUTURE WORK

4.1 Discussion

Decellularisation of xenogeneic tissues from different species has been employed to develop optimal scaffolds for several applications, as prosthetic heart valve manufacturing. Decellularisation aims at the complete elimination of the immunological cues whilst preserving tissue structure (Brown and Badylak 2014). Valvular bioprostheses currently applied in the clinical sector require glutaraldehyde fixation of xenogeneic tissues to avoid severe immune rejection due to the presence of xenogeneic epitopes. On the other side, homografts are limited to the organ donors' availability and not sufficient for the clinical requirements. The unlimited source of xenografts as well as similar structure of homografts (in case of porcine valves), are major advantages of the xenografts. In order to avoid the immune rejection issues previously referred, the decellularisation of these scaffolds provide an insight of the promising application of this decellularised tissues.

Despite the promising results obtained in terms of producing biocompatible decellularised xenogeneic scaffolds (Korossis, Booth et al. 2002, Schenke-Layland 2003, Iop, Renier et al. 2009, Zhou, Fritze et al. 2010, Mendoza-Novelo, Avila et al. 2011, Naso, Gandaglia et al. 2011, Gallo, Naso et al. 2012, Theodoridis, Tudorache et al. 2015), many studies are addressed to lower the risk of stenosis and calcification while promoting the repopulation of the scaffolds after implantation and the preservation of mechanical performances able to withstand the functional requirements of systemic circulation (Iop, Bonetti et al. 2014) (Spina, Ortolani et al. 2003, Hopkins, Jones et al. 2009) (Theodoridis, Tudorache et al. 2015) (Syedain, Reimer et al. 2015). In addition, a further limitation is the intrinsic possible risk of zoonosis related to the utilization of scaffold of animal origin. Currently, an effective sterilisation of the scaffold prior to implantation.

With regards to the homografts, procedures employed in tissue banks are optimized for the treatment of fresh harvested tissues, with the main aim of preserving cells and ECM by treatments with antibiotics and cryopreservation with dimethyl sulfoxide (DMSO) as cryoprotectant. Sterility assessment is performed in several points of the tissue processing and, in case of contamination, the tissue is discarded. Indeed, discards due

to contaminations can reach 15%, further reducing the already limited number of the available homografts.

In this PhD project, two different protocols for the sterilisation of decellularised xenogeneic tissues were tested. In addition, a method to assess the effectiveness of such a sterilisation method on biological decellularised scaffolds. A sterilisation method can be optimized according to the material/device, in this case biological decellularised (thus, devoid of issues related to maintenance of cell viability/phenotype) scaffolds mainly composed of collagen and GAGs. The sterilisation procedure should be adapted to such a scaffold and, at the same time, provide information able to cover the requirements from regulatory authorities such as FDA and European Commission. So, questions such "How many contaminants are present in the tissue?" and "Which contaminants (bioburden) are present?" should be addressed. Furthermore, a simulation of the worst-case scenario with high bioburden of bacteria currently present in biological scaffolds, resistant to the disinfection/sterilisation protocols adopted can provide understanding of how the protocols can be optimized.

To fulfil these requirements, a comprehensive sterility assessment protocol has been designed. It comprises the verification of the sterility of the sample with a simple method, approved by the European Pharmacopoeia. Furthermore, the protocol provides qualification and quantification of microorganisms by MALDI-TOF and MPN method.

In order to simulate the worst-case scenario, a methodology for CC was established. Bacterial strains of *Staphylococcus aureus*, *Enterococcus faecalis*, *Escherichia coli* and *BacP* were applied. CC methodology simulates microorganism contamination in the scaffolds and it was adequate to assess the effectiveness of the developed sterilisation methods. *Staphylococcus aureus*, *Enterococcus faecalis* and *Escherichia coli* are bacteria commonly found in cardiovascular homografts and are reported as high virulent and opportunistic microorganisms (Villalba, Solis et al. 2012) (van Kats, van Tricht et al. 2010) (Fan, Van Hoeck et al. 2012). On the other side, *BacP* is the biological indicator of γ-irradiation treatment (Pharmacopeia). A biological indicator is routinely used to monitor the efficacy of several sterilisation processes in food, pharmaceutical and medical

industries. Due to the elevated resistance to chemical and physical sterilisation methods, bacterial spores are frequently used as biological indicators, as *Bacillus* strains (Raguse, Fiebrandt et al. 2016).

After the CC, the sterilisation protocols can be applied. Following, the tissue can be subjected to the sterility assessment protocol. Verification of the sterility of the sample follows the European Pharmacopoeia. Ideally, a sample of the material to be tested is inoculated directly in the Thio or TSB medium, however the solution in which the sample is immersed is also indicative whether the sample is contaminated or not, similarly to the procedure currently applied in tissue banks. In case of contamination, the medium will become turbid; otherwise, a clear/non-turbid medium after 14 days of incubation is indicative of a sterile sample. Besides the sterility/non-sterility information, further information of which and how many contaminants are present are essential. Bacteria identification can be performed by inoculation of the Thio or TSB media positive to the contamination test in agar plates. After grow of bacteria, MALDI-TOF can be applied as a rapid and sensitive method to identify contaminants. Furthermore, at this step of the protocol, quantification of the bioburden can be performed on the solution in which the material is immersed. Samples of the biomaterial supernatant can be inoculated in multiwell plate following the MPN method procedure, which provides a reliable and sensitive quantification of the microorganism.

The design of this protocol considered both the feasibility of the procedure and the possible adaptability to diverse biological acellular matrices from different tissues and of different animal origin. This protocol was optimized for pericardial scaffolds, but has potential and feasibility to be applied in several materials (biologic, polymeric, metallic ...) of different investigation fields.

The feasibility of the protocol resides mainly in the employment of known methods already standardized. In addition, the amount of tissue needed for the study is minimum and this allows the applicability of this protocol on material to be stored in tissue banks and subsequently employed for implantation without affecting the integrity of the tissue or the organ. With a limited amount of tissue, it is possible to carry out different types of analysis that cover all the data needed to evaluate both the effective sterility of a

material and the type of contaminants that may be present, in order to identify the source of contamination and eventually optimize the procedure.

The main aim of this PhD project was to investigate the effectiveness of two disinfection and/or sterilisation methods on decellularised tissues. Taking into consideration that one of the main drawbacks of high level disinfection and sterilisation techniques for soft tissues is the possibility to cause damage in tissue components and properties (Qiu, Sun et al. 2011), two distinct protocols were studied for decellularised pericardium of bovine and porcine origin based on the use of AA+PAA (Sterilisation Protocol 1) and γ-irradiation (Sterilisation Protocol 2).

PP and BP were decellularised with established protocols known to provide completely acellular tissues while preserving the ECM of the tissues (Spina, Ortolani et al. 2003) and retaining the potential to be repopulated either *in vitro* or *in vivo* (Iop, Bonetti et al. 2014). Nuclei of porcine and bovine pericardia decellularised with TRICOL protocol were completely removed as observed by histological analyses. Furthermore, major components of the matrix as collagen and GAGs were preserved, as well as mechanical properties after decellularisation (manuscript in preparation).

Decellularisation of PP and BP under sterile conditions using the TRICOL decellularisation procedure provides sterile and acellular scaffolds, proving the disinfection potential of the protocol. However, the TRICOL decellularisation procedure resulted effective as a disinfection method for tissues with a lower bioburden, confirming that the effect of a sterilisation treatment is dependent on the initial bioburden present in the tissues.

The CC is a simulation of high levels of bioburden in the scaffold. Preferential sites of contaminants adhesion on decellularised pericardial scaffolds were evaluated by Gram staining, while confirmation of the high bioburden was obtained by MPN and the identification of bacteria inoculated by MALDI-TOF. Application of CC on pericardium reveal preferential bacteria adherence in fibrosa in comparison with serosa surface, where no contaminants were observed histologically. Surface roughness is a preferential characteristic that promote bacteria adhesion to surfaces, as reported by Díaz, et al. (Díaz, Cortizo et al. 2007). Furthermore, Dantas, et al. refer that pits and grooves in rougher surfaces reduce the influence of shear forces in decreasing initial bacteria

adhesion, while characteristics as hydrophobicity and surface charge also play a role (Dantas, da Silva-Neto et al. 2016).

The disinfection/sterilisation protocols investigated were AA followed by PAA treatment and γ-irradiation treatment. Regarding the first protocol, the first step was treatment with AA. This treatment was performed at 37 °C, differently from most common practices in tissue banks. The temperature has influence in the efficacy of the AA treatment. In a study by Germain et al., 10 heart valves were treated with cocktail of antibiotics for 24h at 4 °C and at 37 °C. The rinsing solutions were then tested for contaminations (Germain, Thibault et al. 2010). All valves treated at 4 °C revealed contaminations, whereas only 2 out of 10 present contaminations after treatment at 37 °C. The treatment at wet ice temperatures reduces the efficacy of antibiotics treatment. Besides, microorganisms are actively replicating at 37 °C which can increase the effectiveness of the treatment.

AA treatment was efficient in reducing the bioburden in the tested decellularised tissues. PPD and BPD present a reduction factor of 10^3 which was found statistically significant in the case of BPD. Analysis of the contaminants present after AA treatment revealed that the most common microorganisms were *Enterococcus faecalis* and *Escherichia coli.* These bacteria have the ability to produce pili to improve attachment to surfaces, therefore complete elimination can be harder to achieve when compared with other bacteria (Nallapareddy, Singh et al. 2006) (Pizarro-Cerda and Cossart 2006) (Nielsen, Guiton et al. 2012).

PAA treatment at both concentrations revealed to be efficient in the complete elimination of all microorganisms in all tissues and provided sterile scaffolds after 14 days of inoculation. The oxidizing potential of PAA in the cell membrane or capsid of microorganisms lead to this treatment to have bactericidal, fungicidal and sporicidal properties (Qiu, Sun et al. 2011), therefore is known to be effective in the complete elimination of contaminants. Furthermore, the utilization of PAA proven effective elimination of viruses after 0.18% PAA treatment of SIS matrices (Hodde and Hiles 2002).

As effectiveness of PAA was already been proven (Lomas, Huang et al. 2004), also its potential to induce detrimental effects on biological tissues was documented.

Treatment with 0.1% PAA can cause loose of collagen waveform in decellularised tendon allografts (Huang, Ingham et al. 2013). Since the scaffolds object of this study are selected to be employed as starting materials for the construction of cardiovascular prostheses, one fundamental requirement for a sterilisation method is the maintenance of the structural and functional features of the tissues. We thus investigated whenever PAA could cause alterations in the ECM at the structural and functional level. Structural modifications of the ECM have been investigated by different means: histological and immunofluorescence analysis for general ECM overview, biochemical quantification of major components of tissue ECM (collagen and GAGs), biomechanical properties to evaluate if the tissue can withstand cardiovascular mechanical requirements, surface analysis by SEM and finally cytotoxicity and cell proliferation after cell seeding.

Histological and immunofluorescence analysis on PPD and BPD revealed unaffected scaffolds after 0.05% PAA treatment, while some ECM damages were present after treatment with 0.1% PAA in PPD.

Quantification of the components of the tissue ECM such HYP and GAGs provides an insight in the preservation of the tissue characteristics after a sterilisation treatment. Studies have also reported preservation of components of soft scaffolds. A study with 0.1% PAA treatment in decellularised human amniotic membrane verified that GAGs and HYP content was preserved as well as tissue histoarchitecture and major components as collagen type IV and I, laminin and fibronectin were also preserved (Wilshaw, Kearney et al. 2006). Also, collagen, GAGs, laminin and fibronectin were preserved after 0.1% PAA treatment in SIS matrices (Hodde, Janis et al. 2007) (Gilbert, Sellaro et al. 2006). These studies support the results obtained for the quantification of HYP and GAGs in decellularised scaffolds.

GAGs content was preserved in both porcine and bovine pericardial scaffolds after all sterilisation performed, while for HYP a significant increase was observed on bovine scaffolds after 0.05% PAA treatment. The normalization for the area of tissue can justify the differences observed in the biochemical analysis of the scaffolds. Despite the possible expectation of reduction of the main components of the ECM of pericardial scaffolds, they were preserved after all treatments applied.

SEM analysis of both serosa and fibrosa surface of porcine and bovine pericardial scaffolds reveal cobblestone-like morphology, whereas a smoothing of both fibrosa and serosa surface was detected for PAA treated porcine scaffolds. However, for bovine scaffolds, this effect was not observed at the same extension. The cobblestone-like morphology was also observed by Roosens et al., in porcine pericardial scaffolds (Roosens, Somers et al. 2016). Furthermore, the oxidation potential of PAA treatment on virus and bacteria can be also translated to damages in surface of scaffolds as referred by Zhou et al. (Zhou, Zhang et al. 2014).

PAA effect on biomechanical properties has been reported to be contradictory. As referred by Rauh et al. in a study of cancellous bone graft treated with PAA and ethanol, levels of compressive strength, Young's modulus and fracture energy were significantly decreased after the treatment (Rauh, Despang et al. 2014). However, decellularised human amniotic membrane treated with PAA revealed no significant reduction in UTS, extensibility and elasticity (Wilshaw, Kearney et al. 2006). Also, ultimate tensile stress and Young's modulus were maintained in human patellar tendon allografts treated with 0.1% PAA (Lomas, Jennings et al. 2004); and a report by Scheffler et al. demonstrate the preservation of viscoelastic and mechanical properties of human bone-patellar tendon-bone grafts treated with PAA and ethanol (Scheffler, Scherler et al. 2005).

Biomechanical properties of the decellularised pericardia assessed by uniaxial tensile test reveal that bovine tissue have a uniform behaviour in all groups and for both UTS and failure strain no significant differences were observed. However, AA and PAA 0.1% treatment induces a significant decrease in failure strain of porcine tissue and significant differences were observed after PAA 0.05% treatment in UTS. Regarding Young's modulus, it was maintained for both treated porcine and bovine scaffolds. From these observations, it can be suggested that bovine tissue maintains the biomechanical properties after all treatments applied and presents a more constant behaviour in terms of the three components analysed. Also for the porcine tissue, there was no change in the Young's Modulus indicating no alteration in the stiffness of the tissues. However, the treatments resulted in a decrease of the failure strain of the porcine scaffolds, but the same trend was not observed for the UTS that was maintained except for one treatment. This indicated that the mechanical properties of porcine tissue are more

susceptible to the sterilisation methods applied since some components were altered and the scaffolds presented more variability. In general, a decrease in the failure strain indicate that the tissue ruptured at a lower deformation, suggesting some damages in the ECM structure caused by the treatments.

In summary, both tissues fail at the same deformation level, while porcine scaffold is stiffer than bovine, since it resists more to the deformation than bovine when applied the same force and elongation. The difference in the thickness of tissues and alignment of the collagen fibres during the elongation to rupture influence the mechanical properties observed. The ECM damages observed after histological analyses for 0.1% PAA treated porcine tissue were revealed after the mechanical test.

Biocompatibility of the scaffolds was assessed after cell seeding. The major requirements of a biocompatible material are the lack of cytotoxicity and the potential to sustain cell attachment, proliferation and differentiation. These features were investigated in this project through the quantification of LDH activity and a proliferation assay on hBM-MSCs-seeded sterilized scaffolds. These studies provide an insight of possible effect provoked by the sterilisation protocols that might interfere with endogenous cell adhesion and proliferation of the scaffolds once implanted.

The treatments applied to both porcine and bovine scaffolds result in a similar behaviour of their decellularised controls that has already demonstrated to not be cytotoxic or interfere with cell proliferation. They did not appear to lead to cytotoxicity or interfere with cell attachment and proliferation. Besides, histological analyses reveal a cell monolayer on both scaffolds after 14 days of hBM-MSC seeding. Our results are in line with previous observations. A report by Wilshaw et al. in decellularised human amniotic membrane 0.1% PAA treated revealed a biocompatible matrix, that promotes cell grow in contact and no decrease in cell viability (Wilshaw, Kearney et al. 2006). Also, similar results were obtained for decellularised SIS and urinary bladder matrix 0.1% PAA treated, where the matrices support cell grow and proliferation presenting a single layer confluence (Hodde, Record et al. 2002) (Gilbert, Sellaro et al. 2006).

The developed protocol was optimized for the treatment of pericardial scaffolds. However, this protocol is compatible with other decellularised scaffolds: it preserves the

structure and components of the ECM, mechanical properties and do not cause cytotoxicity neither interfere with cell attachment and proliferation. Also, it does not require specific or expensive laboratory equipment or reagents.

To this aim, we broadened the application of the AA+PAA protocol on other decellularised tissues routinely employed for the construction of cardiovascular substitutes. Decellularised porcine AV and PV were submitted to this protocol. The preliminary results obtained are comparable with the ones presented for pericardial scaffolds: the sterility was achieved after PAA treatment and structure and components of the ECM were preserved (Figure 4.1, Figure 4.2 and Figure 4.3). This indicates the feasibility of this protocol be efficient in the effective sterilisation of other scaffolds besides pericardium.

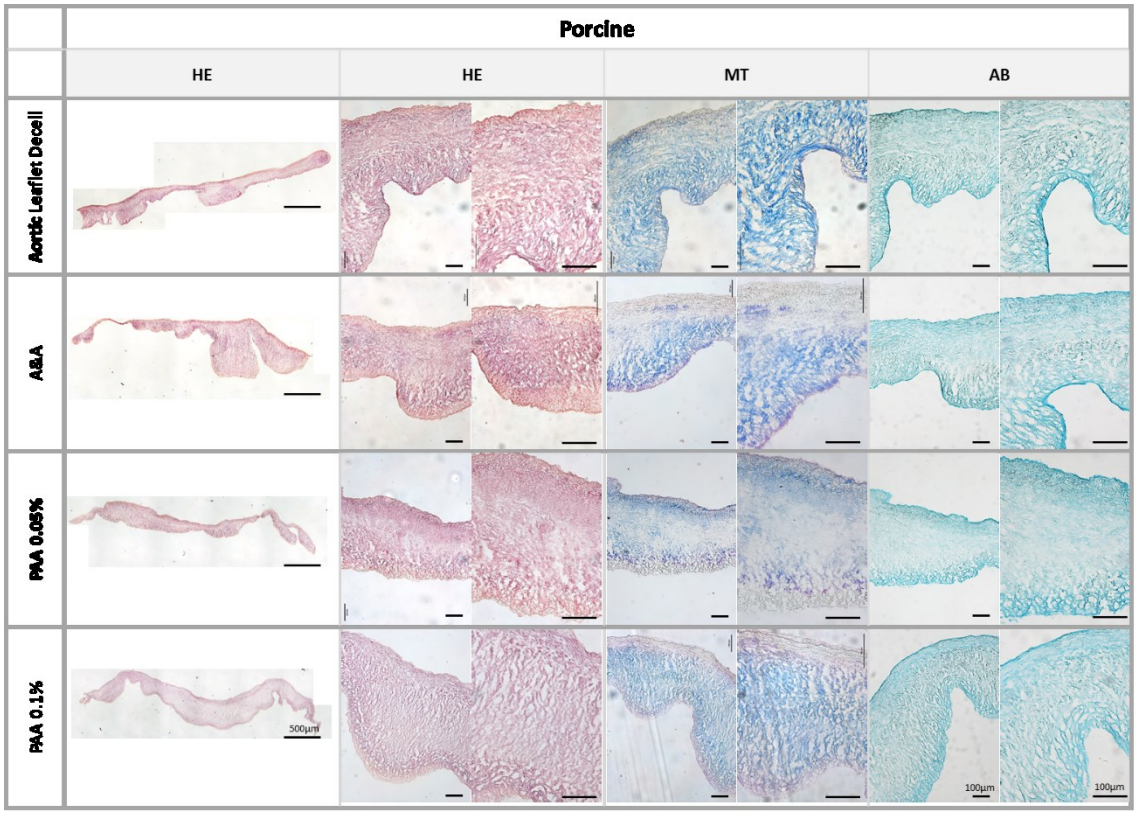

Figure 4.1 HE, MT and AB staining of aortic leaflet decellularised and after Sterilisation Protocol 1 treatments. Scale bar 500 and 100 µm.

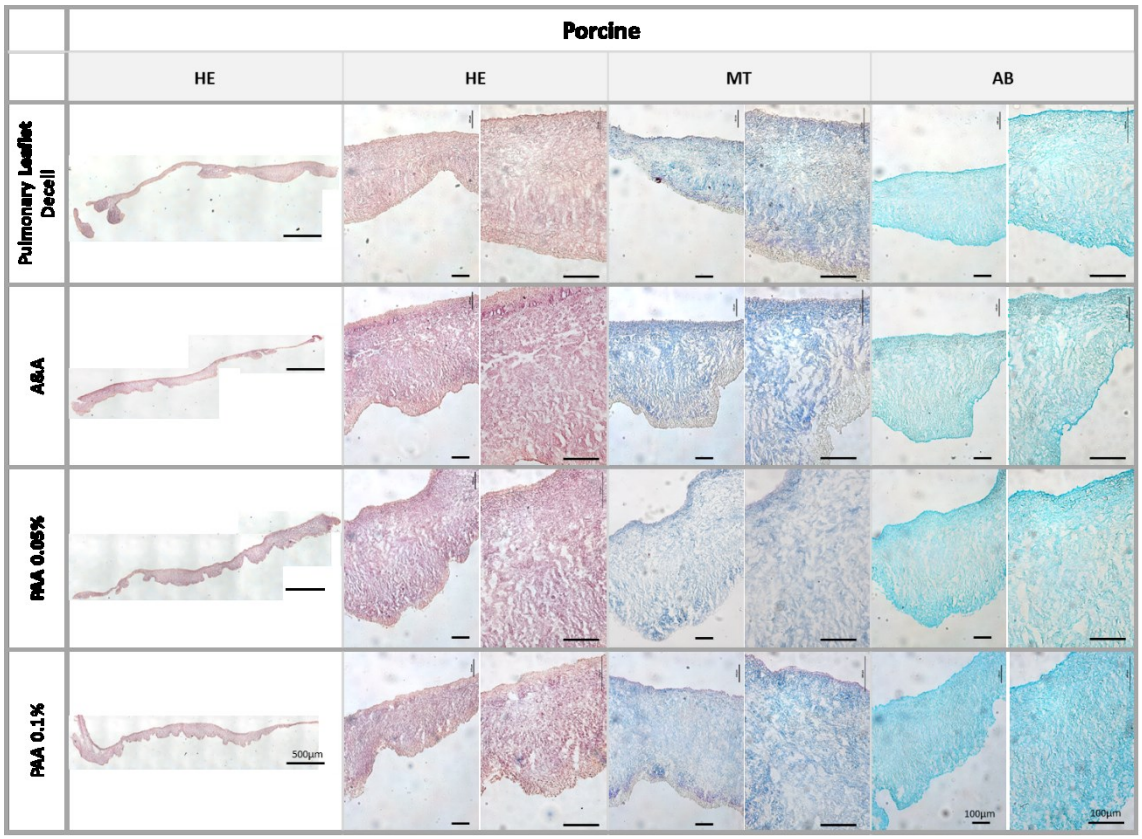

Figure 4.2 HE, MT and AB staining of pulmonary leaflet decellularised and after Sterilisation Protocol 1 treatments. Scale bar 500 and 100 µm.

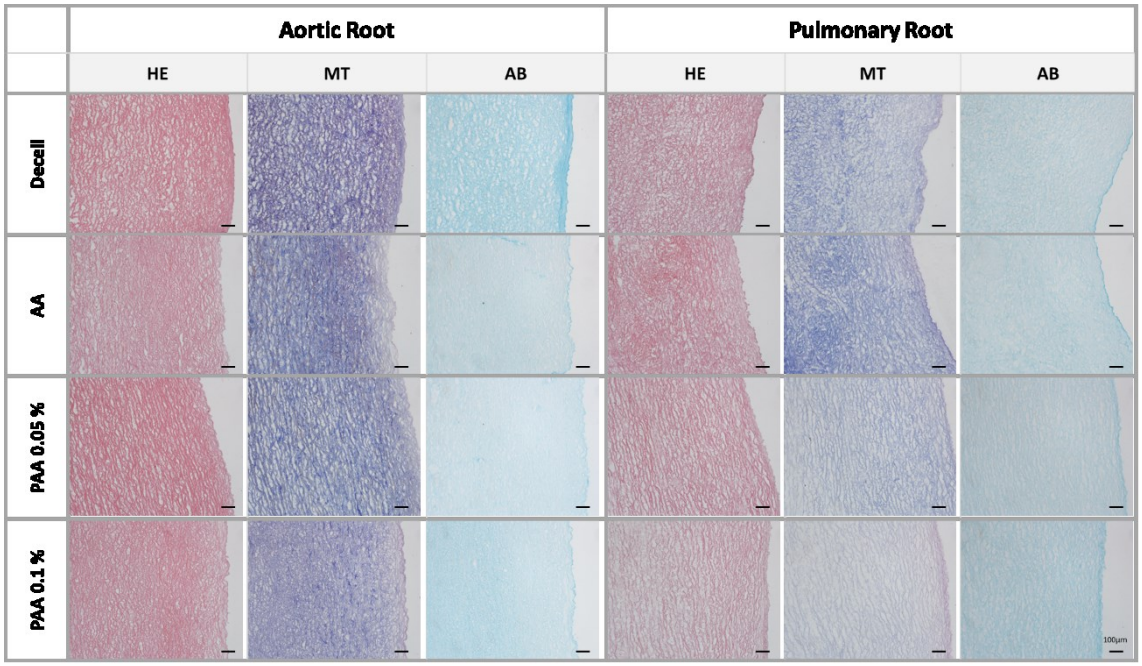

Figure 4.3 HE, MT and AB staining of aortic and pulmonary root decellularised and after Sterilisation Protocol 1 treatments. Scale bar 100 µm.

The second protocol developed, based on the use of γ-irradiation treatment. This treatment is a well-established method for terminal sterilisation of tissues. Major advantages are high efficiency, lack of chemical residues and the fact that the treatment is performed in the final package and no further handling is required, while damages in structure of scaffolds are appointed as disadvantages. In this project, γ-irradiation was tested in five different dosages: 1.5, 5, 10, 15 and 25 kGy. 25 kGy is the 'gold standard' for medical devices, but also known to cause damages in tissue matrix. Lower dosages were applied to the aim of reaching a sterility level without affecting the properties of the tissues in so high extension.

All contaminants were completely eliminated by all the tested dosages, independently of the type of CC performed on the decellularised scaffolds, including the spore form of *BacP*. Despite the high level of bioburden inoculated in the tissues with the CC, the sterilisation protocol resulted effective.

These results overcome previous observations with low-dosage γ-irradiation. A recent study by Helder et al. where decellularised heart valves were treated with 1, 3 and 10 kGy demonstrate that valves treated with low-dosage (1 kGy) present contaminants after inoculation in bacteria media (Helder, Hennessy et al. 2016).

In a study by Gouk et al., histological analyses of γ-irradiation treated acellular human dermal tissue matrix reported increased damages of tissues treated with 2.5, 12.7 and 25.9 kGy (Gouk, Lim et al. 2008). For the pericardial scaffolds treated, a similar result was expected: higher ECM damages with the increasing of the dosage applied. Histological and immunofluorescence assessment of the ECM structure of PPD and BPD revealed that after the treatment, the decellularised scaffold showed some changes compared to the untreated scaffold. However, the trend indicated by Gouk et al. was not observed as in general ECM histoarchitecture of treated PPD and BPD was preserved even with the higher dosages. Therefore, these findings for the dermal scaffolds are not correlated with the results obtained for pericardial scaffolds. This suggest that the pericardial tissues are more stable towards γ-irradiation treatment.

Despite the structural changes that can be induced by γ-irradiation treatment, HYP content was reported to be preserved in acellular porcine tendon (Edwards, Herbert et

al. 2016), while GAGs amount was maintained for treated acellular human tissue matrix (Gouk, Lim et al. 2008). After γ-irradiation treatment on bovine and porcine scaffolds, the amount of HYP was maintained in comparison with the decellularised tissue for porcine scaffolds, while for bovine ones it was observed an increase after 15 and 25 kGy treatment. The treatment did not reduce the total amount of collagen present in the tissues. As previously mentioned, normalization by the area of the tissue can justify the differences observed. For both bovine and porcine scaffolds, GAGs amount did not decrease when compared to the decellularised tissues. Preservation of GAGs and HYP amount in the scaffold is important for the maintenance of mechanical properties of the scaffolds, since a decrease in these components can be reflected in the reduction of mechanical parameters of the scaffold.

The reported structural damages by condensation of collagen fibres, extensive protein scission and rupture of hydrogen bonds can cause extensive alteration of tissue microstructure observed by SEM in collagen-based scaffolds (Gouk, Lim et al. 2008) (Matuska and McFetridge 2015). However, surface analysis by SEM reveal an altered surface from the decellularised to the treated scaffolds, where more evident fibres were observed. However, no major differences were observed with the different dosages applied in both scaffolds.

Treatment with γ-radiation is required to be, as from ISO guidelines, a terminal sterilisation in which the final sterilized product cannot be following subjected to further procedures or handling. This implies that γ-irradiation is carried out on the end product in its final package designed for the storage prior to implantation. In the design of Sterilisation Protocol 2 this directive was taken into account which render this protocol feasible and applicable for tissue banks.

4.2 Conclusions

The work conducted in the project focused initially on the development of an optimized sterilisation assessment method (qualitative and quantitative), fundamental for the achievement of sterilisation protocols dedicated to decellularised scaffolds. An effective and feasible sterilisation assessment method that can be applied to several types of scaffolds and tissues in the clinical sector has been developed. The method consists in an effective CC with known amount and type of bacteria that can be tailored for the purpose, as in the case of the use of *BacP,* biological indicator for γ-irradiation treatment. The method for discrimination between sterile and contaminated samples presented is in agreement with guidelines of European Pharmacopoeia, while identification and contamination of contaminants are obtained through standardized and effective techniques. The protocol developed, a part from the device needed for identification of the contaminants through MALDITOF, requires easily available and low cost equipment and reagents and enables this protocol to be applied by different research laboratories. The developed protocol was following applied to evaluate the effectiveness of the two sterilisation methodologies in study.

The results obtained for Sterilisation Protocol 1 are quite promising since they indicated that sterile tissues can be produced, without major ECM damage that has been reported using other sterilisation methods (Delgado, Pandit et al. 2014). Moreover, PAA treatment was performed at a very low concentration as it is already applied for SIS disinfection procedures (Freytes, Badylak et al. 2004). Treatment with AA reduces bioburden while PAA treatment achieve sterile scaffolds. Tissue ECM structure, surface and components were preserved, as well as biomechanical properties, mainly for bovine tissues. Biocompatibility of all scaffolds was preserved after cell seeding. The methodology developed was optimised for the tissues in study and can be feasible to consider the application in tissue banks and other tissues, since they do not require expensive and complex equipment to be implemented such as plasma treatment and SC-CO_2 treatments.

Regarding the Sterilisation Protocol 2, based on γ-irradiation treatment with five dosages sterility was achieved even with the lower dosage applied (1.5 kGy). Tissue

assessment reveal a general well preserved ECM structure, surface and components for all dosages tested. Since this procedure is applied in the final package, reduced manipulation of scaffolds is required and application in tissue banks for homografts treatment can be possible.

Supercritical CO_2 treatment require complex equipment to achieve the supercritical state at which the treatment is feasible and chemical sterilants as PAA were reported to be necessary to accomplish terminal sterilisation. In this case, the detrimental effects caused on the tissues ECM could be superior when compared with the treatments in study. Furthermore, complex equipment was necessary to perform this methodology.

For plasma treatment, the main disadvantage is related with the low penetration of the plasma in the material treated, decreasing the effectiveness in thicker materials. Additionally, it is required more handling of the tissue and a complex equipment to carry out the treatment.

4.3 Future Work

Chemical residues after AA and PAA treatments could lead to reduced cell adhesion and proliferation that can result in scaffold rejection after implantation. Besides, chemical residues can induce misinterpretation of sterility test results. In fact, a study by Gatto et al. focused on antibiotics residues in heart valves reveal that antibiotics residues may result in false negative sterility tests due to the masking of microorganisms that can further result in post-surgical infections (Gatto, Giurgola et al. 2013). On the other side, in a report by Jashari et al. low concentration of antibiotics was remaining in cryopreserved heart valves and vascular grafts, but authors refer that these residues may not present a risk for homograft recipient since they could be the reason for increased resistance of tissue to infection in the early period after implantation (Jashari, Faucon et al. 2011). In order to evaluate whether chemical residues can be present in the treated porcine and bovine pericardia, high-pressure liquid chromatography (HPLC) analysis will be performed on the scaffolds after the treatment.

REFERENCES

. "U.S. Food and Drug Administration - BAM Appendix 2: Most Probable Number from Serial Dilutions." BAM Appendix 2: Most Probable Number from Serial Dilutions Retrieved 21 October 2015, from http://www.fda.gov/Food/FoodScienceResearch/LaboratoryMethods/ucm109656.htm.

Acharya, T. (2016). "Preparation of McFarland Turbidity Standards." Bacteriology.

Aguiari, P., M. Fiorese, L. Iop, G. Gerosa and A. Bagno (2016). "Mechanical testing of pericardium for manufacturing prosthetic heart valves." Interact Cardiovasc Thorac Surg **22**(1): 72-84.

Bader, A., T. Schilling, O. E. Teebken, G. Brandes, T. Herden, G. Steinhoff and A. Haverich (1998). "Tissue engineering of heart valves--human endothelial cell seeding of detergent acellularized porcine valves." Eur J Cardiothorac Surg **14**(3): 279-284.

Balsly, C. R., A. T. Cotter, L. A. Williams, B. D. Gaskins, M. A. Moore and L. Wolfinbarger, Jr. (2008). "Effect of low dose and moderate dose gamma irradiation on the mechanical properties of bone and soft tissue allografts." Cell Tissue Bank **9**(4): 289-298.

Baraki, H., I. Tudorache, M. Braun, K. Hoffler, A. Gorler, A. Lichtenberg, C. Bara, A. Calistru, G. Brandes, M. Hewicker-Trautwein, A. Hilfiker, A. Haverich and S. Cebotari (2009). "Orthotopic replacement of the aortic valve with decellularized allograft in a sheep model." Biomaterials **30**(31): 6240-6246.

Barbosa, I., S. Garcia, V. Barbier-Chassefiere, J. P. Caruelle, I. Martelly and D. Papy-Garcia (2003). "Improved and simple micro assay for sulfated glycosaminoglycans quantification in biological extracts and its use in skin and muscle tissue studies." Glycobiology **13**(9): 647-653.

Bateman, M. G., A. J. Hill, J. L. Quill and P. A. Iaizzo (2013). "The clinical anatomy and pathology of the human arterial valves:

implications for repair or replacement." J Cardiovasc Transl Res 6(2): 166-175.

Bouten, C. V. C., P. Y. W. Dankers, A. Driessen-Mol, S. Pedron, A. M. A. Brizard and F. P. T. Baaijens (2011). "Substrates for cardiovascular tissue engineering." Advanced Drug Delivery Reviews 63(4–5): 221-241.

Brockbank, K. G. and P. E. Dawson (1993). "Cytotoxicity of amphotericin B for fibroblasts in human heart valve leaflets." Cryobiology 30(1): 19-24.

Brown, B. N. and S. F. Badylak (2014). "Extracellular matrix as an inductive scaffold for functional tissue reconstruction." Transl Res 163(4): 268-285.

C. Wells, F. (2013). The heart of Leonardo: foreword by HRH Prince Charles, the Prince of Wales. New York, Springer %@ 9781447145301.

Cartmell, J. S. and M. G. Dunn (2000). "Effect of chemical treatments on tendon cellularity and mechanical properties." J Biomed Mater Res 49(1): 134-140.

Chiu, L. L. Y. and M. Radisic (2013). "Cardiac tissue engineering." Current Opinion in Chemical Engineering 2(1): 41-52.

Cigliano, A., A. Gandaglia, A. J. Lepedda, E. Zinellu, F. Naso, A. Gastaldello, P. Aguiari, P. De Muro, G. Gerosa, M. Spina and M. Formato (2012). "Fine structure of glycosaminoglycans from fresh and decellularized porcine cardiac valves and pericardium." Biochem Res Int 2012: 979351.

Commission, E. P. (2005). European Pharmacopoeia 5.0. 2.6 - Biological Tests; 2.6.1 Sterility.

Conrad, B. P., M. Rappe, M. Horodyski, K. W. Farmer and P. A. Indelicato (2013). "The effect of sterilization on mechanical properties of soft tissue allografts." Cell Tissue Bank 14(3): 359-366.

Currin, C. S. P.-W. J. (2012). "Streptococcus uberis- a pratical summary for controlling mastitis." from https://pubs.ext.vt.edu/DASC/DASC-8P/DASC-8P_pdf.pdf.

D'Ambra, L., S. Berti, C. Feleppa, P. Magistrelli, P. Bonfante and E. Falco (2012). "Use of bovine pericardium graft for abdominal wall reconstruction in contaminated fields." World J Gastrointest Surg **4**(7): 171-176.

Dantas, L. C., J. P. da Silva-Neto, T. S. Dantas, L. Z. Naves, F. D. das Neves and A. S. da Mota (2016). "Bacterial Adhesion and Surface Roughness for Different Clinical Techniques for Acrylic Polymethyl Methacrylate." Int J Dent **2016**: 8685796.

de By, T. M., R. Parker, E. M. Delmo Walter and R. Hetzer (2012). "Cardiovascular tissue banking in Europe." HSR Proc Intensive Care Cardiovasc Anesth **4**(4): 251-260.

De Geyter, N. and R. Morent (2012). "Nonthermal plasma sterilization of living and nonliving surfaces." Annu Rev Biomed Eng **14**: 255-274.

Delgado, L. M., A. Pandit and D. I. Zeugolis (2014). "Influence of sterilisation methods on collagen-based devices stability and properties." Expert Rev Med Devices **11**(3): 305-314.

Delmo Walter, E. M., T. M. de By, R. Meyer and R. Hetzer (2012). "The future of heart valve banking and of homografts: perspective from the Deutsches Herzzentrum Berlin." HSR Proc Intensive Care Cardiovasc Anesth **4**(2): 97-108.

Devriese , L. A., Kilpper-Balz, R. and Schleifer, K. H. (1988). "Streptococcus hyointestinalis sp. nov. from the gut of swine." International Journal of Systematic Bacteriology **38**(4): 440-441.

Dhandayuthapani, B., Y. Yoshida, T. Maekawa and D. S. Kumar (2011). "Polymeric Scaffolds in Tissue Engineering Application: A Review." International Journal of Polymer Science **2011**: 1-19.

Díaz, C., M. C. Cortizo, P. L. Schilardi, S. G. G. d. Saravia, M. Mele and A. F. Lorenzo (2007). "Influence of the nano-micro structure of the surface on bacterial adhesion." Materials Research **10**: 11-14.

Dodge-Khatami, A., V. Tsang, D. Roebuck and M. Elliott (2000). "Management of congenital tracheal stenosis: a multidisciplinary approach." Images Paediatr Cardiol **2**(1): 29-39.

Dohmen, P. M., F. da Costa, S. Yoshi, S. V. Lopes, F. P. da Souza, R. Vilani, A. F. Wouk, M. da Costa and W. Konertz (2006). "Histological evaluation of tissue-engineered heart valves implanted in the juvenile sheep model: is there a need for in-vitro seeding?" J Heart Valve Dis **15**(6): 823-829.

Dong, X., X. Wei, W. Yi, C. Gu, X. Kang, Y. Liu, Q. Li and D. Yi (2009). "RGD-modified acellular bovine pericardium as a bioprosthetic scaffold for tissue engineering." J Mater Sci Mater Med **20**(11): 2327-2336.

Dziedzic-Goclawska, A., A. Kaminski, I. Uhrynowska-Tyszkiewicz and W. Stachowicz (2005). "Irradiation as a safety procedure in tissue banking." Cell Tissue Bank **6**(3): 201-219.

Eastlund, T. (2006). "Bacterial infection transmitted by human tissue allograft transplantation." Cell Tissue Bank **7**(3): 147-166.

Edwards, C. A. and W. D. O'Brien, Jr. (1980). "Modified assay for determination of hydroxyproline in a tissue hydrolyzate." Clin Chim Acta **104**(2): 161-167.

Edwards, J. H., A. Herbert, G. L. Jones, I. W. Manfield, J. Fisher and E. Ingham (2016). "The effects of irradiation on the biological and biomechanical properties of an acellular porcine superflexor tendon graft for cruciate ligament repair." J Biomed Mater Res B Appl Biomater.

Fan, Y. D., B. Van Hoeck, V. Holovska and R. Jashari (2012). "Evaluation of decontamination process of heart valve and artery tissues in European Homograft Bank (EHB): a retrospective study of 1,055 cases." Cell Tissue Bank **13**(2): 297-304.

Farrington, M., T. Wreghitt, I. Matthews, D. Scarr, G. Sutehall, C. J. Hunt, T. Santiago, E. Gruys, W. Voorhout, T. Ramos and D. E. Pegg (2002). "Processing of cardiac valve allografts: 2. Effects of antimicrobial treatment on sterility, structure and mechanical properties." Cell Tissue Bank **3**(2): 91-103.

Flynn, L., J. L. Semple and K. A. Woodhouse (2006). "Decellularized placental matrices for adipose tissue engineering." J Biomed Mater Res A **79**(2): 359-369.

Freytes, D. O., S. F. Badylak, T. J. Webster, L. A. Geddes and A. E. Rundell (2004). "Biaxial strength of multilaminated extracellular matrix scaffolds." Biomaterials **25**(12): 2353-2361.

Gall, K., S. Smith, C. Willmette, M. Wong and M. O'Brien (1995). "Allograft heart valve sterilization: a six-year in-depth analysis of a twenty-five-year experience with low-dose antibiotics." J Thorac Cardiovasc Surg **110**(3): 680-687.

Gallo, M., F. Naso, H. Poser, A. Rossi, P. Franci, R. Bianco, M. Micciolo, F. Zanella, U. Cucchini, L. Aresu, E. Buratto, R. Busetto, M. Spina, A. Gandaglia and G. Gerosa (2012). "Physiological performance of a detergent decellularized heart valve implanted for 15 months in Vietnamese pigs: surgical procedure, follow-up, and explant inspection." Artif Organs **36**(6): E138-150.

Gatto, C., L. Giurgola and J. D'Amato Tothova (2013). "A suitable and efficient procedure for the removal of decontaminating antibiotics from tissue allografts." Cell Tissue Bank **14**(1): 107-115.

Gauvin, R., G. Marinov, Y. Mehri, J. Klein, B. Li, D. Larouche, R. Guzman, Z. Zhang, L. Germain and R. Guidoin (2013). "A comparative study of bovine and porcine pericardium to highlight their potential advantages to manufacture percutaneous cardiovascular implants." J Biomater Appl **28**(4): 552-565.

Germain, M., D. M. Strong, G. Dowling, J. Mohr, A. Duong, A. Garibaldi, N. Simunovic, O. R. Ayeni, C. Bioburden Steering and g. Cardiac Tissue Working (2016). "Disinfection of human cardiac

valve allografts in tissue banking: systematic review report." Cell Tissue Bank.

Germain, M., L. Thibault, A. Jacques, J. Tremblay and R. Bourgeois (2010). "Heart valve allograft decontamination with antibiotics: impact of the temperature of incubation on efficacy." Cell Tissue Bank **11**(2): 197-204.

Gilbert, T. W., T. L. Sellaro and S. F. Badylak (2006). "Decellularization of tissues and organs." Biomaterials **27**(19): 3675-3683.

Gouk, S. S., T. M. Lim, S. H. Teoh and W. Q. Sun (2008). "Alterations of human acellular tissue matrix by gamma irradiation: histology, biomechanical property, stability, in vitro cell repopulation, and remodeling." J Biomed Mater Res B Appl Biomater **84**(1): 205-217.

Grande-Allen, K. J., B. P. Griffin, N. B. Ratliff, D. M. Cosgrove and I. Vesely (2003). "Glycosaminoglycan profiles of myxomatous mitral leaflets and chordae parallel the severity of mechanical alterations." Journal of the American College of Cardiology **42**(2): 271-277.

Grieb, T. A., R. Y. Forng, S. Bogdansky, C. Ronholdt, B. Parks, W. N. Drohan, W. H. Burgess and J. Lin (2006). "High-dose gamma irradiation for soft tissue allografts: High margin of safety with biomechanical integrity." J Orthop Res **24**(5): 1011-1018.

Hafeez, Y. M., A. B. Zuki, N. Yusof, H. Asnah, M. Y. Loqman, M. M. Noordin and M. Y. Ainul-Yuzairi (2005). "Effect of freeze-drying and gamma irradiation on biomechanical properties of bovine pericardium." Cell Tissue Bank **6**(2): 85-89.

Helder, M. R., R. S. Hennessy, D. B. Spoon, B. J. Tefft, T. A. Witt, R. J. Marler, S. V. Pislaru, R. D. Simari, J. M. Stulak and A. Lerman (2016). "Low-Dose Gamma Irradiation of Decellularized Heart Valves Results in Tissue Injury In Vitro and In Vivo." Ann Thorac Surg **101**(2): 667-674.

Heng, W. L., H. Albrecht, P. Chiappini, Y. P. Lim and L. Manning (2013). "International heart valve bank survey: a review of

processing practices and activity outcomes." J Transplant 2013: 163150.

Hodde, J. and M. Hiles (2002). "Virus safety of a porcine-derived medical device: evaluation of a viral inactivation method." Biotechnol Bioeng 79(2): 211-216.

Hodde, J., A. Janis, D. Ernst, D. Zopf, D. Sherman and C. Johnson (2007). "Effects of sterilization on an extracellular matrix scaffold: part I. Composition and matrix architecture." J Mater Sci Mater Med 18(4): 537-543.

Hodde, J. P., R. D. Record, R. S. Tullius and S. F. Badylak (2002). "Retention of endothelial cell adherence to porcine-derived extracellular matrix after disinfection and sterilization." Tissue Eng 8(2): 225-234.

Hoerstrup, S. P., R. Sodian, S. Daebritz, J. Wang, E. A. Bacha, D. P. Martin, A. M. Moran, K. J. Guleserian, J. S. Sperling, S. Kaushal, J. P. Vacanti, F. J. Schoen and J. E. Mayer, Jr. (2000). "Functional living trileaflet heart valves grown in vitro." Circulation 102(19 Suppl 3): III44-49.

Holzapfel, G. A. (2000). Biomechanics of Soft Tissue. Handbook of Material Behaviour - Nonlinear Models and Properties J. Lemaitre. France

Hopkins, R. A., A. L. Jones, L. Wolfinbarger, M. A. Moore, A. A. Bert and G. K. Lofland (2009). "Decellularization reduces calcification while improving both durability and 1-year functional results of pulmonary homograft valves in juvenile sheep." J Thorac Cardiovasc Surg 137(4): 907-913, 913e901-904.

Huang, Q., E. Ingham, P. Rooney and J. N. Kearney (2013). "Production of a sterilised decellularised tendon allograft for clinical use." Cell Tissue Bank 14(4): 645-654.

Ingham, E., J. Fisher, S. A. Korossis, H. E. Wilcox and R. L. Knight (2008). "The use of acellular matrices for the tissue engineering of cardiac valves." Proceedings of the Institution of Mechanical

Engineers, Part H: Journal of Engineering in Medicine 222(1): 129-143.

Iop, L., A. Bonetti, F. Naso, S. Rizzo, S. Cagnin, R. Bianco, C. Dal Lin, P. Martini, H. Poser, P. Franci, G. Lanfranchi, R. Busetto, M. Spina, C. Basso, M. Marchini, A. Gandaglia, F. Ortolani and G. Gerosa (2014). "Decellularized allogeneic heart valves demonstrate self-regeneration potential after a long-term preclinical evaluation." PLoS One 9(6): e99593.

Iop, L., V. Renier, F. Naso, M. Piccoli, A. Bonetti, A. Gandaglia, M. Pozzobon, A. Paolin, F. Ortolani, M. Marchini, M. Spina, P. De Coppi, S. Sartore and G. Gerosa (2009). "The influence of heart valve leaflet matrix characteristics on the interaction between human mesenchymal stem cells and decellularized scaffolds." Biomaterials 30(25): 4104-4116.

Isbary, G., J. L. Zimmermann, T. Shimizu, Y. F. Li, G. E. Morfill, H. M. Thomas, B. Steffes, J. Heinlin, S. Karrer and W. Stolz (2013). "Non-thermal plasma—More than five years of clinical experience." Clinical Plasma Medicine 1(1): 19-23.

Ishihara, T., V. J. Ferrans, M. Jones, S. W. Boyce, O. Kawanami and W. C. Roberts (1980). "Histologic and ultrastructural features of normal human parietal pericardium." Am J Cardiol 46(5): 744-753.

Jana, S., B. J. Tefft, D. B. Spoon and R. D. Simari (2014). "Scaffolds for tissue engineering of cardiac valves." Acta Biomater 10(7): 2877-2893.

Jarvis, B., C. Wilrich and P. T. Wilrich (2010). "Reconsideration of the derivation of Most Probable Numbers, their standard deviations, confidence bounds and rarity values." J Appl Microbiol 109(5): 1660-1667.

Jashari, R., F. Faucon, B. V. Hoeck, S. D. Gelas, Y. Fan and S. Vandenbulcke (2011). "Determination of Residual Antibiotics in Cryopreserved Heart Valve Allografts." Transfus Med Hemother 38(6): 379-386.

Jashari, R., Y. Goffin, B. Van Hoeck, A. Vanderkelen, A. du Verger, Y. Fan, V. Holovska, A. Fagu and O. Brahy (2010). "Belgian and European experience with the European Homograft Bank (EHB) cryopreserved allograft valves.--assessment of a 20 year activity." Acta Chirurgica Belgica **110**(3): 280-290.

Jashari, R., Y. Goffin, A. Vanderkelen, B. Van Hoeck, A. du Verger, Y. Fan, V. Holovska and O. Brahy (2010). "European homograft bank: twenty years of cardiovascular tissue banking and collaboration with transplant coordination in Europe." Transplant Proc **42**(1): 183-189.

Jashari, R., B. Van Hoeck, M. Tabaku and A. Vanderkelen (2004). "Banking of the human heart valves and the arteries at the European homograft bank (EHB) – Overview of a 14-year activity in this International Association in Brussels*." Cell and Tissue Banking **5**(4): 239-251.

Jordan, J. E., J. K. Williams, S. J. Lee, D. Raghavan, A. Atala and J. J. Yoo (2012). "Bioengineered self-seeding heart valves." J Thorac Cardiovasc Surg **143**(1): 201-208.

Keane, T. J., I. Swinehart and S. F. Badylak (2015). "Methods of Tissue Decellularization Used for Preparation of Biologic Scaffolds and In-vivo Relevance." Methods.

Kheradvar, A., E. M. Groves, C. J. Goergen, S. H. Alavi, R. Tranquillo, C. A. Simmons, L. P. Dasi, K. J. Grande-Allen, M. R. Mofrad, A. Falahatpisheh, B. Griffith, F. Baaijens, S. H. Little and S. Canic (2014). "Emerging Trends in Heart Valve Engineering: Part II. Novel and Standard Technologies for Aortic Valve Replacement." Ann Biomed Eng.

Knight, R. L., C. Booth, H. E. Wilcox, J. Fisher and E. Ingham (2005). "Tissue engineering of cardiac valves: re-seeding of acellular porcine aortic valve matrices with human mesenchymal progenitor cells." J Heart Valve Dis **14**(6): 806-813.

Kohanski, M. A., D. J. Dwyer and J. J. Collins (2010). "How antibiotics kill bacteria: from targets to networks." Nat Rev Microbiol 8(6): 423-435.

Korossis, S. A., C. Booth, H. E. Wilcox, K. G. Watterson, J. N. Kearney, J. Fisher and E. Ingham (2002). "Tissue engineering of cardiac valve prostheses II: biomechanical characterization of decellularized porcine aortic heart valves." J Heart Valve Dis 11(4): 463-471.

Lambert, B. J., T. A. Mendelson and M. D. Craven (2011). "Radiation and ethylene oxide terminal sterilization experiences with drug eluting stent products." AAPS PharmSciTech 12(4): 1116-1126.

Langer, R. and J. P. Vacanti (1993). "Tissue engineering." Science 260(5110): 920-926.

Lazarou, G., K. Powers, C. Pena, L. Bruck and M. S. Mikhail (2005). "Inflammatory reaction following bovine pericardium graft augmentation for posterior vaginal wall defect repair." Int Urogynecol J Pelvic Floor Dysfunct 16(3): 242-244.

Leeming, J. P., A. M. Lovering and C. J. Hunt (2005). "Residual antibiotics in allograft heart valve tissue samples following antibiotic disinfection." J Hosp Infect 60(3): 231-234.

Leonardo, K. D. Keele, J. Roberts, C. Windsor and A. Metropolitan Museum of (1983). Leonardo da Vinci: anatomical drawings from the Royal Library, Windsor Castle. New York, Metropolitan Museum of Art %@ 0870993623 %L NC257.L4 A4 1983.

Lomas, R. J., Q. Huang, D. E. Pegg and J. N. Kearney (2004). "Application of a high-level peracetic acid disinfection protocol to re-process antibiotic disinfected skin allografts." Cell Tissue Bank 5(1): 23-36.

Lomas, R. J., L. M. Jennings, J. Fisher and J. N. Kearney (2004). "Effects of a peracetic acid disinfection protocol on the biocompatibility and biomechanical properties of human patellar tendon allografts." Cell Tissue Bank 5(3): 149-160.

Matsagas, M. I., C. Bali, E. Arnaoutoglou, J. C. Papakostas, C. Nassis, G. Papadopoulos and A. M. Kappas (2006). "Carotid endarterectomy with bovine pericardium patch angioplasty: mid-term results." Ann Vasc Surg 20(5): 614-619.

Matuska, A. M. and P. S. McFetridge (2015). "The effect of terminal sterilization on structural and biophysical properties of a decellularized collagen-based scaffold; implications for stem cell adhesion." J Biomed Mater Res B Appl Biomater 103(2): 397-406.

Mavrilas, D., E. A. Sinouris, D. H. Vynios and N. Papageorgakopoulou (2005). "Dynamic mechanical characteristics of intact and structurally modified bovine pericardial tissues." J Biomech 38(4): 761-768.

Mendelson, K. and F. J. Schoen (2006). "Heart valve tissue engineering: concepts, approaches, progress, and challenges." Ann Biomed Eng 34(12): 1799-1819.

Mendes, G. C., T. R. Brandao and C. L. Silva (2007). "Ethylene oxide sterilization of medical devices: a review." Am J Infect Control 35(9): 574-581.

Mendoza-Novelo, B., E. E. Avila, J. V. Cauich-Rodriguez, E. Jorge-Herrero, F. J. Rojo, G. V. Guinea and J. L. Mata-Mata (2011). "Decellularization of pericardial tissue and its impact on tensile viscoelasticity and glycosaminoglycan content." Acta Biomater 7(3): 1241-1248.

Merkli, A., J. Heller, C. Tabatabay and R. Gurny (1994). "Gamma sterilization of a semi-solid poly(ortho ester) designed for controlled drug delivery--validation and radiation effects." Pharm Res 11(10): 1485-1491.

Meyer, S. R., B. Chiu, T. A. Churchill, L. Zhu, J. R. Lakey and D. B. Ross (2006). "Comparison of aortic valve allograft decellularization techniques in the rat." J Biomed Mater Res A 79(2): 254-262.

Mirnajafi, A., J. Raymer, M. J. Scott and M. S. Sacks (2005). "The effects of collagen fiber orientation on the flexural properties of pericardial heterograft biomaterials." Biomaterials 26(7): 795-804.

Misfeld, M. and H. H. Sievers (2007). "Heart valve macro- and microstructure." Philos Trans R Soc Lond B Biol Sci 362(1484): 1421-1436.

Moisan, M., J. Barbeau, S. Moreau, J. Pelletier, M. Tabrizian and L. H. Yahia (2001). "Low-temperature sterilization using gas plasmas: a review of the experiments and an analysis of the inactivation mechanisms." Int J Pharm 226(1-2): 1-21.

Mol, A., C. V. Bouten, F. P. Baaijens, G. Zund, M. I. Turina and S. P. Hoerstrup (2004). "Review article: Tissue engineering of semilunar heart valves: current status and future developments." J Heart Valve Dis 13(2): 272-280.

Mol, A., A. I. Smits, C. V. Bouten and F. P. Baaijens (2009). "Tissue engineering of heart valves: advances and current challenges." Expert Rev Med Devices 6(3): 259-275.

Movahedi, S. and W. Waites (2000). "A two-dimensional protein gel electrophoresis study of the heat stress response of Bacillus subtilis cells during sporulation." J Bacteriol 182(17): 4758-4763.

Murray, P. R. (2012). "What is new in clinical microbiology-microbial identification by MALDI-TOF mass spectrometry: a paper from the 2011 William Beaumont Hospital Symposium on molecular pathology." J Mol Diagn 14(5): 419-423.

Nallapareddy, S. R., K. V. Singh, J. Sillanpaa, D. A. Garsin, M. Hook, S. L. Erlandsen and B. E. Murray (2006). "Endocarditis and biofilm-associated pili of Enterococcus faecalis." J Clin Invest 116(10): 2799-2807.

Naso, F., A. Gandaglia, L. Iop, M. Spina and G. Gerosa (2011). "First quantitative assay of alpha-Gal in soft tissues: presence and distribution of the epitope before and after cell removal from xenogeneic heart valves." Acta Biomater 7(4): 1728-1734.

Nguyen, H., A. I. Cassady, M. B. Bennett, E. Gineyts, A. Wu, D. A. Morgan and M. R. Forwood (2013). "Reducing the radiation sterilization dose improves mechanical and biological quality while

retaining sterility assurance levels of bone allografts." Bone 57(1): 194-200.

Nguyen, H., D. A. Morgan and M. R. Forwood (2007). "Sterilization of allograft bone: effects of gamma irradiation on allograft biology and biomechanics." Cell Tissue Bank 8(2): 93-105.

Nguyen, H., D. A. Morgan and M. R. Forwood (2007). "Sterilization of allograft bone: is 25 kGy the gold standard for gamma irradiation?" Cell Tissue Bank 8(2): 81-91.

Nguyen, H., D. A. Morgan and M. R. Forwood (2011). "Validation of 11 kGy as a radiation sterilization dose for frozen bone allografts." J Arthroplasty 26(2): 303-308.

Nielsen, H. V., P. S. Guiton, K. A. Kline, G. C. Port, J. S. Pinkner, F. Neiers, S. Normark, B. Henriques-Normark, M. G. Caparon and S. J. Hultgren (2012). "The metal ion-dependent adhesion site motif of the Enterococcus faecalis EbpA pilin mediates pilus function in catheter-associated urinary tract infection." MBio 3(4): e00177-00112.

Ott, H. C., T. S. Matthiesen, S. K. Goh, L. D. Black, S. M. Kren, T. I. Netoff and D. A. Taylor (2008). "Perfusion-decellularized matrix: using nature's platform to engineer a bioartificial heart." Nat Med 14(2): 213-221.

Pharmacopeia, U. S. Microbiological Tests Biological Indicators for Sterilization. USP29-NF24

Pitt, T. L., K. Tidey, A. Roy, S. Ancliff, R. Lomas and C. P. McDonald (2014). "Activity of four antimicrobial cocktails for tissue allograft decontamination against bacteria and Candida spp. of known susceptibility at different temperatures." Cell Tissue Bank 15(1): 119-125.

Pizarro-Cerda, J. and P. Cossart (2006). "Bacterial adhesion and entry into host cells." Cell 124(4): 715-727.

Prusiner, S. B. (1998). "Prions." Proc Natl Acad Sci U S A 95(23): 13363-13383.

Pruss, A., U. B. Gobel, G. Pauli, M. Kao, M. Seibold, H. J. Monig, A. Hansen and R. von Versen (2003). "Peracetic acid-ethanol treatment of allogeneic avital bone tissue transplants--a reliable sterilization method." Ann Transplant 8(2): 34-42.

Qiu, Q. Q., W. Q. Sun and J. Connor (2011). 4.410 - Sterilization of Biomaterials of Synthetic and Biological Origin. Comprehensive Biomaterials. P. Ducheyne. Oxford, Elsevier: 127-144.

Radjeman, A., S. C. Liew and K. O. Lim (1985). "Anisotropic elasticity of bovine pericardial tissues." Jpn J Physiol 35(5): 831-840.

Raguse, M., M. Fiebrandt, K. Stapelmann, K. Madela, M. Laue, J. W. Lackmann, J. E. Thwaite, P. Setlow, P. Awakowicz and R. Moeller (2016). "Improvement of Biological Indicators by Uniformly Distributing Bacillus subtilis Spores in Monolayers To Evaluate Enhanced Spore Decontamination Technologies." Appl Environ Microbiol 82(7): 2031-2038.

Rauh, J., F. Despang, J. Baas, C. Liebers, A. Pruss, M. Gelinsky, K. P. Gunther and M. Stiehler (2014). "Comparative biomechanical and microstructural analysis of native versus peracetic acid-ethanol treated cancellous bone graft." Biomed Res Int 2014: 784702.

Rémi, E., N. Khelil, I. D. Centa, C. Roques, M. Ba, F. Medjahed-Hamidi, F. Chaubet, D. Letourneur, E. Lansac and A. Meddahi-Pellé (2011). Pericardial Processing: Challenges, Outcomes and Future Prospects. Biomaterials Science and Engineering R. Pignatello.

Rippel, R. A., H. Ghanbari and A. M. Seifalian (2012). "Tissue-engineered heart valve: future of cardiac surgery." World J Surg 36(7): 1581-1591.

Roosens, A., P. Somers, F. De Somer, V. Carriel, G. Van Nooten and R. Cornelissen (2016). "Impact of Detergent-Based Decellularization Methods on Porcine Tissues for Heart Valve Engineering." Ann Biomed Eng 44(9): 2827-2839.

Rosario, D. J., G. C. Reilly, E. Ali Salah, M. Glover, A. J. Bullock and S. Macneil (2008). "Decellularization and sterilization of porcine

urinary bladder matrix for tissue engineering in the lower urinary tract." Regenerative medicine 3(2): 145-156.

Rossner, E., M. D. Smith, B. Petschke, K. Schmidt, M. Vitacolonna, C. Syring, R. von Versen and P. Hohenberger (2011). "Epiflex((R)) a new decellularised human skin tissue transplant: manufacture and properties." Cell Tissue Bank 12(3): 209-217.

Russell, N., A. Rives, M. H. Pelletier, T. Wang and W. R. Walsh (2015). "The effect of supercritical carbon dioxide sterilization on the anisotropy of bovine cortical bone." Cell Tissue Bank 16(1): 109-121.

Rutala, W. A. and D. J. Weber (2013). "Disinfection and sterilization: an overview." Am J Infect Control 41(5 Suppl): S2-5.

Sacks, M. S., F. J. Schoen and J. E. Mayer (2009). "Bioengineering challenges for heart valve tissue engineering." Annu Rev Biomed Eng 11: 289-313.

Saladin, K. S. (2010). Anatomy & Physiology : The Unity of Form and Function. Dubuque, McGraw-Hill.

Scheffler, S. U., J. Scherler, A. Pruss, R. von Versen and A. Weiler (2005). "Biomechanical comparison of human bone-patellar tendon-bone grafts after sterilization with peracetic acid ethanol." Cell Tissue Bank 6(2): 109-115.

Schenke-Layland, K. (2003). "Complete dynamic repopulation of decellularized heart valves by application of defined physical signals—an in vitro study." Cardiovascular Research 60(3): 497-509.

Schmidt, C. E. and J. M. Baier (2000). "Acellular vascular tissues: natural biomaterials for tissue repair and tissue engineering." Biomaterials 21(22): 2215-2231.

Schmidt, D., U. A. Stock and S. P. Hoerstrup (2007). "Tissue engineering of heart valves using decellularized xenogeneic or polymeric starter matrices." Philos Trans R Soc Lond B Biol Sci 362(1484): 1505-1512.

Schoen, F. J. (2008). "Evolving concepts of cardiac valve dynamics: the continuum of development, functional structure, pathobiology, and tissue engineering." Circulation 118(18): 1864-1880.

Schoen, F. J. (2012). "Mechanisms of function and disease of natural and replacement heart valves." Annu Rev Pathol 7: 161-183.

Schoen, F. J. and R. J. Levy (2005). "Calcification of tissue heart valve substitutes: progress toward understanding and prevention." Ann Thorac Surg 79(3): 1072-1080.

Seto, A. U., C. J. Gatt, Jr. and M. G. Dunn (2013). "Sterilization of tendon allografts: a method to improve strength and stability after exposure to 50 kGy gamma radiation." Cell Tissue Bank 14(3): 349-357.

Shearer, H., M. J. Ellis, S. P. Perera and J. B. Chaudhuri (2006). "Effects of common sterilization methods on the structure and properties of poly(D,L lactic-co-glycolic acid) scaffolds." Tissue Eng 12(10): 2717-2727.

Simionescu, D. T. (2006). Artificial Heart Valves. Wiley Encyclopedia of Biomedical Engineering. M. Akay.

Spina, M., F. Ortolani, A. El Messlemani, A. Gandaglia, J. Bujan, N. Garcia-Honduvilla, I. Vesely, G. Gerosa, D. Casarotto, L. Petrelli and M. Marchini (2003). "Isolation of intact aortic valve scaffolds for heart-valve bioprostheses: extracellular matrix structure, prevention from calcification, and cell repopulation features." J Biomed Mater Res A 67(4): 1338-1350.

Srokowski, E. M. and K. A. Woodhouse (2011). "Decellularized Scaffolds." 369-386.

Steinhoff, G., U. Stock, N. Karim, H. Mertsching, A. Timke, R. R. Meliss, K. Pethig, A. Haverich and A. Bader (2000). "Tissue engineering of pulmonary heart valves on allogenic acellular matrix conduits: in vivo restoration of valve tissue." Circulation 102(19 Suppl 3): III50-55.

Sun, W. Q. and P. Leung (2008). "Calorimetric study of extracellular tissue matrix degradation and instability after gamma irradiation." Acta Biomater **4**(4): 817-826.

Sutton, S. (2010). "The Most Probable Number Method and its uses in Enumeration, Qualification and Validation." Journal of Validation Technology **16**(3).

Syedain, Z., J. Reimer, J. Schmidt, M. Lahti, J. Berry, R. Bianco and R. T. Tranquillo (2015). "6-month aortic valve implantation of an off-the-shelf tissue-engineered valve in sheep." Biomaterials **73**: 175-184.

Tabaku, M., R. Jashari, H. F. Carton, A. Du Verger, B. Van Hoeck and A. Vanderkelen (2004). "Processing of cardiovascular allografts: effectiveness of European Homograft Bank (EHB) antimicrobial treatment (cool decontamination protocol with low concentration of antibiotics)." Cell Tissue Bank **5**(4): 261-266.

Tate, P. (2012). Seeley's Principles of Anatomy & Physiology. New York, McGraw-Hill

Tendero, C., C. Tixier, P. Tristant, J. Desmaison and P. Leprince (2006). "Atmospheric pressure plasmas: A review." Spectrochimica Acta Part B: Atomic Spectroscopy **61**(1): 2-30.

Theodoridis, K., I. Tudorache, A. Calistru, S. Cebotari, T. Meyer, S. Sarikouch, C. Bara, R. Brehm, A. Haverich and A. Hilfiker (2015). "Successful matrix guided tissue regeneration of decellularized pulmonary heart valve allografts in elderly sheep." Biomaterials **52**: 221-228.

van Kats, J. P., C. van Tricht, A. van Dijk, M. van der Schans, A. van den Bogaerdt, P. L. Petit and A. J. Bogers (2010). "Microbiological examination of donated human cardiac tissue in heart valve banking." Eur J Cardiothorac Surg **37**(1): 163-169.

Vesely, I. (2005). "Heart valve tissue engineering." Circ Res **97**(8): 743-755.

Villalba, R., P. Alonso, J. M. Villalba, L. F. Rioja and J. L. Gomez Villagran (1995). "The effect of amphotericin B on the viability of cryopreserved human skin." Cryobiology **32**(4): 314-317.

Villalba, R., F. Solis, G. Fornes, A. Jimenez, M. Eisman, A. I. Gonzalez, M. J. Linares, M. Casal and J. L. Gomez Villagran (2012). "In vitro susceptibility of high virulence microorganisms isolated in heart valve banking." Cell Tissue Bank **13**(3): 441-445.

Waite, L. and J. M. Fine (2007). Applied Biofluid Mechanics. New York, McGraw-Hill.

Weber, B. and S. P. Hoerstrup (2011). "Tissue Engineering of Heart Valves." 377-391.

White, A., D. Burns and T. W. Christensen (2006). "Effective terminal sterilization using supercritical carbon dioxide." J Biotechnol **123**(4): 504-515.

Wilshaw, S. P., J. Kearney, J. Fisher and E. Ingham (2008). "Biocompatibility and potential of acellular human amniotic membrane to support the attachment and proliferation of allogeneic cells." Tissue Eng Part A **14**(4): 463-472.

Wilshaw, S. P., J. N. Kearney, J. Fisher and E. Ingham (2006). "Production of an acellular amniotic membrane matrix for use in tissue engineering." Tissue Eng **12**(8): 2117-2129.

Woods, T. and P. F. Gratzer (2005). "Effectiveness of three extraction techniques in the development of a decellularized bone-anterior cruciate ligament-bone graft." Biomaterials **26**(35): 7339-7349.

Zhou, J., O. Fritze, M. Schleicher, H. P. Wendel, K. Schenke-Layland, C. Harasztosi, S. Hu and U. A. Stock (2010). "Impact of heart valve decellularization on 3-D ultrastructure, immunogenicity and thrombogenicity." Biomaterials **31**(9): 2549-2554.

Zhou, M., N. Zhang, X. Liu, Y. Li, Y. Zhang, X. Wang, B. Li and B. Li (2014). "Tendon allograft sterilized by peracetic acid/ethanol combined with gamma irradiation." J Orthop Sci **19**(4): 627-636.

LIST OF FIGURES

LIST OF TABLES

LIST OF ABBREVIATIONS

AA - Antibiotics and Antimycotics

AB- Alcian Blue

AIDS - Acquired Immune Deficiency Syndrome

AL - Aortic Leaflets

AR - Aortic Root

ATP - Adenosine Triphosphate

ATV - Atrioventricular

AV - Aortic Valve

BacP - *Bacillus pumilus*

BacP+HS - *Bacillus pumilus* + heat shock

BHV - Bioprosthetic Heart Valve

BPD - Bovine Pericardium Decellularised

CC - Controlled Contamination

CFU - Colony Forming Units

CHAPS - 3-[3-Cholamidopropyl)dimethylammonio]-1-Propanesulfonate

CI - Confidence Intervals

DMSO - Dimethyl sulfoxide

ECM - Extracellular Matrix

EDTA - Ethylenediaminetetraacetic Acid

EHB - European Homograft Bank

EtO - Ethylene Oxide

FBS - Foetal Bovine Serum

FDA - Food and Drug Administration

GAGs - Glycosaminoglycan

hBM-MSC - human bone marrow mesenchymal stem cells

HCl - Hydrochloric Acid

HE - Haematoxylin & Eosin

HIV - Human Immunodeficiency Virus

HPLC - high-pressure liquid chromatography

HS - Heat Shock

HTLV - Human T-cell Lymphotropic Virus

HYP - Hydroxyproline

ISO - International Organization for Standardization

LDH - Lactate Dehydrogenase

MALDI-TOF - Matrix-Assisted Laser Desorption/Ionization Time-of-Flight

MEMα - Minimum Essential Medium Eagle

MOD - Multi-organ donors

MPN - Most Probable Number

MT - Mallory Trichrome

MTS - tetrazolium compound [3-(4,5-dimethylthiazol-2-yl)- 5 -(3-carboxymethoxyphenyl)- 2 -(4-sulfophenyl)-2H-tetrazolium, inner salt]

MVP - Mitral Valve Prolapse

NBHD - Non-Heart-Beating Deceased Person

OCT - Optimum Cutting Temperature

OD - Over day

ON - Overnight

PAA - Peracetic Acid

PBS - Phosphate-Buffered Saline

PFA - Paraformaldehyde

PGA - Polyglycolic Acid

PHA - Polyhydroxyalkanoates

PI - Protease Inhibitors

PLA - Polylactic Acid

PMSF - Phenylmethylsulfonylfluoride

PP - Porcine Pericardia

PPD - Porcine Pericardium Decellularised

PS - Penicillin Streptomycin

PV - Pulmonary Valve

RHT - Recipients of Heart Transplantation

RT - Room Temperature

SA - Sinoatrial

SAB - Scientific Advisory Board

SAL - Sterility Assurance Level

SB-10 - Sulfobetaine-10

SB-16 - Sulfobetaine-16

SC-CO_2 - Supercritical CO_2

SIS – Small Intestine Submucosa

SDS - Sodium Dodecyl Sulphate

SEM - Scanning Electron Microscopy

SL - Semilunar

TAVR - Transcatheter Aortic Valve Replacement

TCM-199 - Tissue Culture Medium

TE - Tissue Engineering

TEHV - Tissue-Engineered Heart Valve

Thio – Thioglycolate Medium

TnBP - Tri(n-butyl)phosphate

TSB - Tryptone Soya Broth

UTS - Ultimate Tensile Strength

UV – Ultraviolet

VIMM - Venetian Institute of Molecular Medicine

APPENDICES

In the following table are listed the model and supplier of the equipment required to perform the methodologies above mentioned.

Equipment	**Model**	**Supplier**
Autoclave	Steam Sterilizer	Raypa Tradl
Balance	PLS	Kern
Bose Electroforce System	--	Bose Corporation, Eden Prairie, MN, USA
Centrifuge	Minispin Plus	Eppendorf
Centrifuge	S702R	Eppendorf
Cryostat	CM 1850 UV	Leica
Freeze Dryer	Modulyo	Edwards
Incubator Bacteria	Excella	New Brunswick Scientific, Eppendorf
Incubator Cell	CO – 170	Scientific New Brunswick Innova
Magnetic Stirrer	ARE	VELP Scientifica, Sacco
Nikon Eclipse equipped with NIS-Elements D 3.2 Software	50i	Nikon Corporation Shinagawa, Tokyo, Japan
Orbital shaker	----	Vetrotecnica
pH Meter	Crison	Sacco
Plate Reader	Infinite 200Pro	Tecan
Plate Reader2	Fluostar Optima	BMG Labtech
Plate Shaker	Titterbug - 2	Boekel Scientific
Precision Balance	----	Sartorius Research
Spectrophotometer	6305 UV/VIS.	Jenway
Thermoblock	----	Pbi International
Thickness Gauge	Absolute	Mitutoyo
Vortex	----	VELP Scientifica, Sacco
Water Bath	----	MPM Instruments S.r.l

In the table below are listed the model and brand of chemicals and reagents essential to perform the experiments for this project.

Chemical/Reagent	**Supplier**
1,9-Dimethylene-methylene blue zinc	Sigma Aldrich
1-Propanol	Sigma Aldrich
4-(dimethylamino) benzaldehyde	Sigma Aldrich
Acetic acid	Sigma Aldrich
Alcian Blue (AB) Kit	Bio-Optica, Milano, Italy
Amphotericin B	Gibco®, Bleiswijk, Netherlands
Ascorbic acid	Sigma Aldrich
Benzamidine	Sigma Aldrich
Benzonase® Nuclease	Sigma Aldrich
Bovine Fetal Serum	Sigma Aldrich
Calcium chloride	Sigma Aldrich
Cefoxitin (United States Pharmacopeia (USP) Reference Standard)	Fluka, Strasbourg, France
Chloramine-T	Sigma Aldrich
Chocolate Agar Plates (GC II Agar with IsoVitalex)	BD, Heidelberg, Germany
Chondroitin sulfate	Sigma Aldrich
Citric acid	Sigma Aldrich
Citric acid	Sigma Aldrich
Di-hydrogen phosphate	Sigma Aldrich
Dimethyl Sulphoxide	Sigma Aldrich
Dimethyl Sulphoxide Hybri-Max®	Sigma Aldrich
Di-sodium hydrogen phosphate	Sigma Aldrich
Ethanol	Sigma Aldrich
Ethylenediamine tretraacetic acid (EDTA)	Sigma Aldrich
Formic acid	Riedel-de-Haen
Gentamycin Solution	Sigma Aldrich
Glutaraldehyde	Sigma Aldrich
Haematoxylin and Eosin (HE) Kit	Bio-optica, Milano, Italy
Hydrochloric Acid	Carlo Erba, Val de Reuil
Iodoacetamide	Sigma Aldrich
Isopentane	Sigma Aldrich
Isopropanol	Sigma Aldrich
L-cysteine	Sigma Aldrich
L-Glutamine	Sigma Aldrich
LHD kit	Sigma Aldrich
Mallory Trichrome (MT) Kit	Bio-Optica, Milano, Italy

Minimum Essential Medium Eagle (MEMα)	Sigma Aldrich
Mounting Medium	Sigma Aldrich
MTS kit	Sigma Aldrich
N-ethylmaleimide	Sigma Aldrich
Optimum Cutting Temperature (OCT) compound	Tissue-Tek
Papain	Sigma Aldrich
Papain	Sigma Aldrich
Paraformaldehyde	Applichem
Penicillin-Streptomycin	Sigma Aldrich
Peracetic Acid (36-40wt %)	Sigma Aldrich
Perchloric acid	Merck
Phenylmethanesulfonyl fluoride	Sigma Aldrich
Potassium Chloride	Ashaland Chemicals
Potassium phosphate	Sigma Aldrich
Sodium acetate	Sigma Aldrich
Sodium cacodylate	Sigma Aldrich
Sodium Chloride	Sigma Aldrich
Sodium Cholate	Sigma Aldrich
Sodium formate	Sigma Aldrich
Sodium Hydroxide	Sigma Aldrich
Sodium hydroxide	Riedel de Haen
Sodium phosphate	Sigma Aldrich
Sucrose	Sigma Aldrich
Thioglycollate medium	Biolife, Milano, Italy
Trans-4-hydroxy-L-proline	Sigma Aldrich
Triton X-100	Sigma Aldrich
Trypan Blue Solution (0.4%)	Sigma Aldrich
Trypsin	Sigma Aldrich
Tryptone soya broth	Biotec, Cadorago, Italy
Vancomycin Hydrochloride	Sigma Aldrich
Xylene	Sigma Aldrich

SCIENTIFIC PRESENTATIONS AND PUBLICATIONS

I Year

1) **Fidalgo C**., "Preservation and Sterilization of Decellularized Scaffolds", poster and podium presentations at TECAS-ITN (Tissue Engineering Solutions for Cardiovascular Surgery - Initial Training Network) Kick of Meeting on 12th-13th December 2013 in Hannover Medical School, Hannover, Germany;

2) Naso F., Spina M., Iop L., Aguiari P., Areias A.C., **Fidalgo C.M.**, Tuladhar S.R., Gerosa G., "Production of a New Generation of Alpha-Gal-Free Bioprosthetic Tissues: Preliminary Results", Cardiology 2014; 128:106-194, DOI:10.1159/000362180;

3) **Fidalgo C**., "Preservation and Sterilisation of Decellularized Scaffolds", poster and podium presentations at TECAS-ITN Work-in-Progress Meeting on 27th-30th October 2014 in University of Padua, Padua, Italy.

II Year

1) **Fidalgo C.**, Aguiari P., Iop L., Harder M., Mavrilas D., Korossis S. and Gerosa G., podium presentation at TECAS-ITN Half-Year Meeting on 8th-10th June 2015 in Hannover Medical School, Hannover, Germany;

2) **C. Fidalgo**, P. Aguiari, L. Iop, M. Harder, D. Mavrilas, M. Sciro, G. Palù, S. Korossis, G. Gerosa, "Assessment of Disinfection and Sterilization of Decellularized Pericardial Scaffolds", poster presentation, 4th TERMIS World Congress, 8th-11th September 2015, Boston, USA;

3) **C. Fidalgo**, P. Aguiari, L. Iop, M. Harder, D. Mavrilas, M. Sciro, G. Palu`, S. Korossis, G. Gerosa, "Assessment of Disinfection and Sterilization of Decellularized Pericardial Scaffolds", Tissue Engineering: Part A, Volume 21, Supplement 1, 2015, DOI: 10.1089/ten.tea.2015.5000.abstracts;

4) P. Aguiari, L. Iop, S. R. Tuladhar, **C.M. Lourenco Fidalgo**, F. Naso, F. Favaretto, G. Milan, M. Spina, R. Vettor, A. Bagno, G. Gerosa, "A New Pericardial Decellularized Scaffold for the Manufacturing of Cardiovascular Substitutes", Tissue Engineering: Part A, Volume 21, Supplement 1, 2015, DOI: 10.1089/ten.tea.2015.5000.abstracts;

5) **Fidalgo C**., "Assessment of Preservation and Sterilisation Methods for Decellularized Scaffolds", podium presentation at TECAS-ITN Work-in-Progress Meeting on 1st - 4th December 2015 in Helmholtz Institute, Aachen, Germany.

III Year

1) **Fidalgo C**., "Assessment of Preservation and Sterilisation Methods for Decellularized Scaffolds", podium presentation at the Annual Venetian Institute of Molecular Medicine (VIMM) Retreat, on 19th-20th February 2016 in Ponzano Veneto, Treviso, Italy;

2) Cristian Carlos D'Alessandro, Adel Farid Badria, **Cátia Fidalgo**, Gino Gerosa, Sotirios Korossis, Petros Koutsoukos and Dimosthenis Mavrilas, "Development of an improved *in vitro* model for the study of calcification potential of cardiovascular tissue engineering scaffolds", poster presentation at 2nd Biomatsen International Congress on Biomaterials & Biosensors, 1st-3rd June 2016, Istanbul, Turkey;

3) **Fidalgo C.**, Zouhair S., Aguiari P., Iop L., Harder M., Mavrilas D., Bagno A., Wolkers W., Korossis S., Gerosa G., "Advanced Preservation and Sterilization Methodologies", poster presentation for Scientific Advisory Board (SAB) evaluation of VIMM on 30th May 2016 at VIMM laboratories, Padova, Italy.

4) Paola Aguiari, Laura Iop, Francesca Favaretto, **Cátia Marisa Lourenco Fidalgo**, Filippo Naso, Gabriella Milan, Vincenzo Vindigni, Michel Spina, Franco Bassetto, Andrea Bagno, Roberto Vettor and Gino Gerosa, "In vitro comparative assessment of decellularized bovine pericardial patches and commercial bioprosthetic heart valves.", submitted to Biomedical Materials Journal and currently under revision;

5) **C. Fidalgo**, P. Aguiari, L. Iop, M. Harder, D. Mavrilas, A. Bagno, M. Sciro, G. Palù, S. Korossis, G. Gerosa, "Novel Methodology for Effective Sterilization of Xenogeneic Decellularized Pericardial Scaffolds", in preparation.

ACKNOWLEDGEMENTS

This research is part of the TECAS ITN Network and is funded by the People Programme (Marie Curie Actions) of the European Union's Seventh Framework Programme FP7/2007-2013/ under REA grant agreement n° 317512.

For this work to be achieved there are several persons who acknowledgements should be made, since without their support and dedication this will not be possible.

As first, my acknowledgments to my supervisors and tutors at the University of Padova: Professor Gerosa, Dr. Paola Aguiari and Dr. Laura Iop. Thank you for your guidance, moral support, sharing your scientific knowledge, advices, challenges, patience and friendship through my studies.

My thanks also to Dr. Sotirios Korossis for your support and guidance during this three years, especially to the time of my secondment in Hannover. A special thank goes to Dr. Michael Harder. Thank you for sharing the knowledge for the industrial point of view into my research studies and for the many advices given along these three years. Also, I am very thankful for the opportunity you gave me for spending one week at Corlife, where I understood how difficult can be to translate research subjects to the clinical field, but at the same time the impact that it can have in the future. I would like to thank also to Prof. Mavrilas for the scientific advices during my studies.

A general acknowledgement to all TECAS investigators for their advices for my project and sharing their scientific knowledge during the TECAS meetings.

A special thank goes to Professor Palù and to Dr. Manuela Sciro for all experimental part concerning the identification of pathogens and for the fruitful assistance in the microbiology field.

I would like to express my gratitude to Prof. Bagno for his assistance and help during the mechanical testing of the tissues. Thank you for your patience and reply to all my questions. Also, I would like to thank Dr. Furlan for his assistance in the preparation and acquisition of SEM images.

Besides, this work would not have been achieved without support of family and friends. To all the people in the Laboratory of Cardiovascular Regenerative Medicine, thank you so much for all friendship, moral support, motivation and patience in my endless questions and experiment plans. Especially to Eleonora, Sugat, Davide and Sabra, your

company every day in the laboratory make the work much easier and you have become my big family here in Italy!

To my Portuguese friends, that even by physical distance support me with their constant positivity and confidence. Thank you, Sara, Carlos, Carla, Diana, Nilza and Miguel. My visits at home were divided in million plans to be present with each of you for some time and was totally gratifying.

Special thanks are addressed to my family. To my parents that have support me in my decision of develop my studies abroad. Thank you for your moral and financial support, positivity and trust in my work. Thank you for be present in the happy and sad moments and for your constant wise advices. To my sister Liliana and family Ricardo, Rodrigo and Carolina. Thank you for always support me and be such a great family. Without you, all this would never be possible.

For all that were present during these last three years, your presence and support made this amazing experience be possible! Thank you very much!